

CLUSTERS MERGING AND FORWARDING
SCHEMES IN VEHICULAR AD HOC NETWORKS
ON HIGHWAY AND URBAN SCENARIOS

*Presented in Partial Fulfillment of
the Requirements for the Degree of*

DOCTOR OF PHILOSOPHY

with a Major in

Computer Science

in the

College of Graduate Studies

University of Idaho

by

OSAMA ALQAHTANI

*Approved by:
Major Professor*

FREDERICK SHELDON, PH.D.

Committee

TERENCE SOULE, PH.D.

JULIE BEESTON, PH.D.

ROBERT RINKER, PH.D.

Department Administrator

TERENCE SOULE, PH.D.

DECEMBER 2021

ABSTRACT

One of the primary objectives of Intelligent Transportation Systems (ITSs) is providing safety to its users. This can be accomplished by the exchange of information among vehicles, forming a network called vehicular ad-hoc network (VANET). However, such information exchange is a challenge in itself. Safety messages must be timely disseminated throughout vehicles in the vicinity of a detected hazard. The easiest way to do so is to broadcast (and subsequently re-broadcast) safety messages until they reach all vehicles in the vicinity (i.e., whole network). Two problems arise using this approach: (i) the flood of transmitted messages causes massive packet collisions, incurring delays instead of quickly reaching all network nodes — an effect known as broadcast storm — and (ii) wasted bandwidth and processing resources especially because hazard events need not necessarily be required for distant vehicles within the network. That is, distant vehicles would typically discard such messages because they do not have value as for taking an action (yet).

Several studies have appeared in the literature to tackle the aforementioned problems. Some techniques are based on limiting the number of re-broadcasts of a message by using counters, or by allowing re-transmissions only by the vehicles farthest from the original transmitter, or even by making all vehicles share their location to enable selecting the "best" forwarders to be identified (based on a set of predefined criteria). Even though these methods have performed well on highways, their use did not yield good results for typical urban scenarios (e.g., downtown). The higher prevalence of obstacles (buildings) tend to block the highly directive signals used for inter-vehicle communication.

Another class of studies emerged to address this message blocking effect, leveraging so-called forwarder vehicles situated in locations that provide line of sight to avoid the blocking phenomena. Other studies leveraged the wide coverage provided by cellular networks. They considered the Long Term Evolution (LTE) protocol but communication delays were greater than the limit allowed for safety message dissemination. The development of the 5th generation mobile network (5G) however, gave promise that the technology will be able to comply with such hard real-time

requirements. Thus, using both forwarders and (5G) technology for the dissemination of safety warning messages is indeed a promising approach.

In this research, clustering is considered as a means to keep broadcast storms under control. Clustering limits communication among cluster members only. Unfortunately, creating and maintaining clusters is difficult due to multiple factors, including vehicle velocity variance and constantly changing cluster membership topologies.

Therefore, in this work we developed a way to form clusters that will last longer (i.e., merging small clusters together). A cluster merging algorithm was developed therefore. Subsequently, the work proceeds to analyze the use of different combinations of forwarders and 5G infrastructure to optimize warning message dissemination performance considering delay and the percentage of informed vehicles. These studies, consistent with most other studies follow a discrete event simulation approach to assess the aforementioned performance metrics compared to the original our studies and those of other researchers selected from the literature as benchmarks.

ACKNOWLEDGEMENTS

First, I would like to thank the University of Idaho for giving me the opportunity to conduct my Ph.D. studies and for providing great support throughout the whole process. Especially, I thank Dr. Frederick Sheldon for guiding my studies and research, and for being the person I could count on for any advice I needed to complete this work.

I would like to thank Jazan University, KSA, for the financial support during my PhD Studies.

Finally and most importantly, I would like to thank Allah, my family, and my friends for giving me the strength and the emotional support to face all the challenges life in academia can present.

DEDICATION

To my father, who taught me to push through life and never give up.

TABLE OF CONTENTS

ABSTRACT	ii
ACKNOWLEDGEMENTS	iv
DEDICATION.	v
TABLE OF CONTENTS.	vi
LIST OF TABLES	viii
LIST OF FIGURES.	xi
LIST OF ACRONYMS	xiii
1 INTRODUCTION	1
1.1 The Broad Problem in VANETs	1
1.2 The Specific Problems That Add to the Broader Problem	2
1.3 The Current Literature Proposals and Weaknesses	3
1.4 Our Contribution	4
1.5 Problem Statement	5
1.6 Research Motivation and Contributions	6
1.7 Document Organization	6
2 BACKGROUND AND RELATED WORK	8
2.1 VANETs	8
2.2 Warning Messages Dissemination	9
2.3 Related Work	12
3 CLUSTERING IN VANETs	16
3.1 Introduction	16
3.2 Background	17
3.3 Related Work	18
3.4 Cluster Merging Scheme for Reliable Message Dissemination	21
3.5 Simulation Results	26
3.6 Conclusion	28
4 DISSEMINATION PROPOSALS	32
4.1 Introduction	32
4.2 Background	34
4.3 Related Work	37
4.4 Methodology	40
4.5 Results and Discussion	47
4.6 Conclusion	53

5	THREE-FACTOR CLUSTER MERGING	55
5.1	Introduction	55
5.2	Related Work	58
5.3	A New VANET System Model	60
5.4	Results and Discussion	65
5.5	Conclusion	68
6	WEIGHT FACTORS STUDY.	69
6.1	Introduction	69
6.2	Related Work	71
6.3	System Model Summary	72
6.4	Results	74
6.5	Conclusion	81
7	CONCLUSION	83
	BIBLIOGRAPHY.	86
	APPENDICES.	91
A	SUPPLEMENTARY CHARTS TO CHAPTER 6	91
A.1	Data and Figures of the Valencia Scenario	91
A.2	Data and Figures of the San Francisco Scenario	104
B	CLUSTER MERGING IMPLEMENTATION IN OMNET++	117

LIST OF TABLES

TABLE 1	List of acronyms used in the thesis (part 1)	xiii
TABLE 2	List of acronyms used in the thesis (part 2)	xiv
TABLE 3.1	Simulation Parameters	27
TABLE 4.1	Comparison of this study to related work	40
TABLE 4.2	Simulation Parameters	48
TABLE 4.3	Comparison between maps throughout number of vehicles and selected notification times	52
TABLE 5.1	Simulation Parameters	65
TABLE 6.1	Weight Factor Combinations	74
TABLE 6.2	Simulation Parameters	74
TABLE 6.3	Percentage of vehicles informed on the Valencia map (method that achieved the maximum percentage for a given density)	75
TABLE 6.4	Percentage of vehicles informed on the San Francisco map (method that achieved the maximum percentage for a given density)	76
TABLE 6.5	Delays to inform the last vehicle on the Valencia map (method that achieved the minimum delay for a given density)	76
TABLE 6.6	Delays to inform the last vehicle on the San Francisco map (method that achieved the minimum delay for a given density)	77
TABLE 6.7	Percentage of vehicles informed on the Valencia map considering a single method for all densities	78
TABLE 6.8	Percentage of vehicles informed on the San Francisco map considering a single method for all densities	79
TABLE 6.9	Delays to inform the last vehicle on the Valencia map considering a single method across densities	79
TABLE 6.10	Delays to inform the last vehicle on the San Francisco map considering a single method across densities	80
TABLE A.1	Percentage of vehicles informed on the Valencia scenario for the considered car densities, highlighting the highest percentage for each density and weight factors combination (part 1 — weight factor combinations 1–5)..	94
TABLE A.2	Percentage of vehicles informed on the Valencia scenario for the considered car densities, highlighting the highest percentage for each density and weight factors combination (part 2 — weight factor combinations 6–10).	95
TABLE A.3	Delays in seconds to inform the last vehicle on the Valencia scenario for the considered car densities, highlighting the lowest delays for each density and weight factors combination (part 1 — weight factor combinations 1–5)..	98

TABLE A.4	Delays in seconds to inform the last vehicle on the Valencia scenario for the considered car densities, highlighting the lowest delays for each density and weight factors combination (part 2 — weight factor combinations 6–10).	99
TABLE A.5	Sum of the percentages of vehicles informed on the Valencia scenario across all densities, highlighting the highest sum for each weight factors combination (part 1 — weight factor combinations 1–5).	100
TABLE A.6	Sum of the percentages of vehicles informed on the Valencia scenario across all densities, highlighting the highest sum for each weight factors combination (part 2 — weight factor combinations 6–10)..	101
TABLE A.7	Sum of the delays in seconds to inform the last vehicle on the Valencia scenario across all densities, highlighting the lowest sum for each weight factors combination (part 1 — weight factor combinations 1–5).	102
TABLE A.8	Sum of the delays in seconds to inform the last vehicle on the Valencia scenario across all densities, highlighting the lowest sum for each weight factors combination (part 2 — weight factor combinations 6–10).	103
TABLE A.9	Percentage of vehicles informed on the San Francisco scenario for the considered car densities, highlighting the highest percentage for each density and weight factors combination (part 1 — weight factor combinations 1–5)..	107
TABLE A.10	Percentage of vehicles informed on the San Francisco scenario for the considered car densities, highlighting the highest percentage for each density and weight factors combination (part 2 — weight factor combinations 6–10).	108
TABLE A.11	Delays in seconds to inform the last vehicle on the San Francisco scenario for the considered car densities, highlighting the lowest delays for each density and weight factors combination (part 1 — weight factor combinations 1–5).	109
TABLE A.12	Delays in seconds to inform the last vehicle on the San Francisco scenario for the considered car densities, highlighting the lowest delays for each density and weight factors combination (part 2 — weight factor combinations 6–10).	110
TABLE A.13	Sum of the percentages of vehicles informed on the San Francisco scenario across all densities, highlighting the highest sum for each weight factors combination (part 1 — weight factor combinations 1–5)..	111
TABLE A.14	Sum of the percentages of vehicles informed on the San Francisco scenario across all densities, highlighting the highest sum for each weight factors combination (part 2 — weight factor combinations 6–10).	112
TABLE A.15	Sum of the delays in seconds to inform the last vehicle on the San Francisco scenario across all densities, highlighting the lowest sum for each weight factors combination (part 1 — weight factor combinations 1–5).	113

TABLE A.16 Sum of the delays in seconds to inform the last vehicle on the San Francisco scenario across all densities, highlighting the lowest sum for each weight factors combination (part 2 — weight factor combinations 6–10). 114

LIST OF FIGURES

FIGURE 3.1	VANET considered as the scenario in this chapter.	22
FIGURE 3.2	Percentage of informed vehicles on the San Francisco (graphs on the left) and on the Valencia (graphs on the right) scenarios . . .	30
FIGURE 3.3	Number of messages received per vehicle in the San Francisco and in the Valencia scenarios	31
FIGURE 4.1	VANET considered as the scenario in this work.	41
FIGURE 4.2	Percentage of informed vehicles over time for the Valencia scenario with different number of vehicles in the VANET for all proposed methods and benchmarks	49
FIGURE 4.3	Delay for informing the last vehicle for all proposed methods and benchmarks	50
FIGURE 4.4	Percentage of informed vehicles over time for the San Francisco scenario with different number of vehicles in the VANET for all proposed methods and benchmarks	51
FIGURE 4.5	Delay for informing the last vehicle for all proposed methods and benchmarks	51
FIGURE 5.1	Percentage of informed vehicles over time for the Valencia scenario with different number of vehicles in the VANET for all proposed methods and benchmarks	66
FIGURE 5.2	Delay for informing the last vehicle for all proposed methods and benchmarks for the Valencia scenario	66
FIGURE 5.3	Percentage of informed vehicles over time for the San Francisco scenario with different number of vehicles in the VANET for all proposed methods and benchmarks	67
FIGURE 5.4	Delay for informing the last vehicle for all proposed methods and benchmarks for the San Francisco scenario	67
FIGURE A.1	Percentage of informed vehicles crossing car densities for the Valencia scenario with different weight factor combinations in the VANET for all proposed methods and benchmarks (part 1 — weight factor combinations 1–5).	92
FIGURE A.2	Percentage of informed vehicles crossing car densities for the Valencia scenario with different weight-factor combinations in the VANET for all proposed methods and benchmarks (part 2 — weight factor combinations 6–10)..	93
FIGURE A.3	Delays to inform the last vehicle crossing car densities for the Valencia scenario with different weight-factor combinations in the VANET for all proposed methods and benchmarks (part 1 — weight factor combinations 1–5).	96

FIGURE A.4	Delays to inform the last vehicle crossing car densities for the Valencia scenario with different weight-factor combinations in the VANET for all proposed methods and benchmarks (part 2 — weight factor combinations 6–10).	97
FIGURE A.5	Percentage of informed vehicles crossing car densities for the San Francisco scenario with different weight-factor combinations in the VANET for all proposed methods and benchmarks (part 1 — weight factor combinations 1–5).	105
FIGURE A.6	Percentage of informed vehicles crossing car densities for the San Francisco scenario with different weight-factor combinations in the VANET for all proposed methods and benchmarks (part 2 — weight factor combinations 6–10).	106
FIGURE A.7	Delays to inform the last vehicle crossing car densities for the San Francisco scenario with different weight-factor combinations in the VANET for all proposed methods and benchmarks (part 1 — weight factor combinations 1–5).	115
FIGURE A.8	Delays to inform the last vehicle crossing car densities for the San Francisco scenario with different weight-factor combinations in the VANET for all proposed methods and benchmarks (part 2 — weight factor combinations 6–10).	116

LIST OF ACRONYMS

TABLE 1: List of acronyms used in the thesis (part 1)

Acronym	Term
2f_E2F2C	2-Factor Event Node to Forwarder to Cluster
2f_EN2IwF	2-Factor Event Node to Infrastructure with Forwarder
2f_HM	2-Factor Hierarchic Model
2f_HMwF	2-Factor Hierarchic Model with Forwarder
2F-CM	2-Factor Cluster Merging
3f_E2F2C	3-Factor Event Node to Forwarder to Cluster
3f_EN2IwF	3-Factor Event Node to Infrastructure with Forwarder
3f_HM	3-Factor Hierarchic Model
3f_HMwF	3-Factor Hierarchic Model with Forwarder
3F-CM	3-Factor Cluster Merging
4G	4th Generation Mobile Network
5G	5th Generation Mobile Network
AC	Additional Coverage
APAL	Adaptive Probability Alert Protocol
ARQ	Automatic Repeat Request
BS	Base Station
BSM	Basic Safety Message
CE	Cluster Member
CF	Cluster Forwarder
CM	Cluster Master
CMC	Cluster Master Candidate
CSMA/CA	Carrier Sense Multiple Access/Collision Avoidance
DENM	Decentralized Environment Notification Message
DSRC	Dedicated Short-Range Communication
E2F2C	Event Node to Forwarder to Cluster
eMDR	Enhanced Message Dissemination for Roadmaps
EN2IwF	Event Node to Infrastructure with Forwarder
ERGS	Experimental Route Guidance System

TABLE 2: List of acronyms used in the thesis (part 2)

Acronym	Term
eSBR	Enhanced Street Broadcast Reduction
EWM	Emergency Warning Messages
FCC	Federal Communications Commission
FEC	Forward Error Correction
GPS	Global Positioning System
HM	Hierarchic Model
HMwF	Hierarchic Model with Forwarder
ITS	Intelligent Transportation System
LoS	Line-of-Sight
LTE	Long-Term Evolution
MAC	Medium Access Control
MANET	Mobile Ad Hoc Network
NJL	Nearest Junction Located
OBU	On-Board Unit
OMNeT++	Objective Modular Network Testbed in C++
OSM	Open Street Map
RSS	Received Signal Strength
RSU	RoadSide Unit
SNR	Signal-to-Noise Ratio
SRB	Selective Reliable Broadcast
SUMO	Simulation of Urban Mobility
TLO	The Last One
UMTS	Universal Mobile Telecommunications System
V2I	Vehicle-to-Infrastructure
V2V	Vehicle-to-Vehicle
V2X	Vehicle-to-Everything
VANET	Vehicular Ad Hoc Network
WF	Weight Factor

CHAPTER 1

INTRODUCTION

The world has witnessed drastic growth in the volume of vehicles. As a result, road traffic and accidents increase dramatically causing injuries and deaths. Thus, the need for driver assistance systems such as a communication portal becomes necessary. Conventional VANETs encounter numerous technical drawbacks in their applications and management due to low flexibility, low scalability, poor connectivity, and insufficient intelligence (Shrestha *et al.*, 2018).

Reliability is considered to be a major concern in VANETs. Generally, VANETs are expected to enable the transfer of information between automobiles or between vehicles and sensors installed along highways and, therefore, enhance the performance of an ITS, as well as the safety of drivers and passengers. The process of transmitting information, such as traffic data, highway conditions, and other related data, often uses multi-hop communications. Nevertheless, only transmitting traffic information does not guarantee improved highway safety (Kounga *et al.*, 2009). The exchanged information is also required to be reliable. In this study, a reliable safety message refers to any warning information or alert that must often represent the situation that can be seen by a driver at the exact position it happened. Therefore, unreliable information is not a reflection of the real condition or event.

1.1 THE BROAD PROBLEM IN VANETS

Some broad problems in VANETs include time sensitivity of safety messages, broadcast storms, and signal attenuation. With the advent of new technologies and the drastic rise in the volume of smart automobiles, conventional VANETs experience numerous technical problems in deployment and management due to limited flexibility, weak connectivity, low scalability, and insufficient intelligence (Shrestha *et al.*, 2018).

The main problem VANETs message dissemination faces is the broadcast storm. A broadcast storm, as exhibited in most urban centers, is a condition in which a

network system is completely overwhelmed by excessive multicast traffic. The condition consists of numerous broadcasts that consume all the bandwidth within the network traffic and thereby prevents more devices from communicating effectively, at the same time degrading the performance of the entire network system. In modern research the broadcast storm has been found to cause more unwanted responses from temporary hosts created by the network, which alternatively create what is known as the snowball effect. In more populated and network jammed areas like urban centers, the severity of the condition can cause complete blockage of the entire VANETs network system (Huang and Chiu, 2013).

Clustering is practically possible, leading to the introduction of Cluster Masters (CMs), with specific vehicles chosen as Cluster Forwarders (CFs). The process requires resourceful and effective algorithms. Broadcast storms have been predicted to cause VANETs meltdown if the message dissemination delays are not solved properly, considering the fact that there are still unreliable dissemination approaches in the dedicated short-range communication DSRC broadcast interface models (Huang and Chiu, 2013).

1.2 THE SPECIFIC PROBLEMS THAT ADD TO THE BROADER PROBLEM

The specific problems caused by the broadcast problem are mainly message delays and a network overwhelmed traffic. Developing a proper message transmission system, relying on fast and reliable network systems is the objective of VANETs, in a bid to solve the dissemination delays. Presumably, the dissemination delay may potentially lead to unwanted situations for example accidents on roads (Feukeu and Zuva, 2020). The increase in the number of vehicles online have always consistently led to subsequent increase in road accidents. In the current transportation system, drivers do communicate using various methods, like the rear lights, high beams, and horns. VANETs are projecting a future in which the vehicles are supposed to communicate among themselves and intelligently act properly to prevent accidents

(Huang and Chiu, 2013). The main objective is to increase safety and reliability with the communication channels effectively.

The question of reliability and dependability of the ITSs of the future is embedded in the complete resilience of network communication efficiency. A quick message dissemination system enhances safety and complete efficiency of the network system (AlQahtani *et al.*, 2021). Multiple applications that require stable communication are the applications that support Internet driving, inter-vehicle communication, Internet access on the vehicles, and significantly safer driving — which requires dense warning messages dissemination. The timely and reliable delivery of these messages depends on the solutions provided to combat the ostensibly imminent broadcast storm condition. Efficient solutions for the network message delays requires solving the broadcast storm fast. However, it is imperative to understand that the objective is an algorithmic solution supported by faster and reliable networks (such as 5G and LTE) as well as cost reduction on implementation strategies.

1.3 THE CURRENT LITERATURE PROPOSALS AND WEAKNESSES

The solution to broadcast storms and subsequent message dissemination delay is to include the vehicle-to-infrastructure (V2I) communication (Tseng *et al.*, 2002). The model relies on the availability of the vehicular ad hoc network (VANET) infrastructure system to enhance communication and ensure safety of the broadcast messages (Martinez *et al.*, 2010). Based on this option, the ITS targets implementing LTE and early 5G network technology into improving the communication process. The 5G infrastructure is very reliable in terms of speed and data security. However, there are a few problems that this technique faces (Feukeu and Zuva, 2020). The cellular network works best, according to the tested VANET vehicles, close to the base stations and as such broadcasting to every vehicle will lead to more wasted messages since vehicles far away from the target will also receive the warning messages targeting specific areas only (Tseng *et al.*, 2002). This formal broadcasting technique increases communication latency further.

The other option proposed by the literature are the vehicle-to-vehicle (V2V) communication models with algorithmic solutions. In this model, there are different cluster techniques, where the vehicles are organized into clusters that act as 'nodes' (Feukeu and Zuva, 2020). Clustering increases the efficiency of message dissemination but with dense areas it will cause flooding due to the increase of the number of forwarding messages (Sanguesa *et al.*, 2013). Specifically, different algorithmic approaches have been designed to help with the broadcast storm problem. However, these methods are also limited by the network density, distance, and communication latency. Applying V2V technologies to disseminate warning messages even with algorithmic solutions to avoid broadcast storms, might not warn nearby vehicles due to the presence of obstacles that interfere with the signaling. Therefore, relying on hybrid communication with cluster forwarders to avoid signal blockage might guarantee all needed vehicles will be informed of a nearby accident.

1.4 OUR CONTRIBUTION

This study proposes a model in which 5G and CFs are integrated, effectively and accurately implementing the message dissemination. The model will significantly reduce broadcast flooding and signal attenuation effectively. Moreover, the model is not subject to the impacts of network latency. The algorithmic concept takes into account integrating the DSRC technologies within the ITS infrastructure. Specifically, the model targets implementing a concrete cluster merging algorithm within the 5G network including the support of cluster forwarders for getting around obstacles.

The 5G network provides advanced communication support ranges with low latency. The clustering will leverage the best features of V2I technologies (specifically 5G network) to provide better coverage (AlQahtani *et al.*, 2021). The hybrid V2V communication strategy is integrated with V2I setup aims at providing a reliable and dependable infrastructure through which the vehicles can communicate effectively, with extremely reduced message delays, increased availability of connectivity, and a subsequently reduced signal latency. GPS modules are required on vehicles, though.

Deploying the cluster merging and cluster forwarding techniques with V2I support increases the efficiency of the messaging process — only when the cluster masters are as few as possible. The algorithm should be able to select as few nodes as possible to be cluster forwarders and cluster masters. The substantial number of messages wasted on broadcast and multicast are highly reduced, which increases the network viability further and proves the effectiveness of the integration.

The other major solvable challenge with this technique is the DSRC directive communication that will be easily blocked by obstacles. The 5G network and cluster forwarders provide multiple alternatives to solve the obstacles problem. This would further provide for more robust communication around obstacles.

1.5 PROBLEM STATEMENT

In most cases, VANETs are required to relay crucial road details, such as accident reports rapidly and consistently. However, it is still a major problem to transmit critical details timely and reliably to a specific point under the current challenges. The delay of crucial information is attributed to medium access control (MAC) contention, which is considered to be unsuitable in VANETs (Shrestha *et al.*, 2018). The inability to distribute vital information timely and accurately can affect road safety especially since VANETs require periodic extensive and massive data. Nevertheless, communication technologies, such as DSRC, are unable to underpin ITSs fully in a setting with excessive loads, increased coverage, and highly active network. To gather and analyze massive sets of real-time traffic data, vehicles have to be connected through different communication channels and organized by clustering techniques.

One of the most basic methods to send safety messages is broadcasting. It is considered a major function in a network that resolves several issues. In a VANET, due to host mobility, operations are anticipated to be performed more regularly, such as finding a route to a certain car or disseminating an alert signal. In the process, radio signals can easily overlap in a specific geographical location, leading to redundancy and collision, which is commonly known as the broadcast storm problem. This

study seeks to identify clusters merging and forwarder schemes that can help reduce broadcast storm problems and signal attenuation in VANETs.

1.6 RESEARCH MOTIVATION AND CONTRIBUTIONS

VANETs have played a critical role in promoting sustainable urban transportation systems and highways. However, latency and coverage of informed vehicles are crucial when it comes to sensitive safety applications. Thus, a minor fault could have detrimental impacts that affect the time of receiving alert messages. Another major issue that impedes the adoption of VANET is lack of flexibility and reliability. Thus, this thesis examines how clusters merging and forwarder schemes can improve flexibility and reliability in VANETs.

1.7 DOCUMENT ORGANIZATION

In Chapter 2, concepts and technologies used on VANETs are presented, as well as the theory of VANETs themselves. On top of that, work related to the presented items and related to the contributions of this thesis are enumerated.

Chapter 3 drives the discussion towards clustering in VANETs, commenting on the latest clustering proposals. Moreover, a new cluster merging scheme is devised considering the combination of V2V and V2I, and its performance — in terms of percentage of vehicles informed on the network and number of messages received by vehicles — is compared to other clustering schemes via simulation. The inputs and outputs of the simulations are provided in the chapter.

In Chapter 4, several communication chains considering a 5G base station, cluster masters, cluster members, and introducing cluster-forwarder vehicles are defined and simulated. Then, they are combined with the cluster merging scheme, presented in Chapter 3, and the percentage of informed vehicles and the delays to inform the last vehicle are compared throughout the defined chains and previous proposals. The inputs and outputs of the simulations are provided in the chapter.

In Chapter 5, a new factor is introduced to the cluster merging scheme, influencing the cluster master election towards the selection of a node closer to the base station compared to the previous version of the scheme. Again, the communication chains created on Chapter 4 are simulated for both versions of the scheme on the same performance metrics investigated before. The inputs and outputs of the simulations are provided in the chapter.

In Chapter 6, several combinations of the factors used for cluster master election on the merging scheme are studied via simulation, as opposed to their equal weights assumed in Chapter 5. Once more, the percentage of informed vehicles and the delays to inform the last vehicle are used for the identification of both the factors importance on the merging scheme and the communication chain that achieves the highest performance. The simulation inputs are provided in the chapter, but only the processed results are given in the chapter due to their size. The remainder of the outputs are shown in Chapter A.

The conclusions of the thesis are drawn in Chapter 7 and some support data are shown on the Appendices. Appendix A brings support data to improve the understanding of the results presented in Chapter 6 and Appendix B shows the implementation of both the two-factor and the three-factor cluster merging schemes on the used OMNeT++ simulator environment.

CHAPTER 2

BACKGROUND AND RELATED WORK

Before going deeper, we need to know the background and corresponding works. Each of the subsections is organized to provide a detailed background along with its related work, whereas the final subsection presents work related to all contributions throughout this thesis.

2.1 VANETS

2.1.1 *What are VANETs?*

VANETs are vehicular ad-hoc networks, a class of mobile ad-hoc networks (MANETs) featuring high node mobilities and frequent topology changes (Chiti *et al.*, 2019). Their aim for creating an intelligent transport system (ITS) is to achieve safer, more secure, and more convenient driving experiences (Zhou *et al.*, 2017).

2.1.2 *Requirements of VANETs*

In order to save some of the almost 40 thousand lives that are lost on road accidents every year in the U.S. and to avoid the waste of almost US\$200 billion in traffic congestion, high reliability and low latency are required from new solutions to make the best use of available resources in VANETs (Ullah *et al.*, 2019).

Since broadcast storms are proportionally more severe with the number of vehicles in an area, it is paramount for VANET applications to be able to scale well. Proposals that are only considered for safety applications in low-density areas are likely to fail when operating in more realistic scenarios (Gao and Peh, 2014).

Moreover, messages exchanged for safety applications are usually urgent and life-critical. Some malicious actor could modify or insert false or repeated messages into the VANET, which would certainly reduce the efficacy of the solutions. Therefore, security also becomes an important aspect for VANETs. Similarly, such a malicious actor could overhear messages and extract network users' information for its own

purposes. Thus, not only security, but also privacy is of concern in VANETs (Al-Ani *et al.*, 2018).

2.1.3 Types of VANET Communication

There are three main types of communication in a VANET:

- **Vehicle-to-Vehicle (V2V):** Vehicles communicate with each other to establish a network (Nshimiyimana *et al.*, 2017). Commonly uses DSRC (IEEE 802.11p) technology.
- **Vehicle-to-Infrastructure (V2I):** Vehicles communicate with existing telecommunication infrastructure (Feukeu and Zuva, 2020), such as cellular networks, Wi-Fi access points, and roadside units (RSUs) (Xu *et al.*, 2017).
- **Vehicle-to-Everything (V2X):** Vehicles communicate with anything that has a wireless interface, such as Internet clouds, pedestrians (via smartphones or other devices), and bicyclists (Auer *et al.*, 2016).

2.2 WARNING MESSAGES DISSEMINATION

2.2.1 What are the Benefits of Connected Vehicles?

VANETs enable a series of applications for vehicles and its users. Road-safety applications can be supported by the dissemination of warning messages (Martinez *et al.*, 2010), and some specific ones are (Al-ani, 2018): lane change warnings, forward collision warnings, head-on collision warnings, intersection collision warnings, and emergency vehicle warnings.

Other facilities that can be provided are inter-vehicles communication, file sharing, and real-time traffic information, which enables route planning and traffic congestion control (Martinez *et al.*, 2010).

Thus, one can infer that vehicle users are not only able to experience more comfort with applications such as file sharing and inter-vehicle communication, but also save time and money via route planning and traffic congestion control, and even reduce risks when on the road through the safety applications.

2.2.2 *Safety Messages*

Safety messages are disseminated via broadcasting and they can be either periodic or event-driven. Basic Safety Messages (BSMs), also known as beacons, are periodical vehicle status messages, including information such as current time, position, speed, direction, and vehicle size (Liu and Jaekel, 2019). Decentralized Environment Notification Messages (DENM) are event-driven messages, periodically sent in the vicinity of the event with a given periodicity until the expiry of the event (Ansari *et al.*, 2020).

2.2.3 *DSRC*

DSRC stands for dedicated short-range communication. It is a wireless technology used for vehicular communication, both among vehicles and between vehicles and Roadside Units (RSU) to communicate with the infrastructure network. It is subject to different standards in North America, Europe, and Japan, which leads to incompatibility problems between those regions (Abboud *et al.*, 2016a).

This technology is widely used on VANETs and ITS applications. However, DSRC presents poor performance both in low and high density scenarios. The former happens because of the small coverage of Internet gateways. Since it leads to short connectivity periods between vehicles and such gateways, multihop communication is a possible solution to extend coverage. However, in low density scenarios, the probability of having a path between the vehicle requesting Internet access and the gateway is low. In addition, the frequent topology changes due to the vehicles movement reduce even more the connectivity probability. The latter scenarios present performance issues due to the access to the communication medium. Carrier Sense Multiple Access (CSMA)/Collision Avoidance (CA) is the DSRC protocol for medium access. When many vehicles try to access the medium, collisions happen and the delay to successfully access the medium increases. The same problem with collisions affects broadcasting, which is used by security applications on VANETs (Abboud *et al.*, 2016a).

2.2.4 RSU

The ITS aims at improving the safety and efficiency of transportation systems, namely avoiding collisions between vehicles and reducing road traffic. That is achieved both by enabling communication between vehicles and between vehicles and infrastructure. The latter is possible via the roadside units (RSUs) (Auer *et al.*, 2016).

In VANETs, as previously mentioned, V2V is used to exchange messages between nearby vehicles in short-range communications. Communication ranges can be extended through the use of the multi-hop technique, however delays start increasing as the messages are forwarded through more vehicles. Therefore, another method is required for long-range communication. Using the infrastructure for relaying messages over longer distances is one reliable option. For that, RSUs are used as an interface between vehicles and the infrastructure network (Paranjothi *et al.*, 2019).

The first RSUs appeared as a result of the Experimental Route Guidance System (ERGS) project in the late 1960s. Several prototype RSUs were deployed at intersections, working as a proof of the concept. However, the infrastructure network at the time was expensive, which led to the termination of the project (Auer *et al.*, 2016).

Another missing part at the time was a suitable interface between vehicles and RSUs. In 1999, the Federal Communications Commission (FCC) allocated the 5.850 to 5.825 GHz range to dedicated short-range communications (DSRC). The technology that leveraged the new frequency range suited both V2I and V2V communication, providing means to improve traveler safety and to reduce traffic congestion. However, the first RSU equipment units were produced and tested only in 2008, in an effort that proved that V2V and V2I applications were viable.

One example of recent improvements proposed for RSUs can be seen in (Chiti *et al.*, 2019). In this work, RSUs coordinate groups of vehicles for data gathering. Then, the RSU aggregates the data and sends them to centralized servers, where decisions about the traffic flow are made and transmitted back to the vehicles.

2.3 RELATED WORK

This work aims at preventing broadcast storms on VANETs. The solutions presented in the literature, some of which are presented in this section, tackle the problem in different manners. Clustering, or at least some level of coordination between the vehicles, has proven to provide enough control over broadcasts to prevent broadcast storms. The proposals that consider such coordination are also presented in this section, along with the analyzed performance metrics that allowed us to assess and compare our proposed solutions to the selected benchmarks.

Broadcast storms are especially harmful when disseminating *warning messages for road accident prevention*, which must be delivered on strict delay and reliability requirements to be effective. Therefore, communication problems that might hinder the dissemination capacity of VANETs must be carefully scrutinized. Since broadcast storms negatively impact message delivery to all participating vehicles, previous and current attempts to solve the problem and some improvement opportunities are shown here as a baseline.

This first related work shows how clustering can be used to limit broadcasts and the metrics that we considered from Chapter 4 on. Khan and Fan (2018) base their work on the limitations of VANETs operating on V2V only, broadcast storms being one of such limitations. The authors propose the use of 3 metrics — vehicles relative speeds, relative distances, and link lifetimes — to elect zonal heads (similar to CMs) for vehicles clustering. The objectives of the proposed Multi-hop Moving Zone clustering scheme are achieving high packet delivery and low latency. To achieve those, a combination of 5G and DSRC is used for vehicles communication. The presented results show the objectives have been accomplished for 100 vehicles in the VANET. However, more vehicles could make the approach more realistic and, also, 5G and DSRC interactions could affect delays, which seems to require additional study.

Tseng *et al.* (2002) show that by using flooding, many nodes will receive the same message multiple times, constant transmissions on the communication medium will hinder vehicles chances to transmit, and many simultaneous transmissions will cause packet losses. Such analysis give the authors the basis for new proposals to tackle redundancy, contention, and collisions, which they carry out using the 5 schemes

described next. The first is the probabilistic scheme, where nodes are given a probability p of re-broadcasting a message they received. Clearly, the use of this probability has a positive effect on the 3 aspects of broadcast storms by reducing the number of re-broadcasts. The second is a counter-based scheme, where a broadcast message is given a counter, incremented at each re-broadcast, which limits the number of times a single message is re-broadcast. This is even more effective than the probabilistic scheme on reducing the number of re-broadcasts. The third scheme is the distance-based scheme. Re-broadcasts only occur if the receiver of the message is farther than a minimum distance d from the transmitter. More effective coverage on re-broadcasts is achieved, improving on the counter-based scheme results. The fourth scheme is a location-based one, which enhances the previous scheme by calculating the additional coverage a node can provide by re-broadcasting. With more information — the location of previous transmitters — than considering just a minimal distance, even less re-broadcasts and more effective ones are performed. And, a clustering-based scheme is the fifth one proposed. On top of any of the previous schemes, clusters are formed and only CMs or gateway nodes, which communicate different clusters, are allowed to re-broadcast, limiting even further the amount of re-broadcasts without losing effectiveness. Some disadvantages are presented by the previous schemes, though. The probabilistic, counter-based, and distance-based ones work well on sparse networks only. The location-based scheme is computationally complex. And, the cluster-based scheme will carry over the disadvantage of the previous scheme adopted in combination. The idea of having nodes for communication coordination, such as the CM and gateway node, inspired the schemes presented throughout this thesis.

Sanguesa *et al.* (2013) consider four rebroadcast schemes before proposing their own — the counter-based scheme, the distance-based scheme, the enhanced Street Broadcast Reduction (eSBR), and the enhanced Message Dissemination for Roadmaps (eMDR). The counter- and distance-based ones were already discussed in the previous paragraph. The eSBR scheme only allows rebroadcasts if the transmitting and the re-transmitting vehicles are at least d_{min} apart from each other, if these vehicles are in different streets, or if they are sufficiently close to a junction (to avoid signal blockage

from buildings) (Martinez *et al.*, 2010). Finally, eMDR improves upon eSBR by limiting the rebroadcast to other streets to vehicles that are the closest to junctions. Both eSBR and eMDR perform well on sparse urban environments, but not on higher vehicles density situations. Hence, Sanguesa *et al.* (2013) proposed the Nearest Junction Located (NJL), which removes the requirement for a minimum separation between transmitting and re-transmitting vehicles, also limiting rebroadcasts to the vehicles that are the closest ones to junctions. By being more restrictive than previously proposed schemes, NJL aims at performing well on high vehicle density scenarios. Furthermore, by recognizing that there are schemes that better fit either higher or lower vehicle densities, Sanguesa *et al.* (2013) proposed an Optimal Broadcast Selection Algorithm. Such algorithm first simulates the percentage of informed vehicles for each of the five considered schemes. The ones that achieve the highest percentages go to the next step of the algorithm, where the number of messages produced is measured. Then, the scheme that generates less messages in the network, therefore reducing the chances of a broadcast storm, is considered optimal for the given vehicles density. The presented results show that NJL is selected in most cases for densities above 100 vehicles/ km^2 . The Optimal Broadcast Selection Algorithm inspired the first solution in Chapter 6, and the number of messages generated is one of the metrics considered in Chapter 3.

An important aspect to be considered by the simulation of VANETs is the signal attenuation between two communicating vehicles. Urquiza-Aguilar *et al.* (2015) present a study of several realistic models. The authors compare those realistic models to a simpler, less realistic one, where the communication between vehicles is successful only if they are in LoS. The results proved that several metrics such as packet loss and communication delay can be well approximated using the simpler model, which requires far less processing than the more realistic counterparts. Following the presented conclusion, this work also considers full blockage of DSRC signals when vehicles are in non-LoS. Moreover, to enable communication between vehicles in non-LoS, this thesis considers the use of a cellular network as an alternative available for vehicle communication. Because this case requires the use of an additional node within the communication chain, the BS, communications delays are expected, and assessing such influence is within the scope of the present study.

Xu *et al.* (2017) consider the 4G LTE as a possible technology to be used for both V2V and V2I communication. In their work, they highlight that simulations can lead to conclusions that are not aligned to the technology operation in practice. Therefore, they propose a test-bed through which they can test the performance of both LTE and DSRC communications under different delay requirements. In their work, Xu *et al.* mapped delays for different safety applications. According to the authors, pre-crash sensing, which is the application considered in this paper, has a latency requirement of 20ms. However, the results presented by Xu *et al.* show that the LTE RTT is at least 300ms. Thus, this technology cannot be used as support for the collision avoidance scenario studied in our work.

A logical step is to consider 5G as the infrastructure technology used to support V2X communication. According to Ullah *et al.* (2019), 5G for V2I communication will achieve latencies comparable to DSRC (about 10ms), while outperforming both DSRC and LTE on other aspects of V2X communication. Therefore, this work endeavors to validate the use of DSRC and 5G together so as to enable vehicle collision avoidance in urban scenarios.

Lastly, as discussed above, since some of the technologies considered rely on highly directive radio communication, such as DSRC and the possibility of millimeter waves for 5G (Ullah *et al.*, 2019), communication blockage by obstacles must be considered, especially in urban scenarios. Mezher *et al.* (2014) present a simulator capable of determining which vehicles can communicate with each other. Thus, 5G brings the flexibility of using several different access methods and frequency bands to avoid the lack of connectivity among vehicles (Zhou *et al.*, 2017). This is another case that supports the use of 5G as the network infrastructure needed to support DSRC communication, which is accounted for here in our analyses.

CHAPTER 3

CLUSTERING IN VANETS¹

As previously presented on Chapter 2, VANETs are vehicular networks that aim at providing communication between vehicles. For safety applications, as the ones envisioned by ITS, the messages exchanged between vehicles carry data for the calculation of each vehicle's next steps on the roads to prevent accidents. Given the importance of such information, messages need to be delivered with low latencies and high reliability. And, in order to provide communication with such characteristics, the first adopted approach was flooding. However, the uncontrolled re-broadcasting of this an approach might render the communication medium unusable due to constant packet collisions — an effect known as broadcast storm. One of the available techniques for preventing the problem is clustering. By electing cluster masters (CMs), which will be responsible for the communication with a subset of vehicles, it is possible to schedule transmissions within an area, avoiding the aforementioned storms. The price of the technique is the need for communication between CMs to perform inter-cluster communication, which delays the delivery of warning messages. This effect can be worsened if the number of clusters is large. Since the dissemination of warning messages has time constraints, it becomes necessary to study the impact of solving broadcast storms on the dissemination latency. In this chapter, a cluster merging algorithm, the 2-Factor Cluster Merging (2F-CM), is proposed to control the number of clusters and its effectiveness is measured on a roadside scenario.

3.1 INTRODUCTION

ITS is designed for traffic management, including safety applications, relying on VANETs for its implementation, as mentioned in Chapter 2. In turn, VANETs are self-organizing networks like MANETs; however, they are comprised of nodes with higher mobility (Chiti *et al.*, 2019), causing a greater rate of connections and disconnections in the network (Sattar *et al.*, 2018).

¹The content of this chapter is based on our publication (AlQahtani *et al.*, 2021).

Even though no infrastructure is required for vehicles to reach each other, communication with other networks, such as the Internet, might be required. This defines two types of communication within VANETs — V2V and V2I (Ravi; *et al.*, 2018) —, which are achieved via the OBUs in vehicles and RSUs along roads (Sospeter *et al.*, 2019). These assets enable VANETs to fulfill the requirements of safety applications (More and Naik, 2018), which aim at keeping the occupants of vehicles safe (Wang *et al.*, 2019). However, the frequent changes of topology and network fragmentation in VANETs impair the reliability of message dissemination (Zhang *et al.*, 2019). To counter the reliability issue, flooding can be used for safety message dissemination, but it can give rise to broadcast storms depending on the network vehicles' density. Thus, to tackle both reliability issues due to network fragmentation and broadcast storms, a Cluster Merging Scheme is proposed and presented in this chapter. The Scheme is simulated in OMNeT++ to prove it can reduce the number of messages received by the vehicles, thus preventing broadcast storms, without reducing the percentage of informed vehicles.

The remainder of the chapter is organized as follows. In Section 3.2, technologies that are used for message dissemination are presented as background for the chapter. Section 3.3 discusses work related to the proposal of this chapter, which is presented in Section 3.4. Then, simulation parameters and results are shown and discussed in Section 3.5. Last, Section 3.6 brings the conclusions of this chapter.

3.2 BACKGROUND

Around the world, car crashes are one of the main causes of life losses (Khaliq *et al.*, 2017). Creating means for warning nearby vehicles of car crashes is exactly one of the objectives of ITS, and VANETs are the type of network that provides such means. Nonetheless, there are still dissemination challenges in VANETs, especially concerning vehicle speeds, network topologies and fragmentation, and random selection of messages (Khan and Fan, 2018). Even though flooding is a robust way to deal with these VANETs challenges (Galaviz-Mosqueda *et al.*, 2017), the technique might cause broadcast storms, which can greatly impair vehicles communication. To tackle

these storms, one of the proposed solutions in the literature is vehicles clustering, which reduces the scope of broadcasts, therefore mitigating the problem. Clustering works by first electing a CM common to the clusters being merged (Benkerdagh and Duvallet, 2019), which handles intra- and intercluster communication.

5G technology is considered for intercluster communication and 5G base stations are responsible for coordinating CMs election. 5G is an interesting choice for supporting VANETs since vehicular scenarios are foreseen from the technology conception and because 5G will soon become the standard for mobile communication (Gupta *et al.*, 2015). Therefore, 5G BSs are considered as RSUs in this work.

For intracluster communication, the well-known DSRC technology is contemplated (Ucar *et al.*, 2016). The combination of 5G and DSRC for messages dissemination in VANETs will definitely differ from the metrics on a DSRC-only scenario, which is commonly considered, at least regarding communication delays. Thus, it is important to merge clusters to keep intercluster communication delays under control, especially because latency is a critical metric for warning messages.

3.3 RELATED WORK

The objectives of this work are to analyze the dissemination of warning messages and to propose a cluster merging scheme to tackle some of the problems that arise with this type of communication in VANETs. Thus, this section discusses work related to the reliability and strategies for message dissemination, also summarizing some research that addresses broadcast storms.

The improvement of the reliability of warning message dissemination can be undertaken in several phases. Benkerdagh and Duvallet (2019) leveraged this division in phases to propose a solution for VANETs. Warning data is first formatted for a more efficient transmission. Clusters are formed in the second phase to maximize stability. And, last, a routing algorithm controls the dissemination of the message towards relevant vehicles. According to the results presented in (Benkerdagh and Duvallet, 2019), clusters last longer using the proposed solution than with other ones and the proposed solutions is also capable of providing a reliable path for warning

messages. However, the complexity of the solution is high when compared to others in the literature.

In (Shaik *et al.*, 2018), Shaik *et al.* propose an enhancement to a cross-layer routing mechanism. The objective was to elect a relay node that would be able to disseminate safety messages with reduced delays. Even though results show successful dissemination with reduced delays, fewer neighbors ended up being warned of a nearby emergency.

By changing the roles of vehicles close to intersections, the work in (Zhao *et al.*, 2019) proposes a mechanism to improve the reliability of Emergency Warning Messages (EWMs) dissemination. Vehicles can transition to one of five predefined roles — trigger vehicle, following vehicle, adjacent vehicle, normal vehicle or leading vehicle. According to the presented results, the control of the role transitions ensure broadcast consistency, which is proven via decreased delays, decreased redundancy, and increased delivery rates of EWMs.

Khan and Fan (2018) base their work on the limitations of VANETs operating on V2V only, broadcast storms being one of such limitations. The authors propose the use of 3 metrics — vehicles relative speeds, relative distances, and link lifetimes — to elect zonal heads (similar to CMs) for vehicles clustering. The objectives of the proposed Multi-hop Moving Zone clustering scheme are achieving high packet delivery and low latency. To achieve those, a combination of 5G and DSRC is used for vehicles communication. The presented results show the objectives have been accomplished for 100 vehicles in the VANET. However, more vehicles could make the approach more realistic and, also, 5G and DSRC interactions could affect delays, which seems to require additional study.

Tseng *et al.* (2002) break broadcast storms into three aspects — redundancy, contention, and collisions. Through flooding, many nodes will receive the same message multiple times, constant transmissions on the communication medium will hinder vehicles' chances to transmit, and many simultaneous transmissions will cause packet losses, respectively. Such analysis gives the authors the basis for new proposals to tackle the three mentioned problems, which they carry out via 5 schemes described next. The first is the probabilistic scheme, where nodes are given a probability p of

re-broadcasting a message they received. Clearly, the use of this probability has a positive effect on the three aspects of broadcast storms by reducing the number of re-broadcasts. The second is a counter-based scheme, where a broadcast message is given a counter, incremented at each re-broadcast, which limits the number of times a single message is re-broadcast. This is even more effective than the probabilistic scheme on reducing the number of re-broadcasts. The third scheme is the distance-based scheme. Re-broadcasts only occur if the receiver of the message is farther than a minimum distance d from the transmitter. More effective coverage on re-broadcasts is achieved, improving on the counter-based scheme results. The fourth scheme is a location-based one, which enhances the previous scheme by calculating the additional coverage a node can provide by re-broadcasting. With more information — the location of previous transmitters — than considering just a minimal distance, even less re-broadcasts and more effective ones are performed. And, a clustering-based scheme is the fifth one proposed. On top of any of the previous schemes, clusters are formed and only CMs or gateway nodes, which communicate different clusters, are allowed to re-broadcast, limiting even further the amount of re-broadcasts without losing effectiveness. Some disadvantages are presented by the previous schemes, though. The probabilistic, counter-based, and distance-based ones work well on sparse networks only. The location-based scheme is computationally complex. And, the cluster-based scheme will carry over the disadvantage of the previous scheme adopted in combination. However, the idea of having nodes for communication coordination, such as the CM and gateway node, also inspired the proposal presented in this chapter.

Sanguesa *et al.* (2013) consider four rebroadcast schemes before proposing their own — the counter-based scheme, the distance-based scheme, the enhanced Street Broadcast Reduction (eSBR), and the enhanced Message Dissemination for Roadmaps (eMDR). The counter- and distance-based ones were already discussed in the previous paragraph. The eSBR scheme only allows rebroadcasts if the transmitting and the retransmitting vehicles are at least d_{min} apart from each other, if these vehicles are in different streets, or if they are sufficiently close to a junction (to avoid signal blockage from buildings) (Martinez *et al.*, 2010). Finally, eMDR improves upon eSBR by limiting

the rebroadcast to other streets to vehicles that are the closest to junctions. Both eSBR and eMDR perform well on sparse urban environments, but not on higher vehicles density situations. Hence, Sanguesa *et al.* (2013) proposed the Nearest Junction Located (NJL), which removes the requirement for a minimum separation between transmitting and retransmitting vehicles, also limiting rebroadcasts to the vehicles that are the closest ones to junctions. By being more restrictive than previously proposed schemes, NJL aims at performing well on high vehicle density scenarios. Furthermore, by recognizing that there are schemes that better fit either higher or lower vehicle densities, Sanguesa *et al.* (2013) proposed an Optimal Broadcast Selection Algorithm. Such an algorithm first simulates the percentage of informed vehicles for each of the five considered schemes. The ones that achieve the highest percentages go to the next step of the algorithm, where the number of messages produced is measured. Then, the scheme that generates fewer messages in the network, therefore reducing the chances of a broadcast storm, is considered optimal for the given vehicles density. The presented results show that NJL is selected in most cases for densities above 100 vehicles/ km^2 .

3.4 CLUSTER MERGING SCHEME FOR RELIABLE MESSAGE DISSEMINATION

3.4.1 *System Model*

Assume vehicle traffic in one direction on a highway, as shown in Figure 3.1. All vehicles are equipped to communicate with each other via DSRC and with a BS via 5G. Blue circles in Figure 3.1 represent vehicle clusters, which have their communication coordinated by a CM (white vehicle), not necessarily located at the center of the cluster. Only CMs are allowed to communicate with the BS and inter-cluster communication must go through the clusters' CMs.

Even though communication coordination provided by clustering already reduces the broadcast storm problem, clusters fragmentation or very high vehicle densities might still make the VANET prone to broadcast storms. Therefore, the proposed

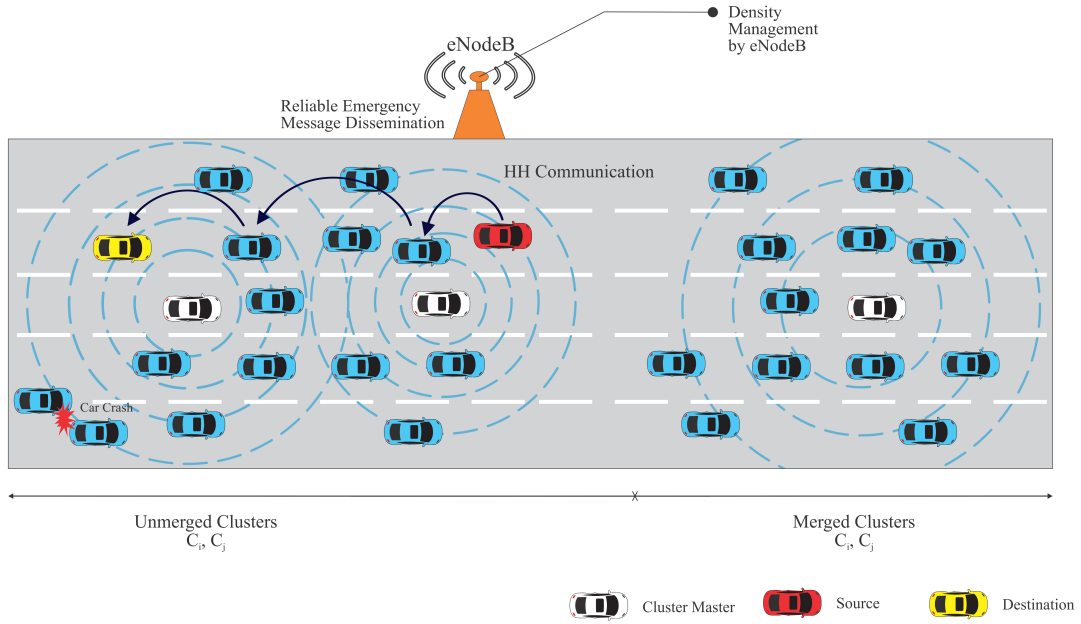


FIGURE 3.1: VANET considered as the scenario in this chapter

cluster merging aims to mitigate the problem by gathering more vehicles under the coordination of a single CM.

In the following subsections, the 2-Factor Cluster Merging (2F-CM) algorithm is proposed to further handle broadcast storms by reducing the number of clusters in VANETs.

3.4.2 Cluster Merging Algorithm Setup

Let a cluster C_i be a set of vehicles that establish the i^{th} cluster in the form $C_i = \{v_{i,1}, v_{i,2}, \dots, v_{i,|C_i|}\}$, where $|C_i|$ is the cardinality of the i^{th} cluster set. Consider a previous cluster formation procedure (not described in this work) elected $v_{i,k}$, with $1 \leq k \leq |C_i|$, the CM of the i^{th} cluster. All the other vehicles in the set, *i.e.*, $C_i \setminus v_{i,k}$, received the status of cluster member (CE). Let $v_{i,k}$, the CM, be in communication range with a BS using 5G and, as discussed before, CEs communicate with the CM via DSRC.

3.4.3 Cluster Handoff

Cluster handoffs from one BS to another are briefly presented here for the sake of completion — this case is out of the scope of this work, however handoffs will occur as vehicles travel on highways.

Along the course of a highway, at some point, a cluster will move away from the BS it is connected to, towards a new BS, considering there is 5G coverage along the entire highway. Eventually, the CM will be able to communicate with both the new and the old BS and, sensing a declining signal level from the currently connected BS, the CM starts the handoff procedure by sending a message to the new BS. Such message informs which vehicle is the CM and which ones are members of the cluster. After the BS acknowledges the information to the CM, such vehicle sends a disconnection message to the old BS, completing the handoff.

3.4.4 Cluster Merge Procedure

Let $v_{i,k}$ and $v_{j,l}$ be the CMs of adjacent clusters \mathcal{C}_i and \mathcal{C}_j , respectively, connected to the same BS.

MERGE REQUEST — Considering $v_{i,k}$ and $v_{j,l}$ came to be within DSRC communication range of each other, they send a cluster merge request message, T_{MR} , with the IDs of the vehicles in each cluster to the BS. If the number of vehicles in the future merged cluster is less than or equal to a given threshold, *i.e.*, $|\mathcal{C}_i \cup \mathcal{C}_j| \leq C^{thr}$, being C^{thr} such threshold, the BS starts the merge. Internally, the BS creates the new cluster set of vehicles, $\mathcal{C}_m = \mathcal{C}_i \cup \mathcal{C}_j = \{v_1, v_2, \dots, v_p\}$, with $p = |\mathcal{C}_i \cup \mathcal{C}_j|$.

MERGER — To start the merge procedure, the BS sends a cluster merge begin message, T_{MB} , to all vehicles within range. Such message carries the merged set, \mathcal{C}_m , so vehicles not in the set that receive the T_{MB} message can discard it. Vehicles v_q , with $q = \{1, 2, \dots, p\}$, in \mathcal{C}_m reply the T_{MB} message with an acknowledgment, $T_{ack,q}$, also containing the replying vehicle number of one-hop neighbors and vectorial speed. After sending $T_{ack,q}$, v_q changes its state to cluster master candidate (CMC). In this work, all $T_{ack,q}$ messages reach the BS in a reasonable time with no losses

or collisions. However, future work should consider such losses and collisions, implementing an acknowledgment timeout to prevent the merge procedure from being blocked indefinitely. Vehicles with failed acknowledgment could be left out of the merging procedure or some technique that considers acknowledgment retries could be devised. Hence, in this work, when the BS receives all $T_{ack,q}$ messages, it can build the set $\mathcal{B} = \{\beta_1, \beta_2, \dots, \beta_p\}$, where β_q represents the suitability value of v_q . The suitability represents a score based on the vehicle speed and number of neighbors, as explained later in the next section, in Eq. 5. Having populated the set \mathcal{B} , the BS is able to determine the highest suitability, β_r , corresponding to vehicle v_r , with $1 \leq r \leq p$, which is elected the CM of the merged cluster \mathcal{C}_m . Then, the BS sends a cluster merge completed message, T_{MC} , informing $v_{m,r}$ has been elected CM of the m^{th} cluster. Finally, the merge ends when all other vehicles in the m^{th} cluster, *i.e.*, $\mathcal{C}_m \setminus v_{m,r}$, set their status to CE.

3.4.5 Cluster Master Selection

The BS is responsible for selecting a CM for the merged cluster based on the information it receives from the vehicles. Such selection is derived from the cluster master election by Tambawal *et al.* (2019), with the following adaptations. Two of the parameters used in (Tambawal *et al.*, 2019) — the node connectivity level and the mean distance — are more meaningful for the same vehicles. The node connectivity level recommends that vehicles that have more neighbors, usually closer to the center of the cluster, must be elected CM, while the mean distance favors vehicles that have the least mean distance to every other vehicle in the cluster — also likely to be a vehicle around the center of the cluster. Therefore, these two parameters are redundant, and only the node connectivity level is kept in the new model presented in this work. Also, the mean speed parameter in (Tambawal *et al.*, 2019) is replaced by the leadership value proposed by Ren *et al.* (2017). Both parameters recommend the vehicle that is closest to the mean speed of the cluster be selected as CM, since it will keep connectivity longer with more vehicles in the cluster. The leadership value was adopted because its computation is simpler than the mean speed parameter, therefore increasing the efficiency of the CM selection process. Thus, with the vehicles number of neighbors

and leadership value, the BS can determine the vehicle most suitable to become the CM of the merged cluster, as presented next.

The suitability of vehicle k , β_k , depends on two factors:

- The number of one-hop neighbors of vehicle k in cluster m , $N_{m,k}$, calculated by

$$N_{m,k} = \sum_{n=1}^{|\mathcal{C}_m|} [\text{dist}(k, n) \leq \text{Tx}_{\text{range}}] \quad (3.1)$$

where $|\mathcal{C}_m|$ is the number of vehicles in the merged cluster m , $[\text{dist}(k, n) \leq \text{Tx}_{\text{range}}]$ evaluates to 1 if the Euclidean distance (see Equation 3.2) between vehicles k and n is less than Tx_{range} , to 0 otherwise, and Tx_{range} is the maximum DSRC communication range.

$$\text{dist}(k, n) = \sqrt{(x_k - x_n)^2 + (y_k - y_n)^2} \quad (3.2)$$

- The leadership value of vehicle k , $L_{m,k}$, meaning how similar the speed of vehicle k is to the speed of all vehicles in the cluster. $L_{m,k}$ depends on a stability factor, given by

$$\text{SF}_{m,k} = \frac{\sum_{n \in \mathcal{C}_m} |\mathbf{s}_n - \mathbf{s}_k|}{|\mathcal{C}_m|} \quad (3.3)$$

where \mathcal{C}_m is the merged cluster set, and \mathbf{s}_n and \mathbf{s}_k are the vectorial speeds of vehicles n and k , respectively. Once $\text{SF}_{m,k}$ is computed, $L_{m,k}$ can be calculated by

$$L_{m,k} = \frac{1}{1 + \text{SF}_{m,k}}. \quad (3.4)$$

The image of $L_{m,k}$ is $[0, 1]$.

Finally, the two previous factors are multiplied by arbitrary weight factors, wf1 and wf2 , and the terms are added to calculate the vehicle suitability

$$\beta_k = (\text{wf1} \times N_{m,k}) + (\text{wf2} \times L_{m,k}) \quad (3.5)$$

subject to

$$wf1 + wf2 = 1. \quad (3.6)$$

The whole process is depicted in Algorithm 1.

Algorithm 1 Cluster Merge Procedure

Require: $\mathcal{C}_i; \mathcal{C}_j$; all vehicles in \mathcal{C}_i and \mathcal{C}_j know their speed; CMs of \mathcal{C}_i and \mathcal{C}_j within DSRC communication range of each other; $wf1; wf2$; and $wf1 + wf2 = 1$.

```

1: if  $|\mathcal{C}_i \cup \mathcal{C}_j| \leq C^{\text{thr}}$  then
2:   CM of  $\mathcal{C}_i$  sends  $T_{\text{MR}}$  to BS                                ▷ Send merge request
3:   CM of  $\mathcal{C}_j$  sends  $T_{\text{MR}}$  to BS                                ▷ Send merge request
4:    $\mathcal{C}_m \leftarrow |\mathcal{C}_i \cup \mathcal{C}_j|$                                 ▷ Merged cluster set
5:   for all vehicle  $v_q \in \mathcal{C}_m$  do
6:     BS sends  $T_{\text{MB}}$  to  $v_q$                                     ▷ Merge begin message
7:      $v_q$  changes state to CM                                  ▷ Vehicle becomes a cluster master candidate
8:      $v_q$  finds one-hop neighbors with Eq. 3.1
9:      $v_q$  replies to BS with  $T_{\text{ack}}$                             ▷ Contains one-hop neighbors and speed
10:  end for
11:   $\beta_r \leftarrow 0$                                           ▷ Suitability initialization
12:  for all vehicle  $v_q \in \mathcal{C}_m$  do
13:    BS calculates  $v_q$  leadership value with Eq. 3.4
14:    BS calculates  $v_q$  suitability with Eq. 3.5
15:    if  $\beta_q > \beta_r$  then
16:       $\beta_r \leftarrow \beta_q$ 
17:       $v_r \leftarrow v_q$                                       ▷ New most suitable VM
18:    end if
19:  end for
20:   $\mathcal{C}_i \leftarrow \emptyset$                                     ▷ Destroy old cluster (now merged)
21:   $\mathcal{C}_j \leftarrow \emptyset$                                     ▷ Destroy old cluster (now merged)
22:   $v_{m,r} \leftarrow v_r$                                       ▷ Final most suitable CM
23:   $v_{m,r}$  changes state to CM
24:  for all vehicle  $v_{m,k} \in \mathcal{C}_m \setminus v_{m,r}$  do
25:     $v_{m,k}$  changes state to CE
26:  end for
27: end if

```

3.5 SIMULATION RESULTS

In this section, details on the performed simulations of the Cluster Merging Scheme are given. Also, simulated results of the percentage of informed vehicles and number

of messages received per vehicle metrics are shown. Comparisons are carried out considering the following proposals — counter- and distance-based schemes (Tseng *et al.*, 2002), eSBR (Martinez *et al.*, 2010), and NJL (Sanguesa *et al.*, 2013).

The tools used on the performance simulations are the OMNeT++ discrete event simulator version 5.1, the INET Framework, for DSRC communication simulation, version 3.6.3, and the Simulation of Urban MObility (SUMO) simulation package version 0.30.0 for vehicle mobility simulation. Since neither the INET Framework nor any other wireless communication framework feature 5G communication, an approximation is considered — direct communication between the nodes is used, computing propagation and transmission delays manually, also trying to account for protocol overheads (which are still under standardization).

Considered parameters for the simulation of all schemes are summarized in Table 3.1. The used simulation scenarios, available from SUMO, are Valencia (more complex — more streets and junctions) and San Francisco (simpler — less streets and junctions).

TABLE 3.1: Simulation Parameters

Parameters	Specifications
Roadmaps	San Francisco, Valencia
Number of Vehicles	25 – 150 vehicles/km ²
Number of BSs	2
Vehicle Speed	35 – 60 m/s
Message Interval	0.1 second
Mobility Type	Krauss Model
Wireless Technology	5G / DSRC
Queue Size	1 MByte

Regarding vehicle traffic safety applications, the percentage of informed vehicles is a key parameter to avoid vehicle collisions and to re-route vehicle traffic in case of road blockage.

The density of vehicles on the network directly affects the chances of broadcast storms, which impair the percentage of informed vehicles. Therefore, densities of 25, 100, and 150 vehicles/km² are simulated in both scenarios to assess the effects of vehicles density on the mentioned metric. The achieved results for 2F-CM and for other previous proposals are shown in Figure 3.2 and discussed next.

In Figure 3.2a, the counter-based scheme, eSBR, and 2F-CM achieve over 95% of informed vehicles for 120 seconds after the event. Those results are for the San Francisco map at a density of 25 vehicles/ km^2 . In contrast, the results for the Valencia map in Figure 3.2b show how obstacles interfere with the dissemination — all schemes simulated achieved less than 50% of informed vehicles.

As the vehicles density increases, all curves become steeper, *i.e.*, dissemination occurs faster since there are more clusters closed together to aid on the dissemination. Also, results from the Valencia map (Figures 3.2d and 3.2f) become more similar to the ones from the San Francisco map (Figures 3.2c and 3.2e) as vehicles density increases. More clusters cause more obstacles to be circumvented.

Even though 2F-CM is not the best evaluated scheme regarding the percentage of informed vehicles, in all cases it is just 3% to 10% below the top performer for each scenario and density. Before it is possible to conclude which scheme should be preferred for VANETs, another metric — the number of messages received per vehicle — is evaluated next. Results for this metric are shown in Figure 3.3.

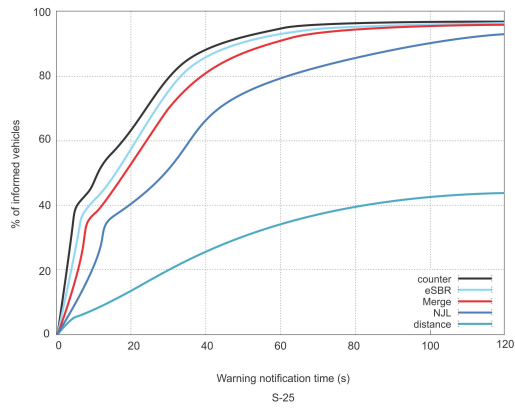
As seen in Figure 3.3a, the counter-based scheme and eSBR were subject to increased messages redundancy. Nevertheless, 2F-CM and the distance-based schemes presented a reduced number of messages received per vehicle and a low dependency on the scenario complexity (from Figures 3a and 3b).

As inferred from the analyzed results from Figures 3.2 and 3.3, 2F-CM results in the best trade-off between the number of informed vehicles (close to the counter-based scheme) and the number of messages received by each vehicle (close to the distance-based scheme), therefore keeping the highest number of vehicles informed without contributing to a potential broadcast storm problem.

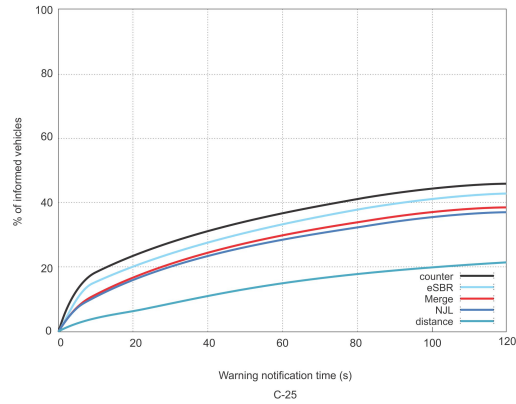
3.6 CONCLUSION

In this chapter, we investigated the impact of broadcast storms inside VANET clusters. The 2F-CM scheme is proposed and compared to other approaches. The intent of cluster merging is to have a better method for disseminating messages to the whole network without increasing the forward flooding. The presented simulation results,

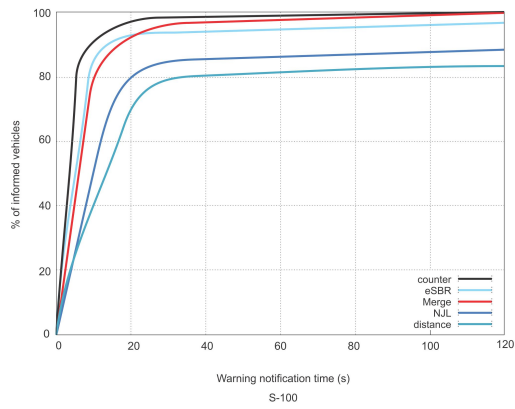
achieved through the OMNeT++ and SUMO simulators, show that our solution reduces the number of messages received per vehicle without affecting the percentage of informed vehicles compared to the counter-based, distance-based, NJL, and eSBR schemes. All results were discussed in the previous section.



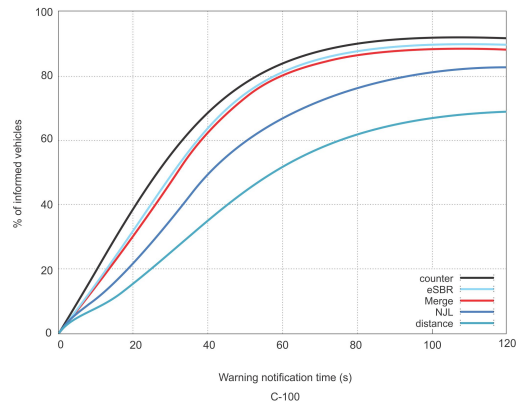
(A) San Francisco (simple), 25 vehicles per km^2



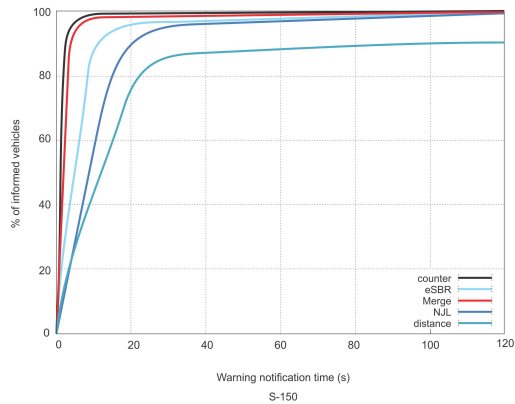
(B) Valencia (complex), 25 vehicles per km^2



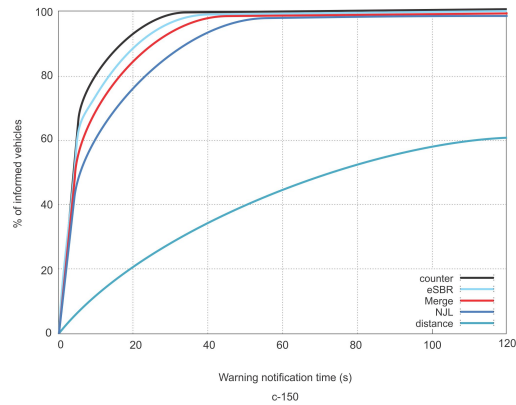
(C) San Francisco (simple), 100 vehicles per km^2



(D) Valencia (complex), 100 vehicles per km^2

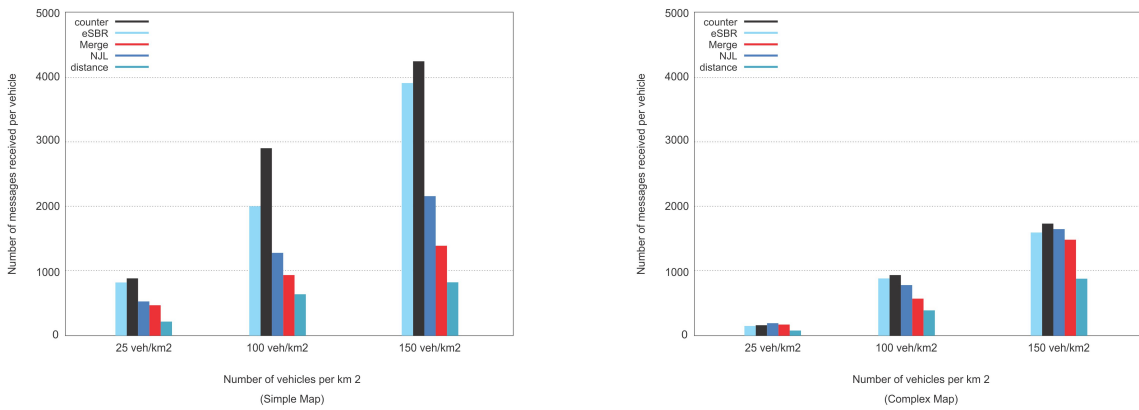


(E) San Francisco (simple), 150 vehicles per km^2



(F) Valencia (complex), 150 vehicles per km^2

FIGURE 3.2: Percentage of informed vehicles on the San Francisco (graphs on the left) and on the Valencia (graphs on the right) scenarios



(A) San Francisco (simple scenario), number of messages received per vehicle

(B) Valencia (complex scenario), number of messages received per vehicle

FIGURE 3.3: Number of messages received per vehicle in the San Francisco and in the Valencia scenarios

CHAPTER 4

DISSEMINATION PROPOSALS²

As shown in Chapter 3, the broadcast storm problem can be alleviated by clustering vehicles and coordinating their communications via CMs — reduced percentages of informed vehicles, especially in urban scenarios, where there are frequent obstacles to the DSRC channels. Therefore, in addition to clustering, this chapter proposes a novel combination of Cluster Forwarders (CFs), that are vehicles elected to help in transmitting messages around obstacles, and 5G as the V2I technology to increase the reach of the disseminated messages. New protocols featuring this combination are proposed next to tackle broadcast storms focusing on keeping the percentage of informed vehicles as high as possible.

4.1 INTRODUCTION

The number of vehicles on roads increases every year, consequently leading to a similar increase in traffic accidents (Sattar *et al.*, 2018). To increase traffic safety, the ITS is a proposed remedy encompassing a range of applications for VANETs, Some of which include automated driving, Internet access, intervehicle communication, and, in the safety category, warning message dissemination (Chiti *et al.*, 2019). However, to achieve increased safety, those warning messages must be delivered reliably and in a timely manner (Sattar *et al.*, 2018).

The dissemination of a warning message to vehicles close to an accident, for example, can be done reliably, to some extent, by pure V2V broadcasting, *i.e.*, starting from the vehicles that detect an event such as an accident, a warning message is broadcast, being re-broadcast by all the other vehicles that receive such a message. DSRC technology is normally used in pure broadcasting, the simplest dissemination method (Chiti *et al.*, 2019). However, depending on the local area vehicle density, its likely that too many re-broadcasts can occur. Thus, this phenomena typically causes

²The contents of this chapter are based on our accepted publication (AlQahtani and Sheldon, 2021).

a large number of packet collisions that makes communications impossible in the vicinity of an accident. This problem is known as the broadcast storm (Khan and Fan, 2018).

One option available to the ITS is the use of V2I communication to broadcast safety messages. This option uses a cellular communication technology, such as 5G, used as the VANET support infrastructure. However, broadcasting to the whole area covered by a base station will deliver the message to vehicles that are so far away that they do not need to be warned. Potentially, many vehicles in this case will receive irrelevant messages, consequently wasting processing resources to discard them. Multicasting could be a solution, but such methods increase communication latency due to the need for the formation of the multicast groups (Abboud *et al.*, 2016b). Thus, other solutions are required to overcome the problem of efficiently using the cellular network infrastructure for message dissemination.

Conversely, only applying V2V technologies to disseminate warning messages with methods to avoid broadcast storms, such as the ones mentioned in Chapter 3, might not warn nearby vehicles due to the presence of obstacles that can interfere with the signaling (Paranjothi *et al.*, 2019). Relying solely on DSRC communication, even with schemes to control broadcast storms, is not enough to guarantee that all needed vehicles are informed because of lost messages caused by signal blockage.

To avoid broadcast storms, vehicle hierarchies are an option and clustering can be used to implement such hierarchies. By grouping vehicles under the coordination of other vehicles, it is possible to organize the communication periods of the different tiers to reduce collisions as opposed to allowing any node to communicate at any time as is the case in pure broadcasting. Moreover, it is known that a hybrid hierarchy using vehicle clusters is possible using DSRC in combination with cellular communications (Abboud *et al.*, 2016b). Therefore, the use of clustering in combination with communication hierarchies allows the network to coordinate in ways that reduce collisions which thereby reduce the likelihood of broadcast storms.

The main contribution of this chapter is the evaluation of several novel protocols featuring different hierarchies and the assessment of the performance of distinct combinations of DSRC and cellular communication, specifically 5G. To find the best

protocol for safety message dissemination, we must understand how these various protocols can impact the percentage of informed vehicles and message delays. Vehicle clustering is used to reduce V2V communications where possible, specifically tackling the broadcast storm problem.

The proposed communication methods are simulated using OMNeT++ with the SUMO and Veins add-ons for vehicle communication simulations to test the two mentioned metrics — percentage of informed vehicles and message delays — in urban scenarios.

The remainder of this chapter is organized as follows. Section 4.2 provides a background of ITS, 5G, and DSRC communication, with emphasis on warning message dissemination reliability. Section 4.3 presents current literature related to the proposed methods. In Section 4.4, the cluster merging algorithm as well as the different combinations of V2V and V2I are presented, along with the benchmark methods, the vehicles mobility model, and the approximation used for the 5G communication. Section 4.5 discusses the simulation results from both the proposed and the benchmark methods for two urban scenarios. Finally, in Section 4.6, the conclusions are drawn and considerations for future research are presented.

4.2 BACKGROUND

The movement towards improving technology for better traffic and safety dates back to the 1940s (Auer *et al.*, 2016). Nonetheless, only recently has the emergence of efforts to create Smart Cities carried over to transportation systems, giving rise to the ITS. Consequently, the creation of VANETs has established V2X communication technologies (Abboud *et al.*, 2016b), which have enabled vehicles and infrastructure to connect with each other, coordinate, adapt, and automatically respond to traffic events (Ganin *et al.*, 2019) with the goal of creating a safer transportation infrastructure. This has been made possible via the on-board units (OBUs) (Al-Ani *et al.*, 2018), which provide measurement of the vehicle status and the vehicle surroundings (*i.e.*, situation awareness), as well as enabling vehicles with V2X communications. In this way, transportation systems can provide better efficiency and safety. However, achieving

these improvements is a work in progress — road accidents are still a leading cause of death globally (Abdul *et al.*, 2017).

Tackling the aforementioned problem, safety applications for VANETs aim at reducing the risk of accidents within the ITS. Early examples started with the synchronization of traffic lights (Ganin *et al.*, 2019). These evolved into contact points between vehicles and the infrastructure (Chiti *et al.*, 2019). In turn, contact points motivated the usage of other kinds of RSUs, such as signs, Internet gateways, and even pedestrians (Abboud *et al.*, 2016b), for connectivity. Applications currently being researched include (Al-Ani *et al.*, 2018):

- detection of vehicles on blind spots for lane changes;
- forewarning of potential collision between cars travelling in opposing lanes;
- detection of fast approaching vehicles at intersections, and;
- detection of police cars, fire engines, and ambulances that require free lanes in an emergency.

However, safety applications depend on the efficiency of the dissemination of messages among the vehicles in the system. Specifically, such critical information must be timely (Shah *et al.*, 2019) and reliably (Sattar *et al.*, 2018) delivered to all vehicles in the vicinity of an accident to guarantee safety. One of the solutions for such a problem is one-hop periodical beacons from all vehicles (Al-Ani *et al.*, 2018). This method proposes that vehicles broadcast a beacon message every 100–300 ms. Such messages should contain information on the vehicle position, speed, acceleration, and movement direction, also including safety events, such as accident warnings. A potential problem is that broadcasts can flood the communication medium. Even though using beacons would partly solve this problem, the medium congestion would still increase (Shah *et al.*, 2019). This effect calls for a more centralized solution. A fully-centralized solution, coordinated by a cellular base station, would drastically reduce the medium usage. However, some multiplexing for all vehicles would be necessary, which unfortunately would increase delays beyond the time requirements needed for safety applications. Thus, a less centralized approach, such as vehicles clustering,

should accomplish a balance between medium occupation and communication delays (AlQahtani *et al.*, 2021). Clustering is able to leverage the range of BSs used as RSUs without incurring the penalty of higher delays due to dividing the communication slots among many users. Only the CMs would need to communicate with the BS.

To make the best use of available communication resources, clustering could leverage the best characteristics of both V2I and V2V. A cellular network for V2I combined with V2V in a hybrid fashion (Shah *et al.*, 2019) could achieve a balance that minimizes both medium usage and message delay time. 5G, which features large communication ranges and low latency, may be used as the V2I technology for intercluster communication. The V2V communications, featuring low communication overhead, would then be used for intracluster communication only (Zhang *et al.*, 2019). Generally, the expectation is that network resiliency (*e.g.*, throughput and congestion) will improve through the use of such a hybrid communication protocol:

- broadcast storms and frequent disconnects from V2V-only clustering would be avoided (Khan and Fan, 2018);
- all vehicle communications with the base station in a pure V2I VANET would be prevented, saving resources and avoiding large contention delays; (Zhang, 2015; Nshimiyimana *et al.*, 2017);
- degraded performance of DSRC operating in high-density scenarios due to congestion (Khan and Fan, 2018) and to signal blockage (Martinez *et al.*, 2010) would be circumvented, and;
- broadcasts would be geographically limited to cluster boundaries, reducing messages redundancy on the network, channel contention, and message collisions.

Some unsavory consequences necessitating special requirements are to be expected. GPS would be needed in all vehicles that would benefit (Nshimiyimana *et al.*, 2017). This should pose no challenge for most modern vehicles and would make all necessary data for cluster formation available. Also, connectivity checks between cluster masters and cluster members would create some small amount of overhead local to clusters (Shah *et al.*, 2019). Finally, as few cluster masters as possible should be elected

in a given network locality. This would make efficient use of the cellular network bandwidth as these nodes are responsible for V2I communication. Fewer clusters also means optimizing clusters to be as large as possible, which would also gain better cluster stability (Zhang *et al.*, 2019). This effect favors the use of a cluster merging method, which was proven in Chapter 3 and is now further investigated.

4.3 RELATED WORK

Warning messages for road accident prevention must be delivered on strict delay and reliability requirements to be effective. Therefore, communication problems that might hinder the dissemination capacity of VANETs must be carefully scrutinized. Since broadcast storms negatively impact message delivery to all participating vehicles, previous and current attempts to solve the problem and some improvement opportunities are shown here to baseline our assumptions in this study.

Martinez *et al.* (2010) bundle together several previous proposals to control the broadcast storm problem. Some of them are counter-based schemes, in which a broadcast message contains a counter field that is increased after each re-transmission; vehicles do not re-transmit the message after a limit of C re-transmissions is reached. Another type of approach are the distance-based methods. Nominally, only the vehicles farthest from a transmitter should forward the message to avoid broadcast redundancy close to a transmitter. Also, when considering only the single farthest vehicle for re-transmission, the methods are known as TLO, which naturally, are most suitable for highway communication. Moreover, location-based approaches have also appeared in the literature. By making the precise locations of each vehicle available, these approaches can determine the best forwarders to cover the most area with fewest re-transmissions. There are also probability-based schemes. Even though they have not been proposed to solve broadcast storms, forcing vehicles to access the channel with a controlled probability less than τ can prioritize the communication of the most critical ones, while reducing the number of messages being rebroadcast. Probability-based schemes are especially designed for highway scenarios. Finally, accounting for

all previous proposed approaches, the TLO has been successfully combined with the probability-based schemes for improved medium access control.

Noting that the previous approaches only prevent *some* of the vehicles from broadcasting to reduce broadcast storms, Martinez *et al.* further studied and proposed the eSBR, a scheme (Martinez *et al.*, 2010) aiming at urban scenarios. In considering DSRC communication between vehicles, a well known problem is that buildings do block signal propagation. Therefore, the authors propose rebroadcasting warning messages only for the following two situations: (i) the distance between the transmitter and receiver is larger than a threshold D or (ii) the vehicles are on different streets, *i.e.*, one of them is close to an intersection and can communicate to vehicles on another street.

Sanguesa *et al.* (2013) note that most proposed methods utilize information on vehicle speed, density, and location, but data on the number of nearby vehicles and the scenario topology are important characteristics that should also be accounted for when aiming to efficiently disseminate messages in an obstacle laden urban environment. Hence, they proposed the NJL method, which considers only the vehicle closest to a junction to be the re-broadcaster of the warning message. As a result, the number of messages being broadcast is reduced when compared to other methods, *e.g.*, eSBR, with the only limitation being that of poor performance in vehicle-sparse environments. The study presented in this chapter investigated this gap by adding a cluster merging algorithm that uses the vehicles closest to junctions as re-broadcasters.

Another important aspect to be considered by the simulation of VANETs is the signal attenuation between two communicating vehicles. Urquiza-Aguilar *et al.* (2015) present a study of several realistic models. The authors compare those realistic models to a simpler, less realistic one, where the communication between vehicles is successful only if they are in LoS. The results proved that several metrics such as packet loss and communication delay can be well approximated using the simpler model, which requires far less processing than the more realistic counterparts. Following the presented conclusion, this work also considers full blockage of DSRC signals when vehicles are in non-LoS. Moreover, to enable communication between vehicles in non-LoS, this chapter considers the use of a cellular network as an alternative available

for vehicle communication. Because this case requires the use of an additional node within the communication chain, the BS, communications delays are expected, and assessing such influence is within the scope of the present study.

Xu *et al.* (2017) consider the 4G LTE as a possible technology to be used for both V2V and V2I communication. In their work, they highlight that simulations can lead to conclusions that are not aligned to the technology's operation in practice. Therefore, they propose a test-bed through which they can test the performance of both LTE and DSRC communications under different delay requirements. In their work, Xu *et al.* mapped delays for different safety applications. According to the authors, pre-crash sensing, which is the application considered in this paper, has a latency requirement of 20ms. However, the results presented by Xu *et al.* show that the LTE RTT is at least 300ms. Thus, this technology cannot be used as support for the collision avoidance scenario studied in our work.

A logical step is to consider 5G as the infrastructure technology used to support V2X communication. According to Ullah *et al.* (2019), 5G for V2I communication will achieve latencies comparable to DSRC (about 10ms), while outperforming both DSRC and LTE on other aspects of V2X communication. Therefore, the work in this chapter endeavors to validate the use of DSRC and 5G together so as to enable vehicle collision avoidance in urban scenarios.

Lastly, as discussed above, since some of the technologies considered rely on highly directive radio communication, such as DSRC and the possibility of millimeter waves for 5G (Ullah *et al.*, 2019), communication blockage by obstacles must be considered, especially in urban scenarios. Mezher *et al.* (2014) present a simulator capable of determining which vehicles can communicate with each other. Thus, 5G brings the flexibility of using several different access methods and frequency bands to avoid the lack of connectivity among vehicles (Zhou *et al.*, 2017). This is another case that justifies the use of 5G as the infrastructure network to support DSRC communication, which is accounted for here in our analyses.

A comparison of the considered aspects between similar related work and our study is shown in Table 4.1.

TABLE 4.1: Comparison of this study to related work

Method	V2V	V2I	Clustering	Considers obstacles	Tackles broadcast storms
eSBR (Martinez <i>et al.</i> , 2010)	DSRC	-	No	Yes	Yes
NJL (Sanguesa <i>et al.</i> , 2013)	DSRC	-	No	Yes	Yes
Urquiza-Aguiar (Urquiza-Aguiar <i>et al.</i> , 2015)	DSRC	-	No	Yes	No
Xu (Xu <i>et al.</i> , 2017)	LTE	LTE	No	No	No
Our approaches	DSRC	5G	Yes	Yes	Yes

4.4 METHODOLOGY

This work proposes to measure the effects of using both V2V and V2I over two metrics — the percentage of informed vehicles and the delay from the event to the last informed vehicle. The considered scheme features a VANET operating in a high traffic urban environment containing obstacles that interfere with communications. The event is an accident generating a warning message that must be disseminated to all nearby vehicle clusters. Moreover, the effect of cluster forwarders (CFs) at street junctions is studied and compared. As expected, CFs will extend the reach of message dissemination to other streets, also reducing signal reflections from the inherently complex urban environment. To achieve such assessment, the scenario in Figure 4.1 is adopted.

The benchmark schemes are eSBR (Martinez *et al.*, 2010), suited for sparse vehicle densities, and NJL (Sanguesa *et al.*, 2013), best for high traffic congestion vehicle densities. Both are applied to the scenario given in Figure 4.1. The percentage of informed vehicles and the delay from the crash to the last informed vehicle receiving the warning message generated in the event are measured to establish each benchmark.

To make the best use of the available communication resources, clustering can leverage the best characteristics of V2I via a cellular network and of V2V in a hybrid communication fashion (Shah *et al.*, 2019). 5G, for example, which features large communication ranges and low latency, can be used as the V2I technology for inter-cluster communication, while DSRC, featuring low communication overhead but high susceptibility to obstacle blockage, can be used as V2V. By combining clustering, DSRC for V2V, and 5G for V2I, the first proposed method, the Hierarchic Model (HM), is created, where the crashed vehicle communicates with its CM, which, in turn,

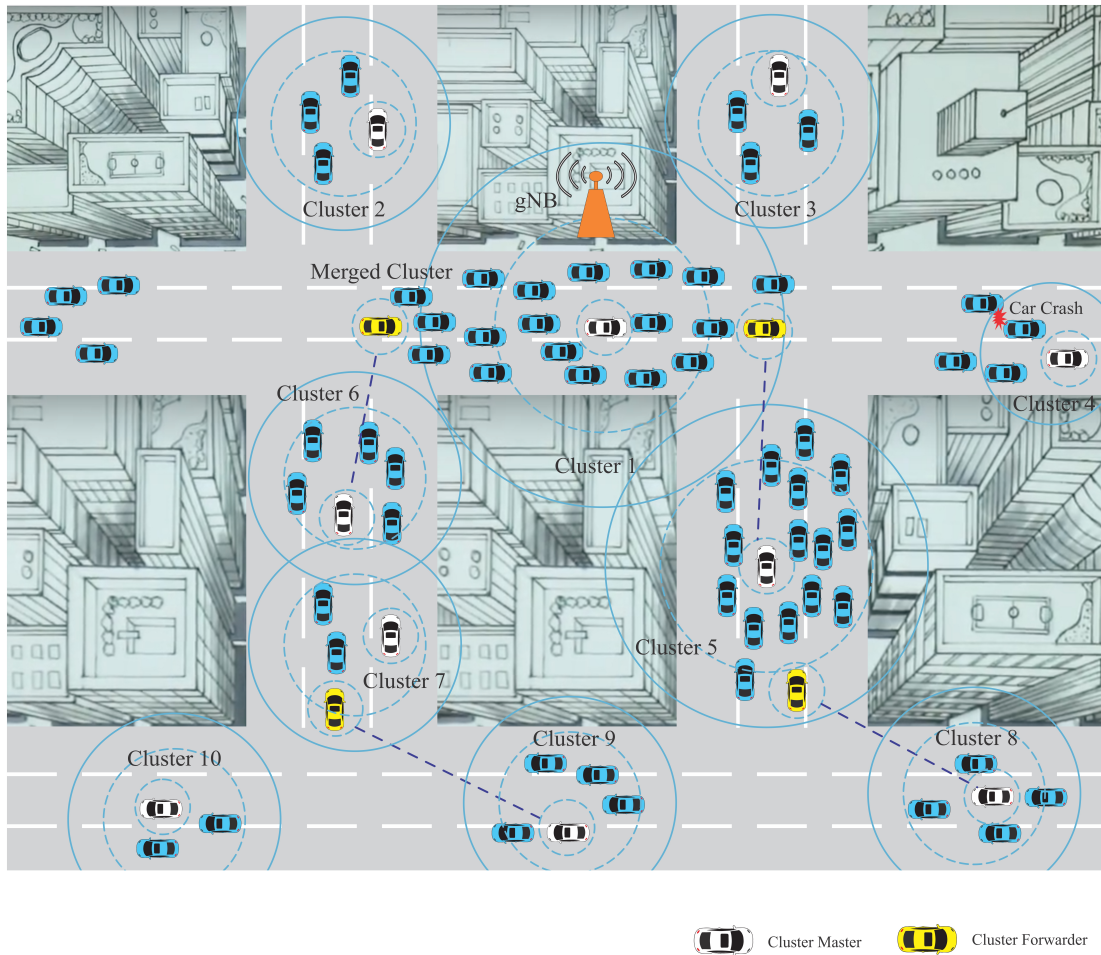


FIGURE 4.1: VANET considered as the scenario in this work

communicates with the 5G infrastructure. The 5G BS then forwards the message to other CMs, finally reaching all cluster members in the region.

Furthermore, to take advantage of the lower latency of the DSRC communication between vehicles when compared to 5G, the Hierarchic Model with Forwarder (HMwF) is proposed. In other words, the crashed vehicle still communicates with its CM, which still forwards the messages to the 5G infrastructure, but, now, the BS only communicates with the CFs, which are responsible for delivering the warning message to the other CMs. Finally, the cluster members receive the message via their CMs.

In a third method, the crashed vehicle communicates directly with the BS in the Event Node to Infrastructure with Forwarder (EN2IwF) method. From there, the warning message is sent to the CFs, then to the CMs, and, finally, to the cluster members.

In the last method, the Event to Forwarder to Cluster (E2F2C), the crashed vehicle contacts the closest CF directly, which will forward the warning message to the CMs and other CFs, reaching the cluster members.

Some caveats apply to the previous cases: (i) In all of the proposed methods, it is assumed that all clusters have already been formed, *i.e.*, delays measured do not include cluster formation time. (ii) There must be an elected CF for each junction at all times, *i.e.*, the most suitable CF is elected using the 5G infrastructure and passed to the closest CMs. (iii) If required, such as in the E2F2C method, all vehicles need to know the current CF at the closest junction.

4.4.1 Cluster Forwarder Election

Periodically, all CMs will receive a query multicast from the BS to find which clusters are closest to which junction, considering all junctions in the area covered by the BS, then proceeding with the CF election according to Algorithm 2.

Let \mathcal{J} be the set of junctions and \mathcal{C} be the set of CM (used in Algorithm 3), both within the BS range. For each junction $j_i \in \mathcal{J}$, create the sets \mathcal{D}_i , which contains all the CMs closest to j_i than to any other junction, by multi-casting a message with the junction number and expecting an acknowledgment from CMs closest to such junction. All vehicles are considered to have GPS and the mapped and numbered junctions received from the BS so they can determine which junction they are closest to. After determining \mathcal{D}_i , the closest vehicle to junction j_i , $v_{i,best}$, is determined according to Algorithm 4. Vehicle $v_{i,best}$ can only be selected from the clusters for which CMs are in \mathcal{D}_i . When $v_{i,best}$ is found, this vehicle is elected the CF for junction j_i and is added into the set of CFs, \mathcal{F} .

Algorithm 2 Cluster Forwarders Election

```

1:  $\mathcal{F} \leftarrow \emptyset$  ▷ Cluster Forwarders set initialization
2: for all  $j_i \in \mathcal{J}$  do
3:    $\mathcal{D}_i \leftarrow \text{GETCLUSTERMASTERSCLOSESTTOJUNCTION}(j_i)$ 
4:    $d_{i,best} \leftarrow \infty$ 
5:   for all  $v_k \in \mathcal{D}_i$  do
6:      $v_{k,best} \leftarrow \text{GETVEHICLEINCLUSTERCLOSESTTOJUNCTION}(v_k, j_i)$ 
7:     if  $\text{DISTANCE}(j_i, v_{k,best}) < d_{i,best}$  then
8:        $d_{i,best} \leftarrow \text{DISTANCE}(j_i, v_{k,best})$ 
9:        $v_{i,best} \leftarrow v_{k,best}$ 
10:    end if
11:  end for
12:   $\mathcal{F} \leftarrow \mathcal{F} \cup \{v_{i,best}\}$ 
13: end for
14: return  $\mathcal{F}$ 

```

Algorithm 3 Finding the set of cluster masters closest to a junction

```

1: procedure  $\text{GETCLUSTERMASTERSCLOSESTTOJUNCTION}(j)$ 
2:    $\mathcal{D} \leftarrow \emptyset$  ▷ Resulting set initialization
3:   for all  $c_k \in \mathcal{C}$  do ▷ Sweep the CMs
4:      $d_{min} \leftarrow \text{DISTANCE}(j, c_k)$  ▷ Minimum distance initialization
5:      $flag \leftarrow true$  ▷ If  $c_k$  is closer to any other junction,
6:      $\cdot$  ▷ this flag gets false
7:     for all  $j_l \in \mathcal{J} \setminus j$  do
8:       if  $\text{DISTANCE}(j_l, c_k) < d_{min}$  then
9:          $flag \leftarrow false$ 
10:        break
11:       end if
12:     end for
13:     if  $flag = true$  then
14:        $\mathcal{D} \leftarrow \mathcal{D} \cup \{c_k\}$ 
15:     end if
16:   end for
17:   return  $\mathcal{D}$ 
18: end procedure

```

4.4.2 Cluster Merging Algorithm

The cluster merging algorithm is the 2F-CM, shown in Algorithm 1 in Chapter 3. This method alone contributes to reducing the number of CMs contending for a chance to communicate with the BS. Therefore, dissemination delays are reduced for the methods that require the use of the cellular system, namely HM, HMwF, and

Algorithm 4 Finding the cluster member closest to a junction

```

1: procedure GETVEHICLEINCLUSTERCLOSESTTOJUNCTION( $v_k, j$ )
2:    $\mathcal{V} \leftarrow \text{GETCLUSTER}(v_k)$             $\triangleright$  Get the cluster  $v_k$  including the CM
3:    $d_{cluster\_best} \leftarrow \infty$ 
4:   for all  $v_i \in \mathcal{V}$  do
5:     if  $\text{DISTANCE}(v_i, j) < d_{cluster\_best}$  then
6:        $d_{cluster\_best} \leftarrow \text{DISTANCE}(v_i, j)$ 
7:        $v_{cluster\_best} \leftarrow v_i$ 
8:     end if
9:   end for
10:  return  $v_{cluster\_best}$ 
11: end procedure

```

EN2IwF. Regarding reliability, the focus of this work is to overcome DSRC signal blockage caused by buildings — therefore, communication errors, likely to happen in practice, are not considered. Since cellular networks are capable of working on highly obstructed environments, such networks can carry out longer range inter-cluster communication better than the highly directive DSRC signals can. As the deployment of 5G approaches and specifications become clearer, more details, such as the aforementioned errors, can be included on future simulations. LTE is already able to operate with less than 5% packet loss ratio for vehicle speeds more common in cities (up to 60km/h) (Xu *et al.*, 2017); therefore, better results are expected for 5G. Even those packet loss ratios can be further improved by using automatic repeat requests (ARQ) and/or forward error correction (FEC), improving dissemination reliability, but this is beyond the scope of this work. The present chapter focuses on proving that dissemination reliability can be improved by using an alternative communication method when DSRC is likely to fail due to signal blockage.

The 2F-CM is used in conjunction with the CF election to keep broadcast storms under control by merging clusters whenever possible. One CM coming into the DSRC communication range of another CM triggers a cluster merging.

In case different clusters cross paths at a junction, they communicate as separate clusters until they are able to merge. When these clusters move out of reach from each other, new CMs are selected for each cluster. They can keep communicating via a CF if needed and if possible.

4.4.3 Vehicle Mobility Simulation

The considered scenarios, vehicle insertion model, and vehicle mobility model are all based on the Simulation of Urban MObility (SUMO) tool (Lopez *et al.*, 2018). The applied workflow and model details are given next.

First, an Open Street Map (OSM) file for the scenario is required. There are many available on the SUMO installation, and two of them were used in this study — Valencia and San Francisco. OSM files contain geographical coordinates of buildings and streets. From one of those files, SUMO can generate a network file, which holds data on all edges (paths vehicles can take), junctions, and connections in the area considered at the OSM file. Then, trip files can be created by randomly selecting departure and arrival places and the respective departure (insertion) times in configurable time periods. For this work, departure and arrival places were taken following a uniform distribution over all the available positions on edges. Using the trip and network files, a route file is created. Routes contain vehicle IDs, departure times, and the sequence of edges, junctions, and connections each vehicle must traverse to reach its destination. With the route file, the simulation can be run.

Vehicles start to be inserted into the network according to their departure positions and times on the route file. If a vehicle fails to be inserted, either because the new vehicle overlaps with an existing vehicle or because inserting the new vehicle at its configured initial speed would cause a collision, no more vehicles are inserted on that edge.

The mobility model itself, *i.e.*, the rules used to update vehicles speeds, follows the Krauss model (Krauss, 1998) as discussed next.

Two types of motion need to be considered when simulating traffic flow on a microscopic level — free motion and motion while interacting with other vehicles. For the former, we assume that vehicle speed v is bounded by a maximum speed v_{max} , which can represent the maximum speed a driver is willing to drive at or the maximum speed achievable by the vehicle (Krauss, 1998; (German Aerospace Center), 2020). For the latter, we assume that vehicles influence one another's speeds because collisions are to be avoided — therefore, v also has to be less than v_{safe} . Also, let v_l

be the speed of a leader vehicle on a given street, v_f be its follower vehicle speed, a is the maximum possible acceleration, and b is the maximum possible deceleration. According to the Krauss' model (Krauss, 1998), the discrete speed update $v(t + \Delta t)$ and the discrete position update $x(t + \Delta t)$ are given by:

$$\begin{aligned}
 v_{safe} &= v_l(t) + \frac{g(t) - \tau v_l(t)}{\tau_b + \tau} \\
 v_{des}(t) &= \min [v_{max}, v(t) + a(v)\Delta t, v_{safe}(t)] \\
 v(t + \Delta t) &= \max [0, v_{des}(t) - \eta] \\
 x(t + \Delta t) &= x(t) + v\Delta t
 \end{aligned} \tag{4.1}$$

where $g(t)$ is the current gap between the leader and the follower vehicle, τ is the drivers' reaction time, τ_b is a time scaling factor $\tau_b = \frac{v_l + v_f}{2b}$, and η is a random perturbation greater than zero that models driving imperfections.

4.4.4 5G Communication Approximation

Since no 5G simulation frameworks for OMNeT++ worked properly with the Veins package that simulates the vehicle's mobility, an approximation was adopted to enable testing of the proposed methods. Hence, 5G communication is generalized as direct communication between the BS and the vehicle of interest with $0.3ms$ propagation delays and $1ms$ transmission delays. Those are intentionally large to capture 5G protocol overheads that would be in place on a real system. To clarify, a propagation delay of $0.3ms$, considering signal propagation at the speed of light, would mean the signal traversed $90km$, much more than the expected $1km$ for 5G in urban environments. Also, a transmission delay of $1ms$ at a bandwidth of $10Mb/s$ (the value used in our simulations), would mean $10kb$ long warning packets, which is too long for these kinds of messages (expected to be less than $1kb$). These values were determined empirically, leading to acceptable results when they became at least comparable to DSRC communication delays. In a real scenario, 5G is expected to perform better.

4.5 RESULTS AND DISCUSSION

The objective of the simulations was to compare the percentage of vehicles informed of a crash event and the delay from the crash to the last vehicle informed. The dissemination methods for which such metrics were simulated are the proposed methods and benchmarks discussed in Section 4.4. The tools chosen for this work were the OMNeT++ discrete event simulator ((OpenSim Ltd.), 2020) version 5.5.1, the SUMO road traffic simulator (Lopez *et al.*, 2018) version 1.6.0, and the Veins framework for VANET wireless communication (Sommer *et al.*, 2011) version 5.0. Due to the authors' previous experience with these tools, they were selected for this work.

Two maps featured by SUMO were used to simulate the benchmarks and proposed methods — Valencia and San Francisco. The former is more complex, with 2829 streets and 2233 junctions, while the latter has 725 streets and 818 junctions. According to the cluster forwarder election procedure proposal shown in Section 4.4, more junctions require more cluster forwarders, adding complexity to the communication between vehicles and clusters. Thus, it is expected that the communication in the Valencia scenario would presents more delays to inform all vehicles of the crash event than in the San Francisco scenario.

When clusters merge during the simulations, the election of the new CM of the merged cluster requires two arbitrary parameters — the number of neighbors weight value ($wf1$) and the leadership weight value ($wf2$). The leadership value that is multiplied by the latter is normalized between 0 and 1, while the number of neighbors multiplied by the former is expected to be around 10. Therefore, the suitable values $wf1 = 0.1$ and $wf2 = 0.9$, empirically found, make the terms of Equation 3.5 comparable, thus balancing the importance of the number of neighbors and of the leadership value of a vehicle for such vehicle election as a CM. A thorough analysis of the system behavior for different values of the weight factors is out of the scope of this work.

The parameters used in our simulations are shown in Table 5.1. Also, the results for each map their comparison are given in the following subsections.

TABLE 4.2: Simulation Parameters

Parameter	Value(s)
Maps	{Valencia, San Francisco}
Vehicles in the network	{25, 50, 100, 150, 200}
Maximum vehicles per cluster	100
Number of events (collisions)	1
Warning message length	256 bytes
Event messages interval	0.1 sec
MAC/PHY	{802.11p (DSRC), approximation of 5G}
Maximum communication range	{300m (DSRC), 1km (5G)}
Neighbors weight factor (wf1)	0.1
Leadership weight factor (wf2)	0.9

4.5.1 Valencia

The percentage of informed vehicles over time for the Valencia map are shown in Figure 4.2.

From Figure 4.2, the first noticeable fact is that the E2F2C method performs poorly on the delivery of the messages to the vehicles. Factors that contribute to these results are that the crashed vehicle tries to send its message to a CF, which needs to route the message to every other CF and CM to reach all vehicles. That is a much slower process than using the 5G infrastructure to reach several CMs and/or CFs at the same time, as done in the other methods. Moreover, the HM, the HMwF, and the EN2IwF methods achieve the top percentage of informed vehicles. For 25 vehicles on the network, in 10 seconds, all messages are delivered with the HM method. As the number of vehicles increases, the usage of the CFs to help spreading the messages outperform the exclusive use of the BS communication with the CMs. That can be seen as the methods that use CFs, namely HMwF and EN2IwF, achieve the maximum of informed vehicles in less time. As for the benchmarks, eSBR only outperforms NJL for 25 vehicles in the network, agreeing with the eSBR authors statement that the method performs better on sparse networks (Martinez *et al.*, 2010). Also agreeing with its authors, NJL performs better on dense networks (Sanguesa *et al.*, 2013), achieving comparable performance to the proposed methods for 200 vehicles in the network.

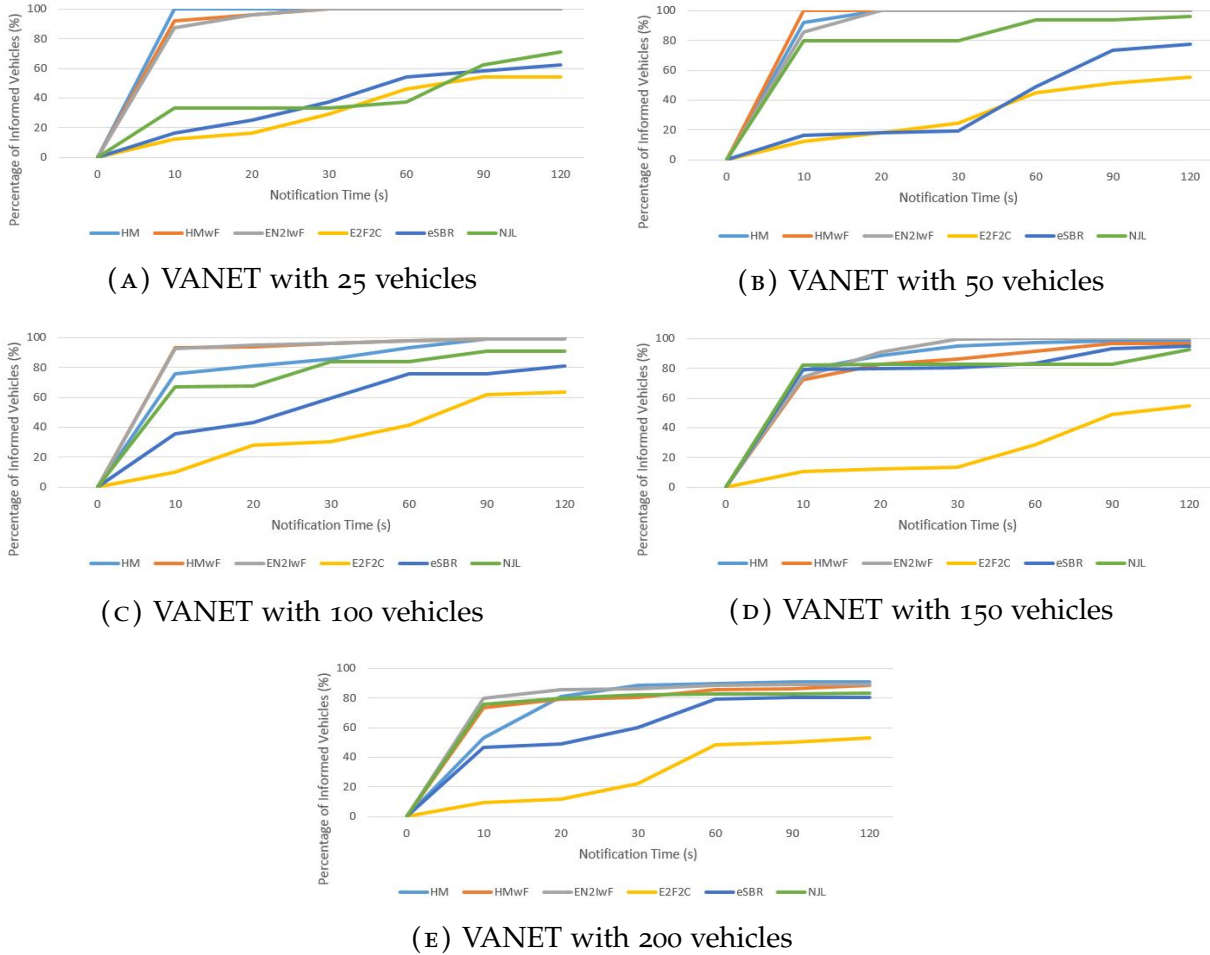


FIGURE 4.2: Percentage of informed vehicles over time for the Valencia scenario with different number of vehicles in the VANET for all proposed methods and benchmarks

The delays for informing the last vehicle for the considered methods are shown in Figure 4.3.

Again, the E2F2C method shows poorer performance than the other methods, even though comparable to the benchmarks. Up to 50 vehicles in the network, the usage of the BS proves to be very efficient, as shown by the low delays for the HM and the HMwF methods. The usage of CFs can keep the delays under 10 seconds for the HMwF, while delays for the HM go up. However, CFs add complexity to the network, so for 150 vehicles and above, BS to CM exclusive communication proves to be better, as seen for the HM.

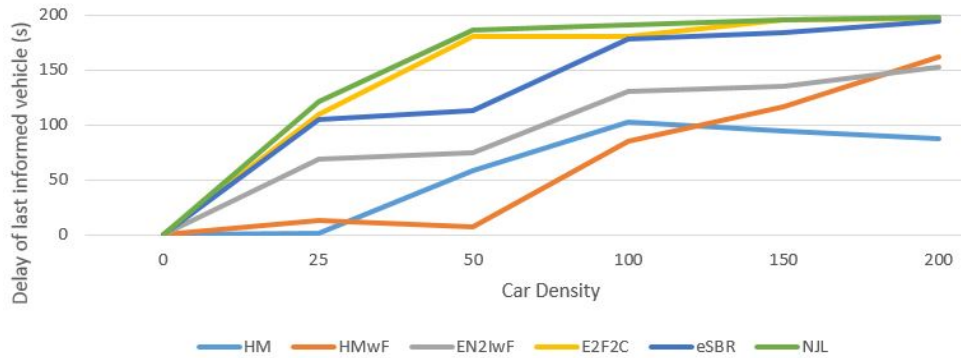


FIGURE 4.3: Delay for informing the last vehicle for all proposed methods and benchmarks

4.5.2 San Francisco

The percentage of informed vehicles has also been simulated at the San Francisco map, which features fewer streets and junctions than the previous one. The results are shown in Figure 4.4.

The E2F2C method still does not achieve good results. As for the other methods and for the benchmarks, the results are similar to the previously shown for the Valencia map, except for NJL. The latter achieves higher percentages of informed vehicles than at the Valencia map, which is explained by the lower availability of roads. This forces vehicles to stay closer and favors the capability of NJL of performing better on higher vehicles densities (Sanguesa *et al.*, 2013). The usage of the 5G infrastructure explains the very similar performance for the proposed methods, which eliminates packet delivery uncertainties as long as the clusters are within the same BS range.

The delays to inform the last vehicle at the San Francisco map are shown in Figure 4.5.

The HM and the HMwF are the best performers, staying below 100 seconds, but NJL delays stand out for 150 vehicles and above. The concentration of vehicles around a few junctions outperform by far the delays added by the communication with the BS. This shows that improving the E2F2C method, which does not communicate with the infrastructure, might prove useful for scenarios where vehicles are concentrated around a few junctions.

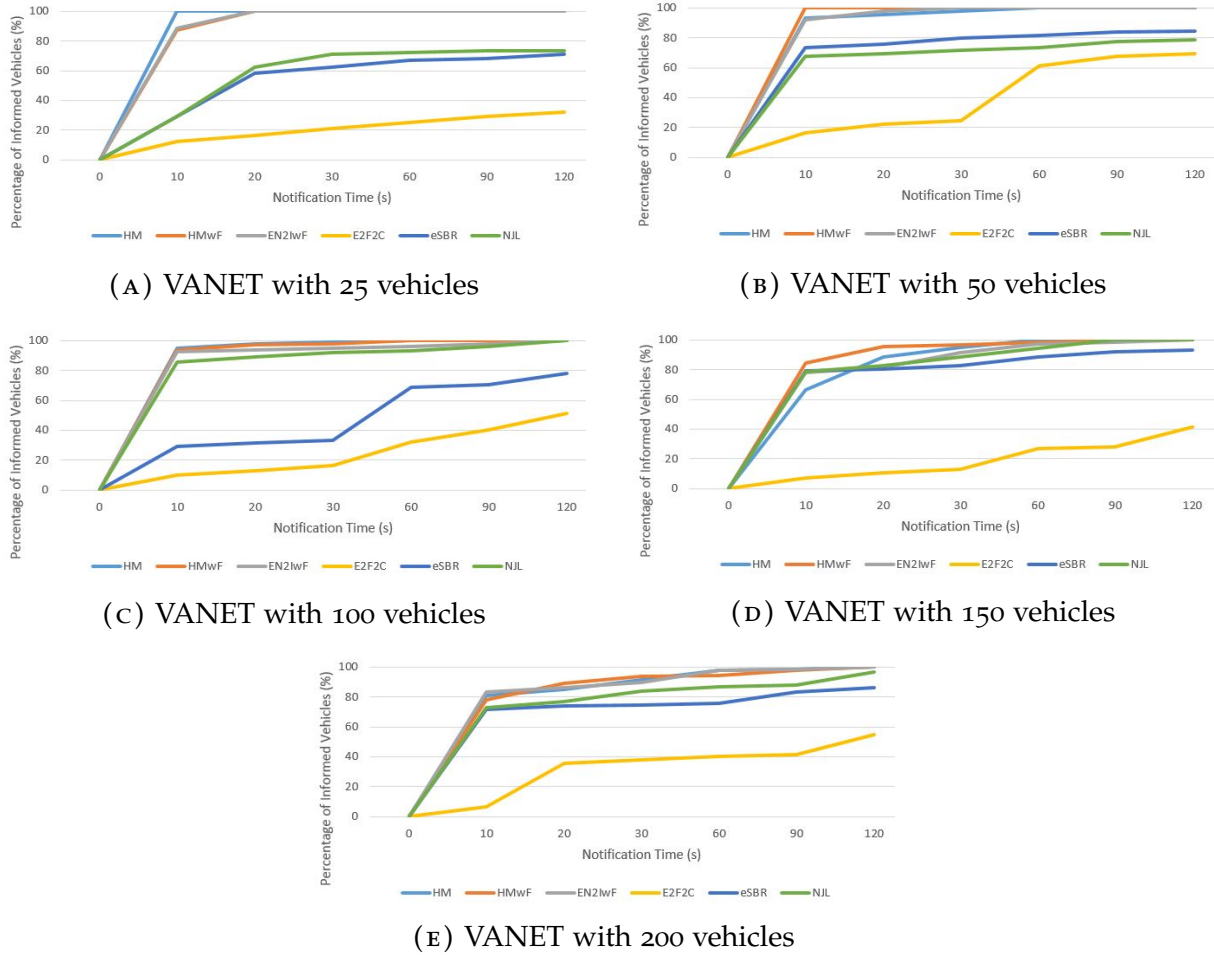


FIGURE 4.4: Percentage of informed vehicles over time for the San Francisco scenario with different number of vehicles in the VANET for all proposed methods and benchmarks

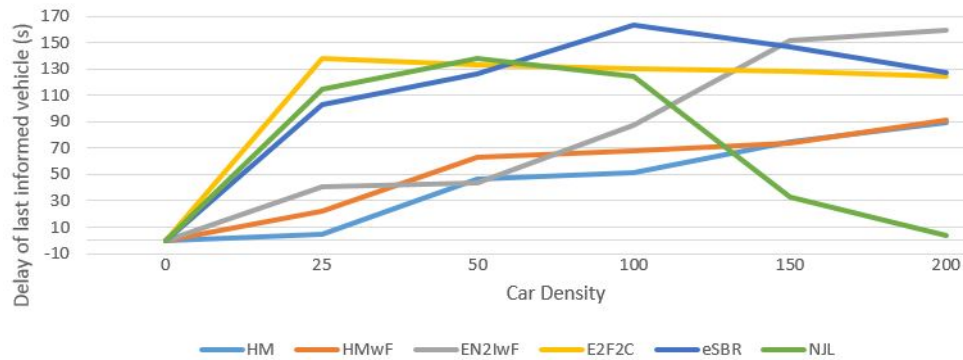


FIGURE 4.5: Delay for informing the last vehicle for all proposed methods and benchmarks

4.5.3 Comparison Across Scenarios

In this subsection, results across the scenarios are discussed. Results for both scenarios are gathered in Table 4.3 to make their analysis possible.

TABLE 4.3: Comparison between maps throughout number of vehicles and selected notification times

method@Notification Time Number of vehicles Map	Percentage of Informed Vehicles									
	25		50		100		150		200	
	SF	Val.	SF	Val.	SF	Val.	SF	Val.	SF	Val.
HM@10sec	100	100	93.4	91.83	94.95	75.76	66.4	78.52	80.9	52.8
HMwF@10sec	87.5	91.7	100	100	93.9	92.93	84.6	72.48	77.8	73.4
EN2IwF@10sec	88.6	87.5	91.8	85.7	92.6	92.3	77.85	73.85	83.4	79.9
E2F2C@10sec	12.5	12.5	16.4	12.4	10.1	10.1	7.4	10.73	6.53	9.54
eSBR@10sec	29.2	16.7	73.4	16.32	29.3	35.4	80.5	79.2	71.4	46.73
NJL@10sec	29.2	33.3	67.4	79.6	85.6	66.7	82.6	81.88	72.87	75.87
HM@60sec	100	100	100	100	100	92.93	100	97.3	97.5	89.44
HMwF@60sec	100	100	100	100	100	97.98	98.65	91.3	94.48	85.4
EN2IwF@60sec	100	100	100	100	96	97.98	97.4	100	97.5	88.4
E2F2C@60sec	25	45.8	61.2	44.9	32.3	41.41	26.8	28.7	40.2	48.3
eSBR@60sec	66.7	54.2	81.64	48.9	68.7	75.76	88.6	83.4	75.9	79.4
NJL@60sec	72.3	37.5	73.5	93.87	93.4	83.83	94.5	82.55	86.5	82.4
HM@120sec	100	100	100	100	100	100	100	98.65	100	90.95
HMwF@120sec	100	100	100	100	100	100	100	96.64	100	88.44
EN2IwF@120sec	100	100	100	100	100	99	100	100	100	89.1
E2F2C@120sec	32.3	54.2	69.1	55.1	51.3	63.6	41.2	55.03	54.8	52.8
eSBR@120sec	71.2	62.5	84.6	77.6	77.8	80.81	93.3	94.63	86.2	80.4
NJL@120sec	73.6	70.83	78.4	95.91	100	90.9	100	92.6	96.5	83.42

In general, the first three methods — HM, HMwF, and EN2IwF — achieve a larger percentage of informed vehicles at the San Francisco map than at Valencia. This happens because, as mentioned previously, the former has fewer streets and junctions, granting vehicles more free space for communication. With fewer obstacles, BS communication, used by the three methods, is able to reach more vehicles than at the latter more complex map. An exception can be seen for HM@10sec, showing 78.52% vehicles are informed at the Valencia map and 66.4% are informed at the San Francisco one. This is caused by randomly having better signals connecting the BS to the vehicles at the Valencia map than at the San Francisco one. However, this is an outlier according to the remainder of the results.

Also, it is possible to infer from the results that, given enough time, *i.e.*, for notification times of 60 and 120 seconds, the use of a forwarder vehicle becomes

less relevant. This can be seen by the increasing proximity between the results for the HM, the HMwF, and the EN2IwF methods. Nevertheless, since critical warning messages have strict delay requirements, reaching the most vehicles in less time becomes important. For notification times of 10 seconds, CF vehicles improve the percentage of informed vehicles given there are enough vehicles that can be reached by the elected CFs. This becomes clear by verifying that the HM (no forwarders) outperforms the HMwF and the EN2IwF for 25 vehicles in the network, but as the number of vehicles increases, the HMwF and the EN2IwF perform better at the Valencia map. The difference between the maps results also suggests that more obstacles (Valencia) also favors the use of CFs.

Moreover, the results corroborate with the Cluster Merging Algorithm objective of maintaining high reliability and low dissemination delays. For the Valencia scenario, considering the notification time of 120 seconds, the percentage of informed vehicles is above 85% for HM, HMwF, and EN2IwF. On the same scenario, HMwF keeps the delay to inform the last vehicle below 20ms considering 50 vehicles in the network, while HM keeps the delay below 100ms considering higher densities. On the San Francisco scenario, the three methods are able to notify 100% of the vehicles in 120 seconds of the notification time, while delays are kept under 90ms by HM and HMwF.

4.6 CONCLUSION

The rise in the number of traffic accidents calls for better management of traffic using ITS. However, the implementation of intelligent systems require efficient and judicious management of the inter-vehicle communications.

A balance between coverage and delays needs to be achieved when disseminating messages to help in preventing accidents. The usage of a cellular network, such as 5G, in combination with V2V technologies can greatly improve coverage, but a study of the added delays is required to optimize and balance the costs and benefits.

In this regard, several methods combining the use of vehicle clusters, cluster forwarders, and a 5G base station were compared to established benchmark proposals, namely, eSBR and NJL.

According to the results shown, a good trade-off was achieved by the HMwF proposed method that features the communication of a vehicle that crashed with its CM, then, with a BS, CFs, other CMs, finally reaching all vehicles. The usage of CFs can speed up the dissemination process for high vehicle densities because there are fewer CFs in HMwF than there would be CMs in HM waiting for BS data. Therefore, even though HMwF has one more tier in the communication chain (the CFs) when compared to the HM chain, having fewer nodes in the BS schedule (less CFs in HMwF versus more CMs in HM) compensates for the additional tier transmission delay. This results in an overall improvement in message delay.

The results achieved by the methods that use the BS on their communication chain also show that the dissemination reliability is improved when compared to previous methods such as eSBR and NJL. In Section 4.3, we mention that safety applications have delay requirements of $20ms$ for the dissemination in the vicinity of the warning event. In this work, only the delay to inform the last vehicle on the network is considered. Such metric is kept under $100ms$ for all vehicle densities, considering HM and HMwF, meaning that $20ms$ only for the proximity of the event should be feasible. Capturing the new metric for this test is deferred to a future work. Notwithstanding, both the delays to inform the last vehicle on the network and the percentage of informed vehicles, considering HM and HMwF, outperform at least one of the benchmark proposals, proving that both reliability and timely dissemination are improved when compared to previous work.

All results were discussed in the previous section.

CHAPTER 5

THREE-FACTOR CLUSTER MERGING³

Several protocols and models have been proposed to address the broadcast problem, for which clustering has proven to be helpful as shown in previous chapters. In Chapter 3, we proposed a cluster merging algorithm with a cluster master selection based on two factors — the vehicles number of one-hop neighbors and their speed similarity. Also, in Chapter 4, we proposed different communication chains, directly related to the clustering due to the use of a 5G base station both for cluster merging and for warning messages dissemination. In this chapter, we re-evaluate all the communication chain models after proposing a new factor for the cluster master election — the estimated received signal power from the base station. Our results show that there is a trade-off between the percentage of informed vehicles and the delays to inform the last vehicles on the network that can be controlled via the weight factors.

5.1 INTRODUCTION

The Intelligent Transportation System (ITS) is one application of VANETs that aims to improve road safety. ITS proposes to achieve such a goal by connecting vehicles and infrastructure, providing communication between vehicles and between vehicles and infrastructure, through which road accidents can be either prevented or communicated via warnings after the fact (Hamdi *et al.*, 2020).

Not only safety applications, but also other uses of VANETs, have requirements regarding a common set of metrics — communication reliability, dissemination delay, and packet delivery ratio. It would be expected that purely rebroadcasting as soon as a vehicle receives a warning message — also known as flooding — would result in high reliability and packet delivery ratio, since there would be high message redundancy, and low dissemination delay because chained rebroadcasts would transport a

³Reference publication.

warning as quickly as possible towards the farthest vehicles. However, in practice, the opposite is observed. The high number of transmitting vehicles (especially in high-density networks, common in urban scenarios) cause long channel contention delays as vehicles wait for a chance to transmit when the channel is not busy. Moreover, the high number of contending nodes increase the probability of concurrent transmissions over the channel, causing collisions. This effect is called broadcast storm (Sospeter *et al.*, 2019), as mentioned in previous chapters.

Next, several schemes proposed to control broadcast storms are analyzed. Even though many of them have already been discussed throughout this thesis, it is worth revisiting those schemes and advancing our knowledge on them.

One of the first approaches that appeared to control broadcast storms was the counter-based scheme. In this approach, each message receives a counter, incremented on every rebroadcast. When a threshold is crossed, the message is not retransmitted any further (Martinez *et al.*, 2010).

Another proposal was the distance-based scheme. In this case, messages are rebroadcast only if the re-transmitter is at least farther than a minimum distance from the last transmitter. This guarantees better additional coverage (AC) is gained with each new rebroadcast.

With the location-based scheme, rebroadcasts only happen if enough AC is attained. However, the AC calculation requires the positions of the last transmitters and the coverage intersection calculations have high computational cost, which motivated the creation of less costly probabilistic schemes.

One of the probabilistic proposals is the weighted p -persistence scheme, where a vehicle rebroadcast a packet with a distance-based probability p . On the slotted 1-persistence scheme, the rebroadcast probability is 1, nevertheless the packet is sent on a time slot calculated based on the vehicle distances. Similarly, the slotted p -persistence scheme uses distance-based time slots, however with rebroadcast probability p (Wisitpongphan *et al.*, 2007).

The Last One (TLO) is another scheme proposed to avoid broadcast storms. Only the farthest vehicle within communication range of the sender is allowed to rebroadcast the message (Martinez *et al.*, 2010). It is clearly a scheme for highways, since

in urban scenarios, the farthest vehicle in four directions (at least) would need to be found, increasing the complexity of the scheme.

An improvement of TLO was proposed — the Adaptive Probability Alert Protocol (APAL) — by using adaptive wait windows and adaptive transmission probabilities, reducing the chances of broadcast storms.

Later, proposals started considering scenarios more complex than highways. The enhanced Street Broadcast Reduction (eSBR) was a scheme proposed to operate in urban scenarios, dealing with signal blockage caused by buildings. Two situations enable rebroadcasts in the eSBR scheme — (i) the distance from the vehicle that sent the message is at least larger than a distance threshold and (ii) vehicles are in different roads. In both cases, it must be the first time the vehicle receives the warning message. In terms of percentage of informed vehicles and number of messages received per vehicle, improvement over previous approaches is only marginal, with some complexity reduction (Martinez *et al.*, 2010).

In Sanguesa *et al.* (Sanguesa *et al.*, 2013), the authors found out that eSBR performance in terms of number of messages received per vehicle was poor in high-density scenarios. Therefore, Sanguesa *et al.* proposed a more restrictive scheme, the Nearest Junction Located, which only allows the vehicles closest to junctions to rebroadcast messages. The authors also show that, even though the percentage of informed vehicles using NJL in sparse scenarios is below the percentage achieved by eSBR, the number of messages received per vehicle is still less in NJL than compared to eSBR.

In our previous work (AlQahtani *et al.*, 2021) presented in Chapter 3, we proposed a scheme to reduce the chances of broadcast storms on highways via cluster merging. In our previously proposed scheme, only cluster masters were allowed to rebroadcast warning messages to their clusters. This means that fewer clusters yield fewer rebroadcasts and, therefore, lower chances of causing broadcast storms. Hence, we focused our proposal on merging clusters, which tend to become fragmented due to the difference in vehicle speeds — some vehicles overtake their clusters, while others are left behind. We used a two-factor selection algorithm to elect the cluster master of a merged cluster, which was able to achieve a percentage of informed vehicles slightly

below other schemes such as NJL and eSBR, while keeping the number of messages received per vehicle way below those same schemes.

The two factors used in our previously proposed algorithm were the number of neighbors of a vehicle and such vehicle speed compared to all the other vehicles in the cluster, the latter captured in a metric called the leadership value. However, we came to the conclusion that neither of the metrics consider the distance between the potential cluster master and the base station, which might prevent the whole cluster from receiving the warning message if the connectivity between the base station and the elected cluster master is bad. Hence, in this work, we propose a third metric — the estimated received power by the vehicle from the base station — and we investigate the impact of adding such a factor to the algorithm on the percentage of informed vehicles and on the delay to inform the last vehicle of the network.

The remainder of this chapter is organized as follows. In Section 5.2, we review work related to broadcast storms and some other proposals that inspired us to include a new factor to the cluster election algorithm. Then, the system model, assumptions, and details about the proposed schemes are shown in Section 5.3. The results and our discussion on the achieved results can be found in Section IV. Finally, Section V concludes the paper with our comments on the value of the achieved results and some venues for future work.

5.2 RELATED WORK

In (Cooper *et al.*, 2017), the authors present a useful survey of clustering techniques for VANETs. Clustering is identified as a mechanism used to help the network scale while maintaining high communication reliability, but also as an infrastructure provider for accidents detection. One of the mentioned proposals coordinates the cluster head selection to enable quickly warning dissemination in the cluster, which can hopefully prevent undesirable coincidental events after an accident has occurred.

The authors of (Sattar *et al.*, 2018) start from plain flooding, which causes broadcast storms. Sattar *et al.* revisit several enhancements of plain flooding in the literature using both the MAC layer and the network layer analyses, also including the use

of the cellular network to improve both reliability and SMD delay. They have also proposed the use of restrictive flooding of safety messages via a control channel, proving that the network layer needs to provide multi-hop capabilities to increase flooding reliability.

Sospeter *et al.* (2019) studied the broadcast storm problem to propose an adaptive dissemination protocol. The authors created the redundancy ratio metric, which measures the ratio between all messages received in the network and the new messages (no re-broadcasts). As the metric increases, indicating the density of the network also increased, vehicles probability of re-broadcast a message decreases, therefore controlling re-broadcasts based on the network density. Moreover, packets travelling along the traffic direction are discarded, since vehicles past the accident do not need to be warned. Also, the waiting time prior to node re-broadcast is calculated according to the distance between receiver and transmitter — the closest the receiver to the accident, the more the receiver vehicle waits before re-broadcasting, which reduces the likelihood of (re)occurrence of a broadcast storm closest to the crashed vehicle.

In (Ren *et al.*, 2021), Ren *et al.* presents several clustering techniques grouped according to their application. On the traffic safety subsection, they cite the Selective Reliable Broadcast (SRB) protocol, where the source of a safety message detects nearby clusters and chooses the farthest nodes in each cluster as the message forwarder. Since only a few vehicles within range are selected to re-broadcast the message, there are less transmissions within range of the first transmitter, which reduces the chance of a broadcast storm. Moreover, the authors study hybrid clustering, which is related to vehicles ability to communicate both via DSRC and via cellular network. Many proposals are analyzed in this work, however none of them considers 5G — only LTE, LTE-A, and UMTS are considered.

In (Cooper *et al.*, 2017), the survey considers the GPS signal loss problem. The authors allude to how signal quality can be used as a clustering metric, since a reliable GPS signal is required for vehicles to precisely determine their position and speed. This work motivated us to study signal quality as a clustering metric, but for wireless interfaces other than the GPS. Kukliński and Wolny (2009) used such a metric considering inter-vehicle signal quality (*i.e.*, between vehicles). The latter authors go

even further, predicting the future link quality to decide whether clustering should be re-created because the link is likely to provide poor quality and, therefore, passing vehicles should not be permitted into the cluster. Given the signal quality metric has already been applied to the GPS signal (Cooper *et al.*, 2017) and to the communication between the vehicles Kukliński and Wolny (2009), we chose to apply the same idea to the link quality between the BS and vehicle. Copper *et al.* determined that the signal to noise ratio (SNR) and the received signal strength (RSS) can together be used as the signal quality metric. Consequently, in this work we used an estimate of the received power, which has computationally a lower cost.

5.3 A NEW VANET SYSTEM MODEL

We consider a VANET operating in an area covered by a 5G BS, where vehicles in an urban scenario are gathered in clusters lead by a cluster master (CM). V2V communication is carried out via DSRC, while V2I, via 5G. Thus, one cluster can reach another cluster via CMs communicating with the BS. Also for inter-cluster communication, another class of vehicles are considered — cluster forwarders (CFs). Such vehicles provide inter-cluster communication avoiding the use of the 5G network.

Two maps are considered in this work — Valencia, a more complex map, featuring 2,829 streets and 2,233 junctions, and San Francisco, a simpler map, comprising 725 streets and 818 junctions.

The considered benchmark proposals are eSBR Martinez *et al.* (2010) and NJL Sanguesa *et al.* (2013), both analyzed in Section 5.1.

Several different communications chains are considered: (i) the Hierarchic Model (HM); (ii) the Hierarchic Model with Forwarder (HMwF); (iii) the Event Node to Infrastructure with Forwarder (EN2IwF); and (iv) the Event node to Forwarder to Cluster (E2F2C). The communication chain for each of those work as follows:

- (i) The message departs from the event node, proceeding to its CM, BS, other CMs, and all cluster members;

- (ii) The warning goes from the event node to its CM, BS, CFs, CMs, finally reaching all members;
- (iii) Now, the event message is sent by the event node to the BS, CFs, CMs, and all cluster members;
- (iv) The message departs from the event node to the closest CF, to other CMs and CFs, reaching all cluster members without using the infrastructure (BS).

Some pre-existing conditions are considered. The clusters must already be formed; CFs need to be elected at all times; and all vehicles know all the CF locations and identities.

The CF for each junction is selected by the BS by detecting the closest vehicle for each of the junctions in the BS coverage area.

A cluster merging algorithm is considered to continuously reduce the number of CMs and, therefore, keep broadcast storms near clusters boundaries under control. Also, since each CM within the BS range requires communication resources to exchange data with the BS, having less CMs in the area — which is exactly what the cluster merging is for — will save communication resources and reduce delays between CMs and the BS. When CMs of different clusters enter in mutual DSRC communication range, the cluster merging begins with the help of the BS. Information about the cluster members is shared and, among the newly formed cluster, a new CM is elected, as discussed below.

Our 2F-CM algorithm (AlQahtani *et al.*, 2021) relied on two metrics of each vehicle — the vehicle number of neighbors and its speed similarity value. In this work, we propose the addition of a (normalized) estimated received power from the BS by each vehicle. Moreover, normalization is also applied to the number of neighbors metric to make it fairer⁴ when compared to the other protocols. The metrics are calculated as follows:

⁴In this context, fairer means that, after the multiplication of the metric and its weight value, it is in the same order of magnitude of the other metrics times their weight factors.

- The number of one-hop neighbors of vehicle k in cluster m , $N_{m,k}$, given by

$$N_{m,k} = \sum_{n=1}^{|\mathcal{C}_m|} [\text{dist}(k,n) < Tx_{range}] \quad (5.1)$$

where $[\text{dist}(k,n) < Tx_{range}]$ is 1 if the Euclidean distance (see Eq. 5.2) between vehicles k and n is less than Tx_{range} , otherwise $[\text{dist}(k,n) < Tx_{range}]$ is 0; $|\mathcal{C}_m|$ is the number of vehicles in the m^{th} cluster; and Tx_{range} is the maximum distance between two vehicles that allows them to communicate with each other.

$$\text{dist}(k,n) = \sqrt{(x_k - x_n)^2 + (y_k - y_n)^2} \quad (5.2)$$

- The speed similarity value of vehicle k in cluster m , $L_{m,k}$, which measures the speed similarity between said vehicle and all others in the cluster. To calculate that, a stability factor, $SF_{m,k}$, which measures the average speed difference between vehicle k and all the others in cluster m must to be calculated first via:

$$SF_{m,k} = \frac{\sum_{n \in \mathcal{C}_m} |\vec{s}_n - \vec{s}_k|}{|\mathcal{C}_m|} \quad (5.3)$$

where \mathcal{C}_m is the set of vehicles in cluster m , \vec{s}_k is the speed of vehicle k , and \vec{s}_n is the speed of vehicle n . Then, the leadership value is defined as:

$$L_{m,k} = \frac{1}{1 + SF_{m,k}}. \quad (5.4)$$

$L_{m,k}$ is normalized between 0 and 1.

- The estimated received power from the BS by vehicle k , given by:

$$P_{m,k} = P_t \times \left(\frac{c}{4\pi d_k f} \right)^2 \quad (5.5)$$

where P_t is the transmission power, c is the speed of light ($300 \cdot 10^6 \text{m/s}$), d_k is the distance between the BS and vehicle k in meters, and f is the BS carrier frequency in hertz.

Before combining all metrics, the number of neighbors, $N_{m,k}$ and the estimated received power, $P_{m,k}$, need to be normalized to enable a fair linear combination with the leadership value, $L_{m,k}$. Thus, $N_{m,k}$ should be divided by the maximum number of neighbors, $N_{m,max}$, and $P_{m,k}$ should be divided by the maximum estimated power, $P_{m,max}$, which are calculated, respectively, via:

$$N_{m,max} = \max_k N_{m,k} \quad (5.6)$$

$$P_{m,max} = \max_k P_{m,k} \quad (5.7)$$

Then, arbitrary weight factors $wf1$, $wf2$, and $wf3$ are associated with each normalized parameter respectively and the vehicle with highest suitability, β_k , calculated as shown in Eq. 5.8 next, is selected as CM.

$$\begin{aligned} \beta_k = & \left(wf1 \times \frac{N_{m,k}}{N_{m,max}} \right) + \\ & + (wf2 \times L_{m,k}) + \left(wf3 \times \frac{P_{m,k}}{P_{m,max}} \right) \end{aligned} \quad (5.8)$$

Subject to:

$$wf1 + wf2 + wf3 = 1 \quad (5.9)$$

Weight factors are evenly distributed ($1/3$ each) as a first step in this work.

The suitability value is determined for all vehicles in the cluster thereby electing a CM for the new merged cluster (*i.e.*, the vehicle with highest suitability value). The whole procedure can be seen in Algorithm 5.

The Krauss (Krauss, 1998) mobility model is used for inserting vehicles into the network and for speed updates. The objective of the model is to distribute the vehicle traffic among the network edges (streets) and avoiding vehicle crashes.

Since no fully-functional frameworks for simulating 5G were found for OMNeT++, an approximation of the technology is used. Very large transmission and propagation

Algorithm 5 Cluster merging algorithm

Require: $\mathcal{C}_i; \mathcal{C}_j$; CMs of \mathcal{C}_i and \mathcal{C}_j within communication range from each other; $wf1$; $wf2$; $wf3$; and $wf1 + wf2 + wf3 = 1$

```

1: if  $|\mathcal{C}_i \cup \mathcal{C}_j| \leq C^{thr}$  then
2:   CM of  $\mathcal{C}_i$  sends intent to merge to BS
3:   CM of  $\mathcal{C}_j$  sends intent to merge to BS
4:   for all vehicle  $v_q$  in  $\mathcal{C}_m$  do
5:     BS sends merge begin to  $v_q$ 
6:      $v_q$  changes state to cluster master candidate
7:      $v_q$  finds its number of one-hop neighbors using Eq. 5.1
8:      $v_q$  estimates the received signal strength from BS using Eq. 5.5
9:      $v_q$  replies to BS with its speed, number of neighbors, and estimated
received signal strength
10:  end for
11:  BS calculates the maximum number of neighbors using Eq. 5.6
12:  BS calculates the maximum received signal strength using Eq. 5.7
13:   $\beta_r \leftarrow 0$ 
14:  for all vehicle  $v_q$  in  $\mathcal{C}_m$  do
15:    BS calculates  $v_q$  speed similarity using Eq. 5.4
16:    BS calculates the suitability  $\beta_q$  using Eq. 5.8
17:    if  $\beta_q > \beta_r$  then
18:       $\beta_r \leftarrow \beta_q$ 
19:       $v_r \leftarrow v_q$ 
20:    end if
21:  end for
22:   $\mathcal{C}_i \leftarrow \emptyset$ 
23:   $\mathcal{C}_j \leftarrow \emptyset$ 
24:   $v_{m,r} \leftarrow v_r$ 
25:   $v_{m,r}$  changes state to CM
26:  for all vehicle  $v_{m,k}$  in  $\mathcal{C}_m \setminus v_{m,r}$  do
27:     $v_{m,k}$  changes state to cluster member
28:  end for
29: end if

```

delays — $1ms$ and $0.3ms$, respectively, empirically determined — are used to simulate the real protocol overheads.

5.4 RESULTS AND DISCUSSION

To simulate the model’s performance, we use version 5.5.1 of the OMNeT++ discrete events simulator, version 1.6.0 of the SUMO road traffic simulator, and version 5.0 of the Veins framework for wireless communication.

The main simulation parameters are shown in Table 5.1. Measurements of the percentage of informed vehicles are taken at six different points in time after the event (crash) happens. The simulations are run for five different numbers of vehicles in the whole network to assess the effects of increasing vehicle density on the network. To calculate the DSRC transmission times, the warning message was assumed to have a fixed size of 256 bytes. Also, the weights used on the 2-factor models are 0.1 and 0.9, respectively, because no normalization was applied to the number of neighbors for the 2-factor models; thus, the first weight factor needs to make the number of neighbors (up to tens) comparable to a normalized speed similarity value. Regarding the 3-factor models, all terms have been previously normalized, allowing the weight factors to be balanced at first.

TABLE 5.1: Simulation Parameters

Parameter	Value(s)
Notification times after event	{10, 20, 30, 60, 90, 120} seconds
Number of vehicles in the network	{25, 50, 100, 150, 200}
Maps	{Valencia, San Francisco}
Warning message length	256 bytes
Maximum communication range	{300m (DSRC), 1km (5G)}
2-factor models weights {wf1, wf2}	{0.1, 0.9}
3-factor models weights {wf1, wf2, wf3}	{0.333, 0.333, 0.333}

As seen in Fig. 5.1, for 25 vehicles on the Valencia map, 3f_HM and 2f_HM are faster in warning the whole network, but the other proposals that use the 5G tier also reach 100% notification. As the number of vehicles increase, the 3-factor models achieve up to 10% fewer informed vehicles than their 2-factor counterparts. This is due to the received signal factor, which pushes the election of the CM to a vehicle which is closer to the BS, leaving vehicles out of the cluster and, therefore, not informed. However, this is compensated by the lower delays to inform the last vehicle, shown in Fig. 5.2, due to the CM being closer to the BS and, thus, experiencing less

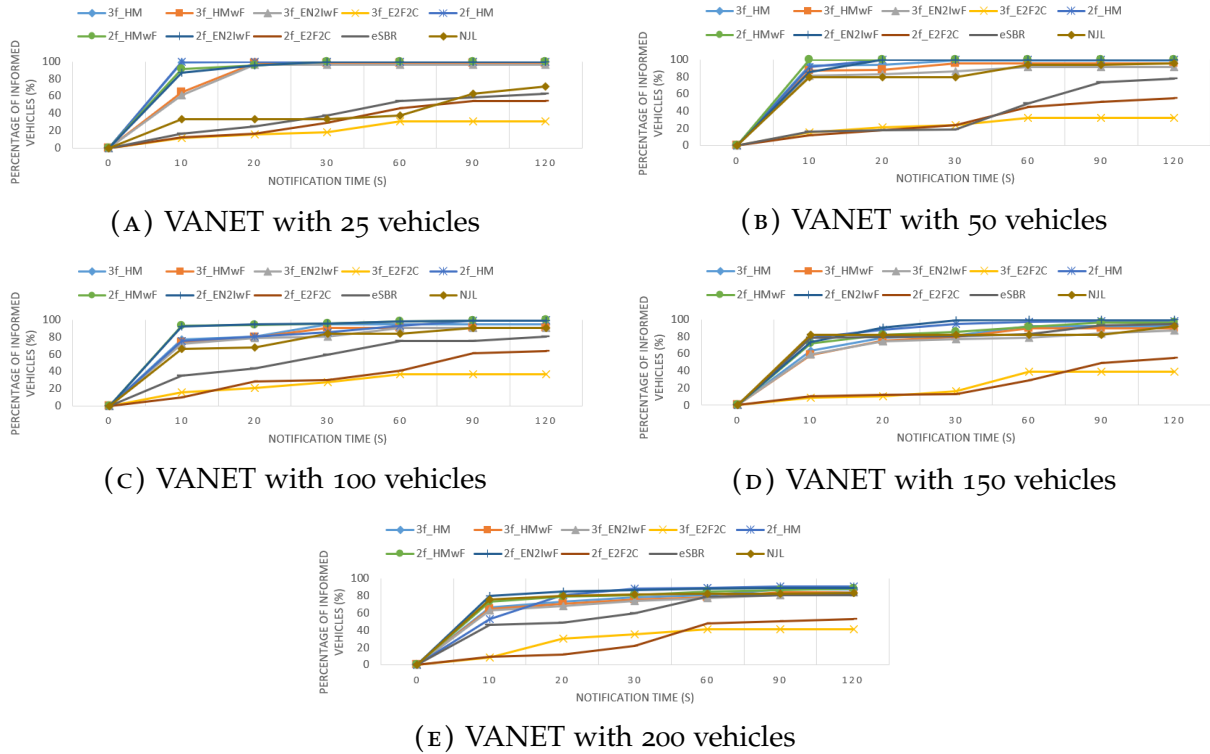


FIGURE 5.1: Percentage of informed vehicles over time for the Valencia scenario with different number of vehicles in the VANET for all proposed methods and benchmarks

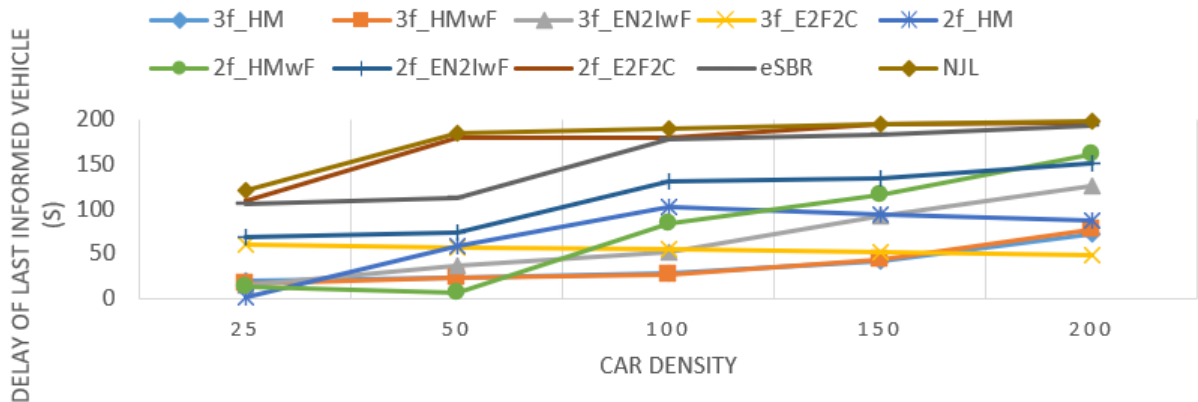


FIGURE 5.2: Delay for informing the last vehicle for all proposed methods and benchmarks for the Valencia scenario

propagation delays. Even though Fig. 5.2 shows lower delays for the 3f_E2F2C model with 200 vehicles in the network, the low number of vehicles informed does not allow a fair comparison to the other models due to the low number of vehicles informed (about 40%). As a result, we see a trade-off between the percentage of informed vehicles and the delays to inform the last vehicle.

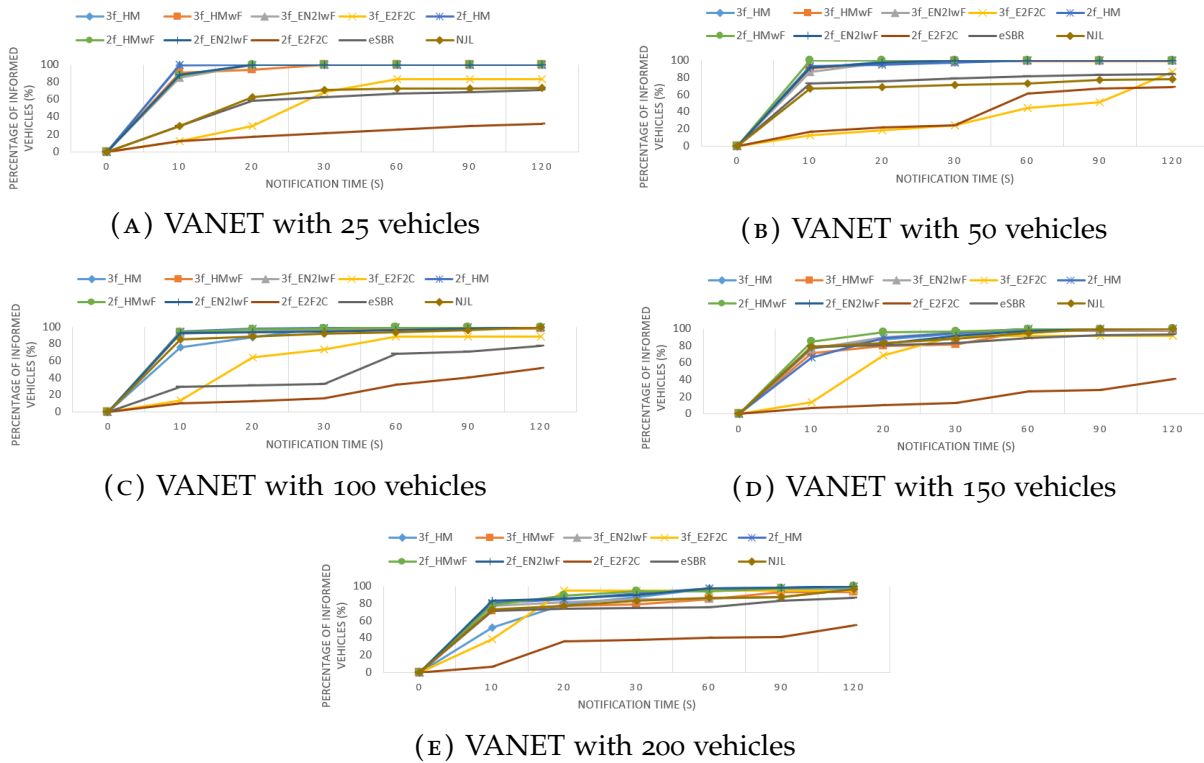


FIGURE 5.3: Percentage of informed vehicles over time for the San Francisco scenario with different number of vehicles in the VANET for all proposed methods and benchmarks

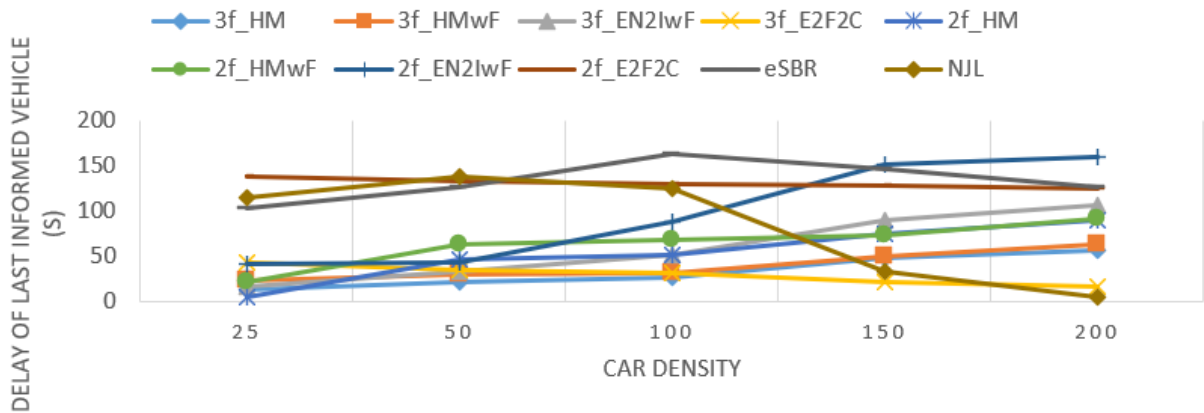


FIGURE 5.4: Delay for informing the last vehicle for all proposed methods and benchmarks for the San Francisco scenario

A similar effect happens on the San Francisco map. As more vehicles are inserted into the network, the 3-factor models may inform up to 7% less than their 2-factor counterparts as can be seen in Fig. 5.3. Again, the 3-factor models achieve up to 25ms reduced delays than their 2-factor counterparts, which can be verified in Fig. 5.4. This

time, $3f_E2F2C$ performs better than on the Valencia map and their delays become significant. The latter model achieves one of the best results due to the concentration of vehicles clustered into a smaller area, with fewer streets and junctions, characteristic of the San Francisco map.

5.5 CONCLUSION

In this chapter, we discussed how broadcast storms can hinder VANET communications in ways that impact SMD and vehicle traffic (*e.g.*, accidents) situation awareness. Moreover, we showed how our previous proposal was able to improve the percentage of informed vehicles and reduce delays when compared to other SMD protocol models.

The addition of a new factor for CM election after a cluster merging is proposed here. Presented results show how electing a CM closer to the BS can improve delays for informing vehicles, even though some vehicles might be left out of clusters. Therefore, we conclude there is a trade-off between the delays and the percentage of informed vehicles, which can be controlled by the weight factors. All results were discussed in the previous section.

In this work, fixed and equal values were considered for $wf1$, $wf2$, and $wf3$, however the next chapter features a study of these factors considering both the delay and informed vehicles metrics.

CHAPTER 6

WEIGHT FACTORS STUDY

As concluded in Chapter 5, the *delays to inform vehicles/percentage of vehicles informed* trade-off can be controlled by varying the weight factors that influence the CM election after a cluster merging. Thus, this chapter builds on our previously proposed cluster merging scheme combined with several communication chains, focusing on different combinations of weight factors that change the importance of a vehicle number of neighbors, speed difference to the cluster average, and received power from the closest base station when electing a cluster master for a merged cluster. The presented results show that such factors have great impact on the number of informed vehicles on the VANET and on the delay to warn the last vehicle.

6.1 INTRODUCTION

The number of vehicles on roads grows at a fast pace, giving rise to the number of road accidents. To tackle the issue, the Intelligent Transportation System (ITS) has been envisioned, making use of vehicular ad-hoc networks (VANETs) to coordinate vehicles via wireless communication to avoid fatalities (Hamdi *et al.*, 2020).

The first method tried for warning messages dissemination, which are meant to give vehicles a better visibility of their surroundings to avoid accidents, was plain flooding. That method instructs vehicles that need to send a warning message to broadcast it and vehicles that receive such warning to re-broadcast it. Since all vehicles in the network will try to broadcast in a short period of time, wireless packet collisions soon make communication impossible. This problem is known as a broadcast storm (Sospeter *et al.*, 2019).

Thus, on further research, several other methods have been tried. Some instructed vehicles within a minimum distance from the sender to refrain from re-broadcasting. Others attached a counter to the broadcast messages, ceasing further broadcasts after a given number of hops. Also, probabilistic methods were used, where each receiving

vehicle has a probability p of re-broadcasting a received message. All of them contained the broadcast storm up to a given vehicle density, however more sophisticated methods were still required. One of them, the enhanced Street Broadcast Reduction (eSBR), used both a minimum re-broadcast distance or the requirement for vehicles to be in different streets. This method improved dissemination even further, however it did not perform well on high-density scenarios (Martinez *et al.*, 2010). Then, the Nearest Junction Located (NJL) method was proposed (Sanguesa *et al.*, 2013), which only considered vehicles in different streets for re-broadcast, which performed better than eSBR in high-density scenarios.

The previously mentioned methods were also combined with clustering, which boosted the containment of broadcast storms (Cooper *et al.*, 2017). However, the highly-directive nature of the dedicated short-range communications (DSRC) interfaces available on vehicles prevented some vehicles from being reached due to the presence of obstacles, such as buildings, that severely attenuate the wireless signal. Then, the concept of forwarder vehicles responsible for transmitting incoming messages from one street towards another one further improved the reach of warning messages without causing broadcast storms (Martinez *et al.*, 2010; Sanguesa *et al.*, 2013).

On top of these previous clustering and forwarding methods, we proposed the 2-factor cluster merging (2F-CM) (AlQahtani *et al.*, 2021), also presented in Chapter 3, and further improved it by including a new factor, creating the 3-factor cluster merging (3F-CM) (AlQahtani and Sheldon, 2021), also presented in Chapter 5. However, the previous 3F-CM work was limited to the comparison with the 2F-CM one, assuming equal weight factors for the election of the new cluster master of the merged cluster. In this work, we propose the study of the effects of each of the factors by including more simulations, still considering the eSBR and NJL benchmark proposals.

The remainder of this chapter is organized as follows. In Section 6.2, we provide a summary of the related work, which lead to the current study. The considered method is summarized in Section 3. Section 4 presents the achieved results and their discussion and, in Section 5, we draw the conclusions of this chapter.

6.2 RELATED WORK

Clustering has been adopted as a logical step to limit broadcast storms, since the independence for broadcasting of all vehicles in the network is divided in smaller groups under the coordination of the cluster masters (CMs), also known as cluster heads (CHs) (Cooper *et al.*, 2017). Such vehicles with coordinating capabilities may also incorporate routing and relaying functions, the latter being considered in this work. As explained further, in Section 6.3, CMs may act as message relays between their cluster members and the infrastructure to reach other clusters or, when the infrastructure is not considered in the communication chain, CMs are relay messages to and from other clusters via their CMs. Nonetheless, the very nature of clustering might be a source of range-constrained broadcast storms depending on the neighborhood discovery process adopted, as in the proactive and reactive examples given next. *Hello messages*, which are proactively sent by all vehicles to allow the CM to determine the members of the cluster, might overwhelm the wireless medium depending on the vehicles density and on the messaging frequency, whereas *inquiry messages* can be sent by the CM, prompting nearby vehicles to react with a reply, therefore, diminishing the risk of a broadcast storm.

Moreover, to reach the entire network, inter-cluster communication is required. Special nodes can be used specifically for forwarding messages from one cluster to another, as in (Tseng *et al.*, 2002), or vehicles can use a longer-range wireless interface to provide such connectivity. When CMs have longer-range interfaces, they could also aggregate the inter-cluster communication functionality by relaying their members messages either to and from the infrastructure or to and from other CMs directly (Ahsan *et al.*, 2020). A combination of both is assumed by some of the communication chains used in this work.

When a cluster is created, the most suitable vehicle needs to be elected CM in order to reach the maximum number of vehicles to make them members and to provide stable communication for the longest period possible. For that, several factors can be used. For instance, in (Khan and Fan, 2018), link lifetime — the duration of the connection between vehicles —, average relative speed, and average relative distance are the factors used for the election of a new CM. The authors show that the

combination of these factors work together to provide connectivity for more vehicles for longer. In this work, we consider the vehicle number of neighbors, which works similarly to the average relative distance, the average relative speed, even though we normalize it, and the normalized signal power received from a base station (BS), for a reason explained in the next paragraph. We believe that the relative distance pushes the CM election to a vehicle close to the center of the cluster, while the relative speed favors the selection of a vehicle that will be able to communicate longer with all the others in the cluster. Both are able to increase link lifetime, which makes the latter somewhat redundant with the other two.

Given the limitations of DSRC to overcome obstacles, alternatives can be considered for longer range communication. As mentioned in (Ren *et al.*, 2021), cellular technologies can be used to reach large areas. However, the work in (Xu *et al.*, 2017) shows that, contrary to DSRC, 4G technology cannot provide sufficient end-to-end communication latency to fulfill safety application requirements. Therefore, as the deployment of 5G approaches, it could be considered as a candidate for vehicle-to-infrastructure (V2I) communication in VANETs, as suggested in (Ullah *et al.*, 2019). Therefore, an approximation of the new 5G technology, for which VANET simulators still lack support, is considered in this work, also taking the signal power received from a 5G BS into account for the CM election, guaranteeing better V2I connectivity.

6.3 SYSTEM MODEL SUMMARY

The clustered VANET operates on two urban scenarios — a simpler (less streets and junctions) and a more complex one —, which means there are buildings that can block the DSRC communication between vehicles. Thus, a 5G interface is also available for vehicles to communicate with the infrastructure (vehicle-to-infrastructure — V2I). There are also cluster forwarder (CF) vehicles, which are the vehicles detected to be closest to junctions to help overcome obstacles depending on the adopted communication model, explained further in this section.

In order to reduce broadcast storms, a cluster merging method we first proposed in (AlQahtani *et al.*, 2021) is applied whenever two CMs come within DSRC commu-

nication range. Moreover, merging clusters help reducing V2I contention, since less CMs will need to communicate with the infrastructure. With the help of the 5G BS, a new cluster is formed and a new CM is elected by choosing the vehicle with the highest suitability. Such metric is derived from the normalized number of neighbors, $N_{m,k}/N_{m,max}$, from the leadership value, $L_{m,k}$, which measures how close the vehicle speed is to the average cluster speed, and from the normalized received signal power from the BS, $P_{m,k}/P_{m,max}$. To combine these factors, they are multiplied by weight factors, which we intend to study in this work, to yield the suitability value of vehicle k as in Equation 6.1.

$$\beta_k = \left(wf1 \times \frac{N_{m,k}}{N_{m,max}} \right) + (wf2 \times L_{m,k}) + \left(wf3 \times \frac{P_{m,k}}{P_{m,max}} \right) \quad (6.1)$$

subject to:

$$wf1 + wf2 + wf3 = 1 \quad (6.2)$$

Regarding the V2V and V2I communication, four different communication chains are considered, as proposed in Chapter 4 and reviewed next. In the Hierarchic Model (HM), a warning message is generated by a vehicle subject to some event, which is sent to the CM. The latter sends the message to the BS, which delivers it to all CMs, in turn, informing their members. The Hierarchic Model with Forwarder (HMwF) adds the CF between the BS and all CMs to HM. In the Event Node to Infrastructure with Forwarder (EN2IwF), the event node bypasses the first CM of HMwF, sending the message straight to the BS. And, last, the Event node to Forwarder to Cluster (E2F2C) model does not consider the use of the infrastructure. The event node sends the warning message to the closest CF, reaching other CFs and CMs, finally reaching all other vehicles.

The considered metrics to assess the effectiveness of clustering and of the communication chains are the percentage of informed vehicles and the delay to inform the last vehicle in the network (Ren *et al.*, 2021).

Vehicles mobility follow the Krauss model (Krauss, 1998) and the 5G communication is simulated by using high transmission and propagation delays to include the

protocol overheads, since there are no satisfactory 5G communication modules for the considered simulator yet.

6.3.1 Weight Factors Study

The weight factors considered in this work to assess the VANET performance according to the aforementioned metrics are given in Table 6.1.

TABLE 6.1: Weight Factor Combinations

#	wf1	wf2	wf3
1	1	0	0
2	2/3	1/3	0
3	2/3	0	1/3
4	1/3	2/3	0
5	1/3	1/3	1/3
6	1/3	0	2/3
7	0	1	0
8	0	2/3	1/3
9	0	1/3	2/3
10	0	0	1

6.4 RESULTS

A VANET comprised of 25 to 200 vehicles is simulated on the Valencia and San Francisco maps, featured by the SUMO mobility simulator, using the OMNeT++ simulator and the Veins communication framework. The main simulation parameters are given in Table 6.2.

TABLE 6.2: Simulation Parameters

Parameter	Value(s)
Number of vehicles in the network	{25, 50, 100, 150, 200}
Maps	{Valencia, San Francisco}
Warning message length	256 bytes
Maximum communication range	{300m (DSRC), 1km (5G)}
3-factor models weights {wf1, wf2, wf3}	Check Table 6.1

Next, we analyze the percentage of informed vehicles for each weight factor combination, presenting the result that achieved the maximum percentage for each of the

considered vehicle density. Then, the percentages are added across densities to find the weight factor combination that achieves the highest sum, which is taken as the best combination for the considered metric.

The highest percentage of informed vehicles across the communication methods for each given density and weight factor combination on the Valencia scenario is presented in Table 6.3. The data for all methods can be seen in Appendix A.1, Table A.1 for weight factor combinations 1–5 and Table A.2 for combinations 6–10. Corresponding charts are in Figure A.1 and Figure A.2, respectively.

TABLE 6.3: Percentage of vehicles informed on the Valencia map (method that achieved the maximum percentage for a given density)

wfs combination	Vehicles density					sum across densities
	25	50	100	150	200	
1	100 (HM)	100 (HM)	97.6 (HM)	94.71 (EN2IwF)	93.5 (HM)	485.81
2	100 (HM)	100 (HM)	98.2 (HM)	96.2 (HM)	96.7 (NJL)	491.1
3	100 (HM)	100 (HM)	97.8 (HM)	96.23 (NJL)	98.84 (NJL)	492.87
4	100 (HM)	99.4 (HM)	95.68 (HM)	97.69 (NJL)	99.3 (NJL)	492.07
5	100 (HM)	99.1 (HM)	96.9 (NJL)	98.48 (NJL)	99.5 (NJL)	493.98
6	95.7 (HM)	95.13 (HM)	94.6 (HM)	92.79 (HM)	91.5 (HM)	469.72
7	98.6 (HM)	96.7 (HM)	95.6 (HM)	94.32 (HM)	92.08 (HM)	477.3
8	100 (HM)	98.14 (HM)	96.9 (HMwF)	95.8 (HM)	94.6 (HM)	485.44
9	100 (HM)	98.9 (HM)	97.48 (HM)	96.9 (HM)	95.78 (HM)	489.06
10	100 (HM)	99.4 (HM)	98.62 (HM)	97.5 (HM)	96.9 (HM)	492.42

It can be seen that there is a high prevalence of the HM across the densities and combinations, but some combinations can benefit from adopting NJL for 150 and 200 vehicles in the network. The highest sum of percentages of informed vehicles is achieved by combination 5 ($wf1 = wf2 = wf3 = 1/3$), but combinations 2, 3, 4, and 10 percentages sum is less than 3% below the highest one and should, therefore, be considered depending on the results of the delays sum, presented further in this section.

The results achieved on the San Francisco map are shown in Table 6.4. Appendix A.2 presents the data for all methods — Table A.9 for weight factor combinations 1–5 and Table A.10 for combinations 6–10, with respective charts in Figure A.5 and in Figure A.6.

On a map with fewer streets and junctions, NJL does not perform as well as on the previous one, however EN2IwF performs best across densities for combinations

TABLE 6.4: Percentage of vehicles informed on the San Francisco map (method that achieved the maximum percentage for a given density)

wfs combination	Vehicles density					sum across densities
	25	50	100	150	200	
1	100 (EN2IwF)	97.76 (EN2IwF)	96.18 (EN2IwF)	94.71 (EN2IwF)	92.64 (EN2IwF)	481.29
2	100 (EN2IwF)	98.1 (EN2IwF)	97.3 (EN2IwF)	95.68 (EN2IwF)	93.79 (HM)	484.87
3	100 (EN2IwF)	98.67 (EN2IwF)	97.8 (EN2IwF)	96.89 (EN2IwF)	94.7 (HM)	488.06
4	100 (EN2IwF)	99.2 (EN2IwF)	98.35 (EN2IwF)	97.14 (EN2IwF)	95.64 (EN2IwF)	490.33
5	100 (HM)	100 (EN2IwF)	99.6 (EN2IwF)	98.5 (EN2IwF)	97.6 (HM)	495.7
6	100 (HM)	99.1 (HMwF)	98.2 (HM)	97.4 (HM)	96.58 (HM)	491.28
7	99.8 (HM)	98.6 (HM)	98.2 (HM)	96.4 (HM)	94.78 (HM)	487.78
8	98.4 (HM)	96.7 (HM)	95.8 (HM)	93.2 (HMwF)	91.38 (HM)	475.48
9	97.8 (HM)	95.6 (HM)	93.7 (HM)	91.4 (HM)	88.48 (HM)	466.98
10	96.7 (HM)	93.28 (HM)	90.8 (HM)	88.4 (HM)	84.2 (HM)	453.38

1 through 4. Nonetheless, the highest sum is achieved again using combination 5 ($wf1 = wf2 = wf3 = 1/3$), even though EN2IwF achieves the best percentages for the three intermediate vehicle densities.

Now, we analyze the sum of the delay to inform the last vehicle in the network. First, the delays for the methods that achieve the minimum delay on the Valencia map are shown in Table 6.5. Once more, the full dataset for all communication methods and weight factor combinations is deferred to Appendix A.1, Table A.3 for weight factor combinations 1–5 and Table A.4 for combinations 6–10. Corresponding charts are presented in Figure A.3 and in Figure A.4, respectively.

TABLE 6.5: Delays to inform the last vehicle on the Valencia map (method that achieved the minimum delay for a given density)

wfs combination	Vehicles density					sum across densities
	25	50	100	150	200	
1	19.3 (EN2IwF)	26.1 (HM)	34.08 (HM)	42.8 (E2F2C)	36.4 (NJL)	158.68
2	11.2 (EN2IwF)	24.8 (HM)	30.29 (HMwF)	41.08 (NJL)	35.89 (NJL)	143.26
3	12.3 (EN2IwF)	24.92 (HMwF)	27.69 (HMwF)	40.2 (NJL)	35.02 (NJL)	140.13
4	13.6 (EN2IwF)	21.9 (HMwF)	24.67 (HMwF)	38.68 (NJL)	34.12 (NJL)	132.97
5	14.28 (EN2IwF)	22.89 (HM)	26.98 (HMwF)	35.29 (NJL)	31.26 (NJL)	130.7
6	15.18 (EN2IwF)	20.67 (HM)	27.9 (HM)	34.79 (NJL)	30.6 (NJL)	129.14
7	16.08 (EN2IwF)	19.64 (HM)	25.8 (HM)	35.2 (NJL)	31.72 (NJL)	128.44
8	17.29 (EN2IwF)	23.47 (HMwF)	28.62 (HM)	37.98 (NJL)	33.65 (NJL)	141.01
9	19.48 (EN2IwF)	25.6 (HMwF)	32.6 (HM)	40.79 (HM)	36.45 (NJL)	154.92
10	22.31 (EN2IwF)	28.95 (HMwF)	35.48 (HMwF)	42.18 (HM)	37.84 (NJL)	166.76

From the table, we see that the weight factor combination 7 ($wf1 = wf3 = 0, wf2 = 1$) achieves the lowest sum of delays across densities. This means that considering only the lowest CM speed difference to the average cluster speed can produce lower delays. However, from Table 6.3, we can see that combination 7 is the one that

yields the second lowest sum of percentage of vehicles informed. Thus, moving to a combination with a better trade-off, considering less than 2.5 seconds above the best sum, combination 5 would be a good choice to achieve the highest percentage of vehicles informed without giving up much on the best result for delays.

The delay results for the San Francisco map are presented in Table 6.6. For the delay results of all communication methods, Table A.11 presents results for weight factor combinations 1–5 and Table A.12 for combinations 6–10, both in Appendix A.2. In the same appendix, corresponding charts can be found in Figure A.7 and in Figure A.8.

TABLE 6.6: Delays to inform the last vehicle on the San Francisco map (method that achieved the minimum delay for a given density)

wfs combination	Vehicles density					sum across densities
	25	50	100	150	200	
1	26.8 (HM)	32.4 (HM)	38.78 (HM)	46.8 (E2F2C)	39.9 (NJL)	184.68
2	22.07 (EN2IwF)	30.7 (HM)	35.26 (HM)	33.6 (E2F2C)	28.03 (E2F2C)	149.66
3	17.6 (EN2IwF)	26.7 (HM)	31.6 (HM)	26.4 (E2F2C)	20.75 (E2F2C)	123.05
4	12.4 (EN2IwF)	22.2 (HM)	34.68 (HM)	41.06 (E2F2C)	23.7 (NJL)	134.04
5	12.7 (HM)	20.9 (HM)	26.3 (HM)	20.4 (E2F2C)	16.5 (E2F2C)	96.8
6	14.8 (HM)	26.5 (HM)	29.4 (HM)	23.4 (E2F2C)	20.64 (E2F2C)	114.74
7	17.8 (HM)	30.2 (HM)	36.5 (HM)	28.7 (E2F2C)	22.6 (E2F2C)	135.8
8	19.8 (HM)	32.6 (HM)	34.7 (E2F2C)	30.2 (E2F2C)	25.8 (E2F2C)	143.1
9	23.5 (HM)	37.48 (HM)	38.4 (E2F2C)	33.46 (E2F2C)	30.7 (E2F2C)	163.54
10	29.48 (HM)	46.78 (HM)	53.62 (HM)	42.15 (E2F2C)	38.74 (E2F2C)	210.77

This time, weight factors combination 5 also yields the lowest sum of delays. However, E2F2C is rarely the best on the percentage of vehicles informed. Therefore, even considering combination 5 for the percentages, using E2F2C would decrease the sum of percentages.

The previous analysis considers the network has some mechanism to sense the VANET vehicle density and adapt to the best method. Therefore, the presented results consider the best method for each density before summing the percentages of informed vehicles and the delays. Such an adaptive system adds much complexity to the network. A more feasible solution would be to compare the sums for a single method across densities, which is presented next.

The highest sums of the percentages of vehicles informed for each weight factor combination on the Valencia map are shown in Table 6.7. The percentages for all

communication chains and all weight factor combinations are available in Appendix A.1 — Table A.5 shows the sums for weight factor combinations 1–5 and Table A.6 for combinations 6–10.

TABLE 6.7: Percentage of vehicles informed on the Valencia map considering a single method for all densities

wfs combination	sum across densities	Method that achieved MAX sum
(1)	485.3	HM
(2)	488.58	HM
(3)	485.54	HM
(4)	480.96	NJL
(5)	485.97	NJL
(6)	469.72	HM
(7)	477.3	HM
(8)	485.33	HM
(9)	489.06	HM
(10)	492.42	HM

The highest sum of percentages corresponds to combination 10 ($wf1 = wf2 = 0, wf3 = 1$). Considering only the received power from the BS as a factor to elect a CM does not seem a stable solution in case there are problems with the BS signal, therefore adopting this combination is risky. The second highest sum is achieved by combination 9 ($wf1 = 0, wf2 = 1/3, wf3 = 2/3$), which also considers the vehicle speeds. In both cases, HM is the chosen method, matching the previous analysis that allowed different methods to be used — HM was the best for all densities.

Table 6.8 presents the highest sums of percentages of informed vehicles for each weight factor combination on the San Francisco map. Besides the highest sums, the metric for the other considered communication methods can be found in Table A.13 for weight factor combinations 1–5 and in Table A.14 for combinations 6–10, both on Appendix A.2.

Combination 5 ($wf1 = wf2 = wf3 = 1/3$) achieves the best result, the same combination that performed best considering different methods across densities, however with a sum less than 1% below the previous case. Particularly, this result shows that the added complexity of having different methods across densities might not be worth

TABLE 6.8: Percentage of vehicles informed on the San Francisco map considering a single method for all densities

wfs combination	sum across densities	Method that achieved MAX sum
(1)	481.29	EN2IwF
(2)	484.2	EN2IwF
(3)	487.62	EN2IwF
(4)	490.33	EN2IwF
(5)	495.1	EN2IwF
(6)	491.08	HM
(7)	487.78	HM
(8)	474.32	HM
(9)	466.98	HM
(10)	453.38	HM

it. Also, the method that worked the best for the simpler map was EN2IwF, which skips the first CM on the HMwF chain.

The lowest sum of delays to inform the last vehicle for each weight factor combination on the Valencia map, taking a single communication method across vehicle densities, is presented in Table 6.9. On Appendix A.1, Tables A.7 and A.8 show the delay sums for other communication methods for weight factor combinations 1–5 and 6–10, respectively.

TABLE 6.9: Delays to inform the last vehicle on the Valencia map considering a single method across densities

wfs combination	sum across densities	Method that achieved MIN sum
(1)	210.12	HM
(2)	203.93	HM
(3)	195.2	HMwF
(4)	180.55	HMwF
(5)	186.79	HM
(6)	179.63	HM
(7)	167.28	HM
(8)	182.51	HM
(9)	195.85	HM
(10)	207.94	HM

The best delays in this case are for combination 7 ($wf1 = wf3 = 0, wf2 = 1$), which only considers the vehicle speeds for the CM election, with the HM method.

Notice this is almost 40 seconds worse than its counterpart considering all methods across densities, but also that the best result came from combination 7. Once more, considering the difference of the speed vehicles to elect the CM achieved the best delays, even though the percentage of informed vehicles decreases significantly. A reasonable trade-off is achieved for combination 8 ($wf1 = 0, wf2 = 2/3, wf3 = 1/3$), with a sum of percentages of informed vehicles about 8% below the best single-method result and about 15s above the best delay to inform the last vehicle.

Last, the lowest sums of delays to inform the last vehicle, considering a single method across densities, for all weight factor combinations on the San Francisco map are shown in Table 6.10. The sums for the other communication methods are available on Appendix A.2, in Table A.15 for weight factor combinations 1–5 and in Table A.16 for other combinations.

TABLE 6.10: Delays to inform the last vehicle on the San Francisco map considering a single method across densities

wfs combination	sum across densities	Method that achieved MIN sum
(1)	247.78	HM
(2)	201.43	E2F2C
(3)	173.33	E2F2C
(4)	210.98	HM
(5)	145.65	E2F2C
(6)	164.81	E2F2C
(7)	196.98	E2F2C
(8)	188.47	E2F2C
(9)	214.06	E2F2C
(10)	262.46	E2F2C

For the San Francisco map, it is possible to see that the E2F2C method is prevalent across the weight factor combinations, also presenting the best delay with such method for combination 5 ($wf1 = wf2 = wf3 = 1/3$). This method is known to achieve lower percentages of informed vehicles, as their presence is not seen for any of the densities in Table 6.3 and in Table 6.4, and also from our previous work by AlQahtani and Sheldon (2021). Therefore, considering the delays for a method that is not E2F2C leaves combination 4 ($wf1 = 1/3, wf2 = 2/3, wf3 = 0$) as the best delay,

with the HM model, even though it is above 100s over the best delay considering all models across densities.

6.5 CONCLUSION

Previously, we proposed a cluster merging scheme and several communication methods to increase the percentage of vehicles informed (PIV) on the VANET and to decrease the delays to inform the last vehicle (DLV). However, important weight factors that are used for the merged cluster master (CM) election had not yet been analyzed. These factors can be used to bias the importance given to the factors that influence the CM election. Thus, depending on the location context, these factors were studied to understand if they may help to optimize the PIV and DLV performance metrics. The weighting factors biased, more or less, i) vehicle number of neighbors, ii) vehicle speed difference with the average cluster speed, and iii) estimated power of the signal received from the base station. This chapter has accomplished such an analysis, for which all results have been discussed in the previous sections. Herein this section we summarize that discussion and draw our conclusion.

The analysis of the weight factors carried out considers two steps. On the first, the network has the ability to adapt to the current vehicles density by picking the communication method that achieves either the best PIV or the method that achieves the best DLV. On the second step of the analysis, the network can no longer adapt to the vehicles density. Thus, we analyzed the performance for each metric and method by finally comparing the sums of the metrics across densities. The method with the best sum (*i.e.*, highest for percentages [PIV], lowest for delays [DLV]) is chosen as the best method for the given weight factors. The second step is simpler to implement in a real test-bed because selecting the best communication method does not require vehicle density measurements.

To summarize, each of the analysis steps is carried out for both scenarios — Valencia and San Francisco —, which are discussed in the next paragraphs.

In the first step of the Valencia scenario analysis, a good trade-off between the PIV and the DLV in the network is achieved when using an even distribution of weight

factors. When prioritizing the PIV, the result favors the use of HM for low densities and NJL for high densities. While prioritizing the DLV, E2C2F is preferred for low densities, HM and HMwF for intermediate densities, and NJL for high densities.

In the second step of the Valencia scenario analysis the highest sum of PIV is achieved when only the power of the signal from the base station is received. That is not a reliable solution because instabilities of the BS signal (in practice) may result on the election of a CM that momentarily presents the best received power. Therefore, the second best result for PIV is considered vital, which uses the speed and power metrics, yielding a more stable result in practice. In which case, the HM is the most suitable communication method. Regarding delays, using only the speed factor achieves the best results, but a good trade-off is seen when considering both the speed and the power factors, as was demonstrated for the PIV.

In the first step of analysis of the San Francisco scenario, an even distribution of weight factors yielded the best results for PIV and for DLV. However, the best method used for each vehicle density were not the same — E2F2C appeared best for delays on higher densities, even though it did not present good PIV results.

For the second step of analysis, an even distribution of weight factors again performs best for both metrics. The sum of percentages across densities is less than 1% below that achieved for the first step of analysis, which suggests that the added complexity of adapting the method to the vehicles density might not be useful. For the delay metric, E2F2C is prevalent across the weight factors.

The even distribution of weight factors seems to be the best choice for both scenarios and both metrics. Consequently, the results of the weight factors study indicate that the number of neighbors, speed differences, and power received from the base station are equally important for the CM selection on a recently merged cluster.

CHAPTER 7

CONCLUSION

The number of vehicle traffic accidents keeps increasing every year as more vehicles join worldwide roads and streets. Technological solutions have emerged to mitigate the problem. One of such solution are the Intelligent Transportation Systems (ITSs), which aim to, among other goals further explored in Chapter 1, improve traffic safety. By enabling vehicles to communicate, it is possible to make use of warning messages to help avoid accidents. Such communication capabilities already exist in vehicular ad-hoc networks (VANETs), which has been the main topic of this study.

Since ITSs are developed around a plethora of concepts and technologies, gathering a knowledge base before diving into the specifics of VANET problems becomes important. The requirements of VANETs, types of communication in these networks — including the technologies used to implement such communications —, messaging for safety applications, and some infrastructure components — are discussed in Chapter 2.

However, the very technology used to prevent accidents by using VANET capabilities faces challenges of its own. Communicating with up to hundreds of vehicles is not trivial, as explained in Chapter 1, broadcast storms being one of the most disruptive problems arising from such high vehicle density scenarios. Among the solutions for such a disruptive problem, clustering (highlighted in this study), provides a way to divide the problem into smaller domains. Unfortunately, as the number of vehicle clusters is allowed to grow large, the vehicles in close proximity to the many adjacent cluster boundaries are still prone to BS. Thus, managing the number of clusters in the VANET is necessary, which is the subject of Chapter 3. A cluster merging scheme based on two different cluster characteristics was proposed and evaluated against previous solutions via simulations, which showed that it is possible to achieve a reduction on the number of messages received by vehicles in the network without impairing the percentage of vehicles being warned within the network.

After managing the number of clusters in the network, a study of the communication chains for warning vehicles in the clusters was performed. This study is presented in Chapter 4 and its objective is to keep communication delays low while still providing high percentages of informed vehicles (PIV) in the network. For that, the 5G infrastructure used in our cluster merging scheme is now used for inter-cluster communication, which can now also be performed by a new class of vehicles — the cluster forwarders (CFs). By combining these assets to form different communication chains, the study showed that the Hierarchical Model (HM) with Forwarder (HMwF) achieves the most (potentially) useful trade-off between delays (DLV) and percentages informed (PIV). Warning messages in the HMwF chain follow the path given next. The event node sends the warning to the event cluster Cluster Master (CM), which forwards it to the Base Station (BS). Then, the BS sends the warning message to all CFs, which, in turn, send it to other CMs. Finally, the warning message reaches all cluster members via their CMs. We found that preventing all CMs from being on the BS schedule for transmission, but still communicating with them, now via CFs, has a beneficial impact on the DLV, which are kept under 100 seconds for all considered vehicle densities.

Then, for the work in Chapter 5, a different metric used for CM election was added to the cluster merging algorithm. Now, the normalized power received by a CM candidate from the BS is used in the election process. This metric favors CM candidates closer to the BS, instead of nodes potentially in the center of the cluster as was done in the previous method. We verified that delays to inform vehicles are reduced, but some negative impact is also seen on the percentage of vehicles informed (PIV) suggesting a trade-off between the two metrics. This trade-off can be biased by manipulating their weight factors to optimize either the PIV or DLV or both. A sensitivity study to understand how those weighting factors may be useful is presented in Chapter 6.

The study of the effects of the weight factors on the PIV and on the DLV carried out in Chapter 6 showed that an even distribution of the weight factors could yield the best performance for both metrics. However, the E2F2C communication method has been shown to add noise to the results dataset — it attains the lowest delays but

unfortunately, this is due to the low percentage of informed vehicles (PIV). Moreover, other interesting results were achieved for weight factor combinations that zeroed out the normalized number of neighbors factor. This suggests that the factor might be redundant with respect to the speed factor — both favor vehicles in the center of the cluster to be elected CM of a merged cluster. Therefore, removing the number of neighbor's factor and the E2F2C chain from subsequent work could provide new interesting results along with lower computational overhead. This aspect is a possible avenue left for future study.

Future work could also consider the initial formation of clusters in the network. The number of vehicles in the simulations could build up over time towards the target density, building clusters and also accounting for cluster divisions and the change of CMs. The hypothesis here is that the simulation of networks operating on a steady state will yield the same PIVs and DLVs as simulations that skip the initial cluster formation, presented in this thesis. Even though results will be influenced by the transient period, in which the number of vehicles increases towards the maximum, the operation of the steady network will remove that initial bias over time.

Another opportunity for future work would include empirical studies to prove the effectiveness of the methods from which our simulation results were shown to be most promising. Other scenarios could be simulated and/or validated in real test-beds according to the procedures that have been established here. Furthermore, these studies might analyze not using the 5G infrastructure when vehicles are gathered around a few junctions, as suggested by some good results achieved by NJL (i.e., nearest junction located). Further, though we have assumed that the environment is free of malicious actors, this assumption is unrealistic. Thus, analyzing the security of the message exchange process between vehicles with the aim of better understanding detection/prevention of hazards/vulnerabilities sourced from malicious actors tampering with warning messages (*e.g.*, jamming or altering) would certainly be desirable.

BIBLIOGRAPHY

- Abboud K., Omar H.A., and Zhuang W. 2016a. Interworking of DSRC and Cellular Network Technologies for V2X Communications: A Survey. *IEEE Transactions on Vehicular Technology* 65:9457–9470.
- Abboud K., Omar H.A., and Zhuang W. 2016b. Interworking of DSRC and Cellular Network Technologies for V2X Communications: A Survey. *IEEE Transactions on Vehicular Technology* 65:9457–9470.
- Abdul K., Qayyum A., and Pannek J. 2017. Performance Analysis of Proposed Congestion Avoiding Protocol for IEEE 802.11s. *International Journal of Advanced Computer Science and Applications* 8.
- Ahsan W., Khan M.F., Aadil F., Maqsood M., Ashraf S., Nam Y., and Rho S. 2020. Optimized node clustering in VANETs by using meta-heuristic algorithms. *Electronics (Switzerland)* 9:1–14.
- Al-Ani R., Zhou B., Shi Q., and Sagheer A. 2018. A Survey on Secure Safety Applications in VANET. *Proceedings - 20th International Conference on High Performance Computing and Communications, 16th International Conference on Smart City and 4th International Conference on Data Science and Systems, HPCC/SmartCity/DSS 2018* pages 1485–1490.
- AlQahtani O. and Sheldon F.T. 2021. Validation of vehicular ad-hoc network (VANET) message dissemination algorithms otherwise vulnerable to broadcast storms in Urban contexts. *Transactions on Emerging Telecommunications Technologies* Accepted f.
- AlQahtani O., Sheldon F.T., Krings A., and Beeston J. 2021. Cluster Merging Scheme in VANETs. *In Proceedings of the Future Technologies Conference 2020* (K. Arai, S. Kapoor, and R. Bhatia, eds.), pages 515–527, Springer, Cham, Vancouver.
- Ansari S., Ahmad J., Aziz Shah S., Kashif Bashir A., Boutaleb T., and Sinanovic S. 2020. Chaos-based privacy preserving vehicle safety protocol for 5G Connected Autonomous Vehicle networks. *Transactions on Emerging Telecommunications Technologies* 31:1–13.
- Auer A., Feese S., and Lockwood S. 2016. *History of Intelligent Transportation Systems*.
- Benkerdagh S. and Duvallet C. 2019. Cluster-based emergency message dissemination strategy for VANET using V2V communication. *International Journal of Communication Systems* 32:e3897.
- Chiti F., Fantacci R., Nizzi F., Pierucci L., and Borrego C. 2019. A distributed token passing protocol for time constrained data gathering in VANETs. *Electronics (Switzerland)* 8:1–17.

- Cooper C., Franklin D., Ros M., Safaei F., and Abolhasan M. 2017. A Comparative Survey of VANET Clustering Techniques. *IEEE Communications Surveys and Tutorials* 19:657–681.
- Feukeu E.A. and Zuva T. 2020. Dynamic Broadcast Storm Mitigation Approach for VANETs. *Future Generation Computer Systems* 107:1097–1104.
- Galaviz-Mosqueda A., Morales-Sandoval M., Villarreal-Reyes S., Galeana-Zapien H., Rivera-Rodriguez R., and Alonso-Arevalo M.A. 2017. Multi-hop broadcast message dissemination in vehicular ad hoc networks: A security perspective review. *International Journal of Distributed Sensor Networks* 13:155014771774126.
- Ganin A.A., Mersky A.C., Jin A.S., Kitsak M., Keisler J.M., and Linkov I. 2019. Resilience in Intelligent Transportation Systems (ITS). *Transportation Research Part C: Emerging Technologies* 100:318–329.
- Gao J.H. and Peh L.S. 2014. Roadrunner: Infrastructure-less vehicular congestion control. *21st World Congress on Intelligent Transport Systems, ITSWC 2014: Reinventing Transportation in Our Connected World* .
- (German Aerospace Center). 2020. SUMO: Simulation/VehicleSpeed.
- Gupta R., Kalyanasundaram S., and Natarajan B. 2015. Dynamic Point Selection Schemes for LTE-A Networks with Load Imbalance. *In Vehicular Technology Conference (VTC Fall), 2015 IEEE 82nd*.
- Hamdi M.M., Audah L., Rashid S.A., Mohammed A.H., Alani S., and Mustafa A.S. 2020. A Review of Applications, Characteristics and Challenges in Vehicular Ad Hoc Networks (VANETs). *HORA 2020 - 2nd International Congress on Human-Computer Interaction, Optimization and Robotic Applications, Proceedings* .
- Huang J.J. and Chiu Y.S. 2013. A scheme to reduce merging collisions in TDMA-based VANETs. *2013 International Symposium on Wireless and Pervasive Computing, ISWPC 2013 pages 1–4*.
- Khaliq K.A., Qayyum A., and Pannek J. 2017. Novel message dissemination mechanism and mathematical model for safety applications in VANET. *In 2017 11th International Conference on Software, Knowledge, Information Management and Applications (SKIMA), pages 1–5, IEEE*.
- Khan Z. and Fan P. 2018. A multi-hop moving zone (MMZ) clustering scheme based on cellular-V2X. *China Communications* 15:55–66.
- Kounga G., Walter T., and Lachmund S. 2009. Proving reliability of anonymous information in VANETs. *IEEE Transactions on Vehicular Technology* 58:2977–2989.
- Krauss S. 1998. Microscopic modeling of traffic flow: investigation of collision free vehicle dynamics. *Forschungsbericht - Deutsche Forschungsanstalt fuer Luft - und Raumfahrt e.V.* .
- Kukliński S. and Wolny G. 2009. Density based clustering algorithm for VANETs. *2009 5th International Conference on Testbeds and Research Infrastructures for the Development of Networks and Communities and Workshops, TridentCom 2009* .

- Liu X. and Jaekel A. 2019. Congestion control in V2V safety communication: Problem, analysis, approaches. *Electronics (Switzerland)* 8.
- Lopez P.A., Behrisch M., Bieker-Walz L., Erdmann J., Flötter Y.P., Hilbrich R., Lücken L., Rummel J., Wagner P., and Wiesner E. 2018. Microscopic Traffic Simulation using SUMO. *The 21st IEEE International Conference on Intelligent Transportation Systems* .
- Martinez F.J., Fogue M., Coll M., Cano J.C., Calafate C.T., and Manzoni P. 2010. Evaluating the impact of a novel warning message dissemination scheme for VANETs using real city maps. *Lecture Notes in Computer Science (including subseries Lecture Notes in Artificial Intelligence and Lecture Notes in Bioinformatics)* 6091 LNCS:265–276.
- Mezher A.M., Oltra J.J., Urquiza-Aguilar L., Paredes C.I., Tripp-Barba C., and Igartua M.A. 2014. Realistic environment for VANET simulations to detect the presence of Obstacles in Vehicular ad hoc networks. *PE-WASUN 2014 - Proceedings of the 11th ACM Symposium on Performance Evaluation of Wireless Ad Hoc, Sensor, and Ubiquitous Networks* pages 77–84.
- More S. and Naik U. 2018. Novel Technique in Multihop Environment for Efficient Emergency Message Dissemination and Lossless Video Transmission in VANETS. *Journal of Communications and Information Networks* 3:101–111.
- Nshimiyimana A., Mupenzi T., and Kanyesheja J.d.D. 2017. V2V Communication in 5G Multi-RATs and VANet Clustering Model from Localization Approaches. *International Journal of Innovative Science, Engineering & Technology* 4:253–258.
- (OpenSim Ltd.). 2020. OMNeT++ Discrete Event Simulator.
- Paranjothi A., Tanik U., Wang Y., and Khan M.S. 2019. Hybrid-Vehfog: A robust approach for reliable dissemination of critical messages in connected vehicles. *Transactions on Emerging Telecommunications Technologies* 30:1–16.
- Ravi; B., Thangaraj; J., and Petale S. 2018. Stochastic Network Optimization of Data Dissemination for Multi-hop Routing in VANETs. *In Proceedings of the 2018 International Conference on Wireless Communications, Signal Processing and Networking (WiSPNET), Chennai, India.*
- Ren M., Zhang J., Khoukhi L., Labiod H., and Veque V. 2017. A study of the impact of merging schemes on cluster stability in VANETs. *IEEE International Symposium on Personal, Indoor and Mobile Radio Communications, PIMRC 2017-October:1–7.*
- Ren M., Zhang J., Khoukhi L., Labiod H., and Vèque V. 2021. A review of clustering algorithms in VANETs. *Annales des Telecommunications/Annals of Telecommunications* .
- Sanguesa J., Fogue M., Garrido P., Martinez F.J., Cano J.C., Calafate C.T., and Manzoni P. 2013. On the selection of optimal broadcast schemes in VANETs. *MSWiM 2013 - Proceedings of the 16th ACM International Conference on Modeling, Analysis and Simulation of Wireless and Mobile Systems* pages 411–418.

- Sattar S., Qureshi H.K., Saleem M., Mumtaz S., and Rodriguez J. 2018. Reliability and energy-efficiency analysis of safety message broadcast in VANETs. *Computer Communications* 119:118–126.
- Shah S.S., Malik A.W., Rahman A.U., Iqbal S., and Khan S.U. 2019. Time Barrier-Based Emergency Message Dissemination in Vehicular Ad-hoc Networks. *IEEE Access* 7:16494–16503.
- Shaik S., Venkata Ratnam D., and Bhandari B.N. 2018. An Efficient Cross Layer Routing Protocol for Safety Message Dissemination in VANETS with Reduced Routing Cost and Delay Using IEEE 802.11p. *Wireless Personal Communications* 100:1765–1774.
- Shrestha R., Bajracharya R., and Nam S.Y. 2018. Challenges of Future VANET and Cloud-Based Approaches. *Wireless Communications and Mobile Computing* 2018.
- Sommer C., German R., and Dressler F. 2011. Bidirectionally Coupled Network and Road Traffic Simulation for Improved IVC Analysis. *IEEE Transactions on Mobile Computing* 10:3–15.
- Sospeter J., Wu D., Hussain S., and Tesfa T. 2019. An effective and efficient adaptive probability data dissemination protocol in VANET. *Data* 4.
- Tambawal A.B., Noor R.M., Salleh R., Chembe C., and Oche M. 2019. Enhanced weight-based clustering algorithm to provide reliable delivery for VANET safety applications. *PLoS ONE* 14:1–19.
- Tseng Y.C., Ni S.Y., Chen Y.S., and Sheu J.P. 2002. The broadcast storm problem in a mobile ad hoc network. *Wireless Networks* 8:153–167.
- Ucar S., Ergen S.C., and Ozkasap O. 2016. Multihop-Cluster-Based IEEE 802.11p and LTE Hybrid Architecture for VANET Safety Message Dissemination. *IEEE Transactions on Vehicular Technology* 65:2621–2636.
- Ullah H., Gopalakrishnan Nair N., Moore A., Nugent C., Muschamp P., and Cuevas M. 2019. 5G communication: An overview of vehicle-to-everything, drones, and healthcare use-cases. *IEEE Access* 7:37251–37268.
- Urquiza-Aguiar L., Tripp-Barba C., Estrada-Jiménez J., and Igartua M.A. 2015. On the impact of building attenuation models in vanet simulations of urban scenarios. *Electronics* 4:37–58.
- Wang J., Shao Y., Ge Y., and Yu R. 2019. A survey of vehicle to everything (V2X) testing. *Sensors (Switzerland)* 19:1–20.
- Wisitpongphan N., Tonguz O.K., Parikh J.S., Mudalige P., Bai F., and Sadekar V. 2007. Broadcast storm mitigation techniques in vehicular ad hoc networks. *IEEE Wireless Communications* 14:84–94.
- Xu Z., Li X., Zhao X., Zhang M.H., and Wang Z. 2017. DSRC versus 4G-LTE for connected vehicle applications: A study on field experiments of vehicular communication performance. *Journal of Advanced Transportation* 2017.

- Zhang D., Ge H., Zhang T., Cui Y.Y., Liu X., and Mao G. 2019. New Multi-Hop Clustering Algorithm for Vehicular Ad Hoc Networks. *IEEE Transactions on Intelligent Transportation Systems* 20:1517–1530.
- Zhang H. 2015. Cooperative Interference Mitigation and Handover Management for Heterogeneous Cloud Small Cell Networks. *IEEE Wireless Communications* pages 92–99.
- Zhao H., Yue H., Gu T., and Li W. 2019. CPS-Based Reliability Enhancement Mechanism for Vehicular Emergency Warning System. *International Journal of Intelligent Transportation Systems Research* 17:232–241.
- Zhou H., Xu W., Bi Y., Chen J., Yu Q., and Shen X. 2017. Toward 5G spectrum sharing for immersive- experience-driven vehicular communications. *IEEE Wireless Communications* 24:30–37.

APPENDIX A

SUPPLEMENTARY CHARTS TO CHAPTER 6

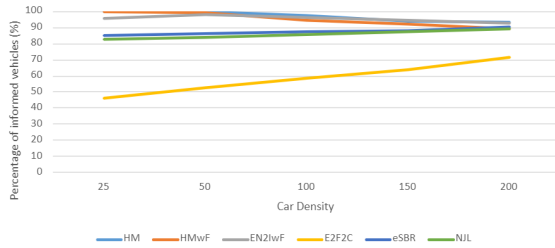
On Chapter 6, the weight factors study is conducted, which required supporting data that would disrupt the content if presented on the chapter itself. This Appendix gathers all simulation data generated in chart and table forms, which have been used to create the tables presented on Chapter 6, divided in two sections — Appendix A.1 shows data for the Valencia scenario and Appendix A.2 for the San Francisco scenario.

A.1 DATA AND FIGURES OF THE VALENCIA SCENARIO

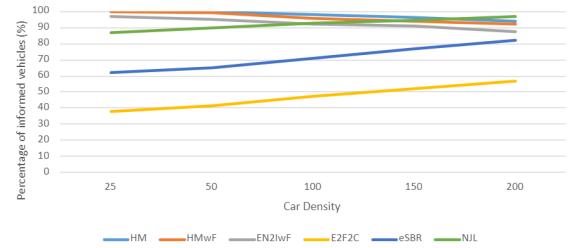
First, the percentage of vehicles informed at each considered vehicle density and for all weight factor combinations is presented on Figure A.1 (part 1 — weight factor combinations 1 through 5) and Figure A.2 (part 2 — weight factor combinations 6 through 10). The same data is shown in tabular form in Table A.1 (part 1) and Table A.2 (part 2). The highlighted values are the ones that appear in Table 6.3.

Then, the delays to inform the last vehicle at each considered density and for all weight factor combinations is shown on Figure A.3 (part 1) and Figure A.4 (part 2). Again, the same data is shown in tabular form in Table A.3 (part 1) and in Table A.4 (part 2), being the highlighted values the same ones presented in Table 6.5.

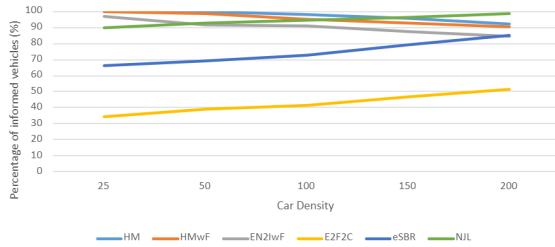
For the single communication method across vehicle densities, the percentages of informed vehicles are presented in Table A.5 (part 1) and in Table A.6 (part 2) (used in Table 6.7), and the delays, in Table A.7 (part 1) and in Table A.8 (part 2) (used in Table 6.9).



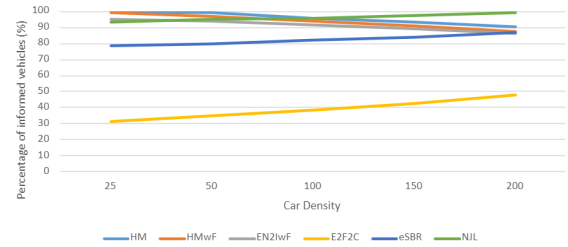
(A) Weight factors combination 1 — $wf1 = 1, wf2 = 0, wf3 = 0$



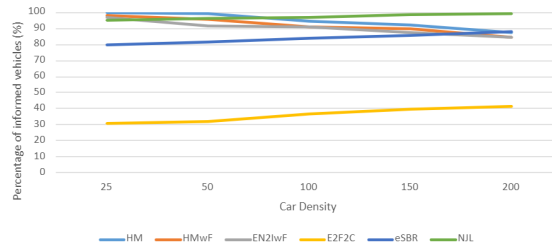
(B) Weight factors combination 2 — $wf1 = 2/3, wf2 = 1/3, wf3 = 0$



(C) Weight factors combination 3 — $wf1 = 2/3, wf2 = 0, wf3 = 1/3$

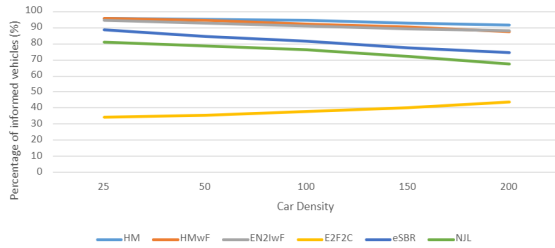


(D) Weight factors combination 4 — $wf1 = 1/3, wf2 = 2/3, wf3 = 0$

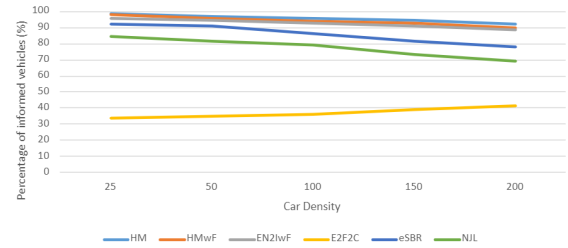


(E) Weight factors combination 5 — $wf1 = 1/3, wf2 = 1/3, wf3 = 1/3$

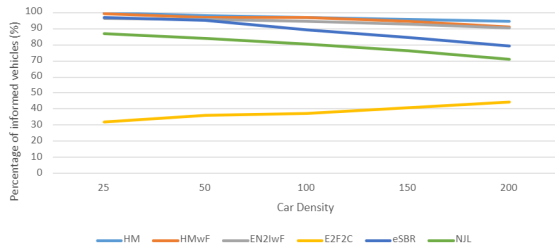
FIGURE A.1: Percentage of informed vehicles crossing car densities for the Valencia scenario with different weight factor combinations in the VANET for all proposed methods and benchmarks (part 1 — weight factor combinations 1–5).



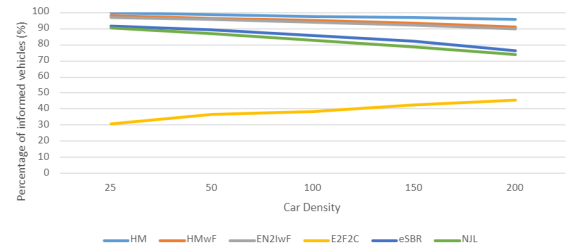
(A) Weight factors combination 6 — $wf1 = 1/3, wf2 = 0, wf3 = 2/3$



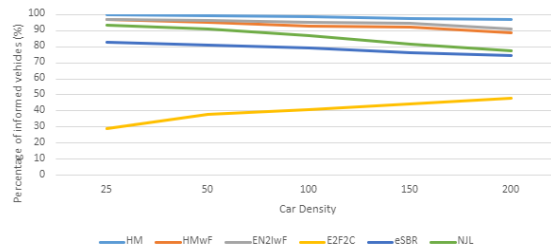
(B) Weight factors combination 7 — $wf1 = 0, wf2 = 1, wf3 = 0$



(C) Weight factors combination 8 — $wf1 = 0, wf2 = 2/3, wf3 = 1/3$



(D) Weight factors combination 9 — $wf1 = 0, wf2 = 1/3, wf3 = 2/3$



(E) Weight factors combination 10 — $wf1 = 0, wf2 = 0, wf3 = 1$

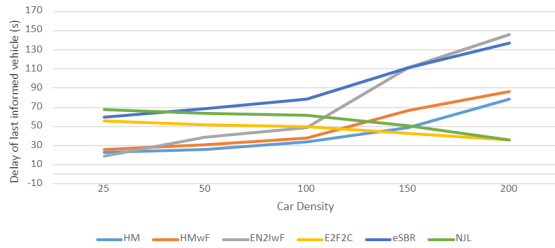
FIGURE A.2: Percentage of informed vehicles crossing car densities for the Valencia scenario with different weight-factor combinations in the VANET for all proposed methods and benchmarks (part 2 — weight factor combinations 6–10).

TABLE A.1: Percentage of vehicles informed on the Valencia scenario for the considered car densities, highlighting the highest percentage for each density and weight factors combination (part 1 — weight factor combinations 1–5).

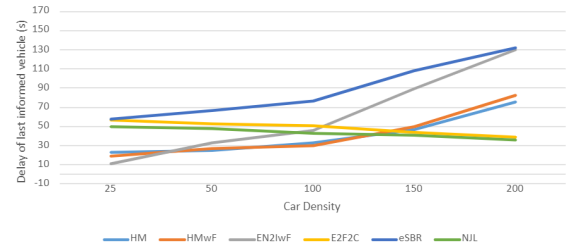
Car density	25	50	100	150	200
Weight factors combination 1					
HM	<u>100</u>	<u>100</u>	97.6	94.2	93.5
HMwF	<u>100</u>	98.95	94.6	92.14	89.4
EN2IwF	95.7	97.76	96.18	94.71	92.64
E2F2C	46.24	52.47	58.6	63.81	71.8
eSBR	84.95	86.2	87.4	88.1	90.5
NJL	82.8	83.7	85.6	87.4	89.2
Weight factors combination 2					
HM	<u>100</u>	<u>100</u>	98.2	96.2	94.18
HMwF	<u>100</u>	99.2	95.7	93.8	92.4
EN2IwF	96.77	94.82	92.14	90.8	87.24
E2F2C	37.63	41.6	47.4	52.18	56.9
eSBR	62.36	65.2	71.2	76.75	82.3
NJL	87.1	89.8	92.7	94.68	96.7
Weight factors combination 3					
HM	<u>100</u>	<u>100</u>	97.8	95.4	92.34
HMwF	<u>100</u>	98.65	95.13	92.78	90.4
EN2IwF	96.77	91.6	90.8	87.48	84.2
E2F2C	34.25	38.9	41.26	46.78	51.4
eSBR	66.4	69.27	72.8	78.9	84.97
NJL	89.6	92.6	94.78	96.23	98.84
Weight factors combination 4					
HM	<u>100</u>	99.4	95.68	93.27	90.48
HMwF	98.92	96.59	94.1	90.68	87.49
EN2IwF	95.18	93.67	91.8	89.25	86.4
E2F2C	31.18	34.79	38.65	42.38	47.96
eSBR	78.5	79.87	82.34	84.1	86.9
NJL	93.55	94.8	95.62	97.69	99.3
Weight factors combination 5					
HM	<u>100</u>	99.1	94.7	92.14	87.56
HMwF	98.2	95.48	91.05	89.7	84.4
EN2IwF	96.77	91.6	90.8	87.48	84.2
E2F2C	30.79	32.16	36.7	39.48	41.26
eSBR	79.5	81.82	83.69	85.7	88.2
NJL	94.89	96.2	96.9	98.48	99.5

TABLE A.2: Percentage of vehicles informed on the Valencia scenario for the considered car densities, highlighting the highest percentage for each density and weight factors combination (part 2 — weight factor combinations 6–10).

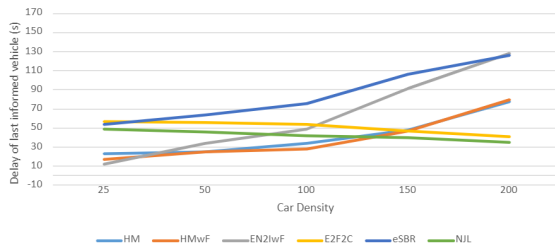
Car density	25	50	100	150	200
Weight factors combination 6					
HM	95.7	95.13	94.6	92.79	91.5
HMwF	95.7	94.78	92.18	90.6	87.42
EN2IwF	94.62	92.76	91.02	89.46	87.8
E2F2C	34.4	35.78	37.9	40.42	43.6
eSBR	88.5	84.76	81.8	77.49	74.6
NJL	80.65	78.7	76.28	71.9	67.1
Weight factors combination 7					
HM	98.6	96.7	95.6	94.32	92.08
HMwF	97.9	95.82	94.16	92.73	89.62
EN2IwF	95.47	94.6	92.84	90.69	88.5
E2F2C	33.74	34.69	36.2	38.79	41.2
eSBR	92.18	90.7	86.24	81.68	77.9
NJL	84.69	81.4	78.9	73.46	69.08
Weight factors combination 8					
HM	100	98.14	96.79	95.8	94.6
HMwF	98.92	97.14	96.9	94.76	91.2
EN2IwF	96.5	95.8	94.62	92.89	90.6
E2F2C	32.26	35.9	37.24	40.8	44.2
eSBR	96.7	94.81	88.9	84.76	79.29
NJL	87.1	83.69	80.5	76.47	71.2
Weight factors combination 9					
HM	100	98.9	97.48	96.9	95.78
HMwF	97.8	96.42	94.95	93.46	90.7
EN2IwF	96.77	95.4	94.12	92.26	89.74
E2F2C	30.97	36.7	38.24	42.6	45.3
eSBR	91.69	89.1	85.74	82.38	76.48
NJL	90.3	86.75	82.8	78.29	73.67
Weight factors combination 10					
HM	100	99.4	98.62	97.5	96.9
HMwF	96.9	95.28	93.01	91.9	88.76
EN2IwF	96.81	96	95.28	94.73	91.09
E2F2C	29.03	37.91	40.8	44.55	47.85
eSBR	82.8	81.06	78.9	76.47	74.18
NJL	93.55	90.86	86.9	81.37	77.49



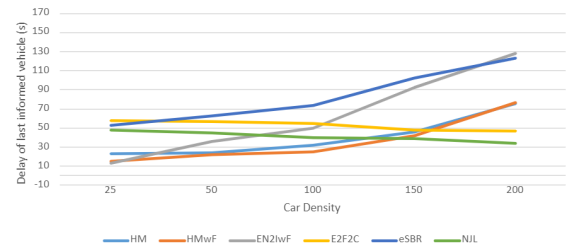
(A) Weight factors combination 1 — $wf1 = 1, wf2 = 0, wf3 = 0$



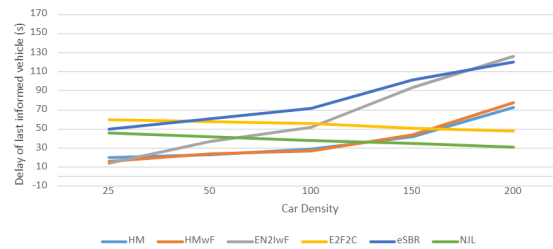
(B) Weight factors combination 2 — $wf1 = 2/3, wf2 = 1/3, wf3 = 0$



(C) Weight factors combination 3 — $wf1 = 2/3, wf2 = 0, wf3 = 1/3$

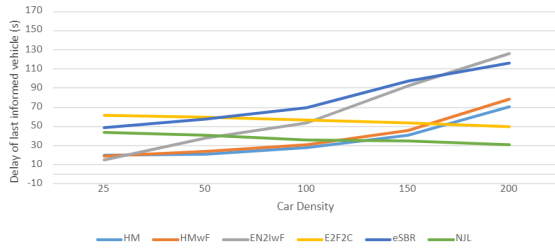


(D) Weight factors combination 4 — $wf1 = 1/3, wf2 = 2/3, wf3 = 0$

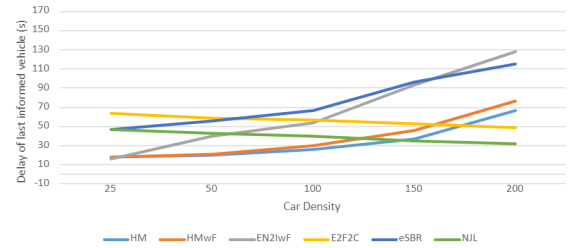


(E) Weight factors combination 5 — $wf1 = 1/3, wf2 = 1/3, wf3 = 1/3$

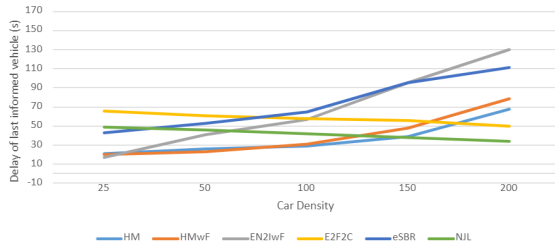
FIGURE A.3: Delays to inform the last vehicle crossing car densities for the Valencia scenario with different weight-factor combinations in the VANET for all proposed methods and benchmarks (part 1 — weight factor combinations 1–5).



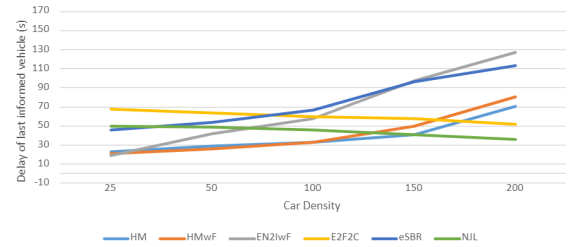
(A) Weight factors combination 6 — $wf1 = 1/3, wf2 = 0, wf3 = 2/3$



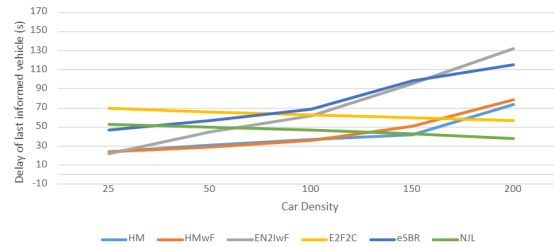
(B) Weight factors combination 7 — $wf1 = 0, wf2 = 1, wf3 = 0$



(C) Weight factors combination 8 — $wf1 = 0, wf2 = 2/3, wf3 = 1/3$



(D) Weight factors combination 9 — $wf1 = 0, wf2 = 1/3, wf3 = 2/3$



(E) Weight factors combination 10 — $wf1 = 0, wf2 = 0, wf3 = 1$

FIGURE A.4: Delays to inform the last vehicle crossing car densities for the Valencia scenario with different weight-factor combinations in the VANET for all proposed methods and benchmarks (part 2 — weight factor combinations 6–10).

TABLE A.3: Delays in seconds to inform the last vehicle on the Valencia scenario for the considered car densities, highlighting the lowest delays for each density and weight factors combination (part 1 — weight factor combinations 1–5).

Car density	25	50	100	150	200
Weight factors combination 1					
HM	22.9	<u>26.1</u>	<u>34.08</u>	48.95	78.09
HMwF	26.2	31.34	37.9	66.48	86.4
EN2IwF	<u>19.3</u>	38.7	49.08	110.8	145.7
E2F2C	55.7	52.06	49.71	<u>42.8</u>	36.45
eSBR	59.4	68.38	78.49	111.55	136.92
NJL	68	63.26	61.79	50.6	<u>36.4</u>
Weight factors combination 2					
HM	23.4	<u>24.8</u>	32.9	46.78	76.05
HMwF	18.97	26.8	<u>30.29</u>	49.73	82.02
EN2IwF	<u>11.2</u>	32.69	46.23	89.65	130.46
E2F2C	56.9	53.14	50.84	44.16	38.9
eSBR	57.7	66.94	76.45	108.26	131.72
NJL	50.02	47.62	43.29	<u>41.08</u>	<u>35.89</u>
Weight factors combination 3					
HM	23.2	25.1	33.68	47.91	77.96
HMwF	16.74	<u>24.92</u>	<u>27.69</u>	46.8	79.05
EN2IwF	<u>12.3</u>	33.95	48.9	91.25	127.64
E2F2C	57.08	55.96	53.48	46.7	41.08
eSBR	54.28	63.8	75.96	106.74	126.4
NJL	49.1	46.07	41.8	<u>40.2</u>	<u>35.02</u>
Weight factors combination 4					
HM	22.6	24.1	31.79	45.6	75.4
HMwF	15.2	<u>21.9</u>	<u>24.67</u>	42.38	76.4
EN2IwF	<u>13.6</u>	35.78	50.28	92.3	128.5
E2F2C	58.12	56.47	54.59	48.2	46.7
eSBR	52.81	62.25	73.48	102.6	123.47
NJL	47.69	45.2	40.1	<u>38.68</u>	<u>34.12</u>
Weight factors combination 5					
HM	20.6	<u>22.89</u>	28.75	42.17	72.38
HMwF	16.47	23.68	<u>26.98</u>	44.05	77.48
EN2IwF	<u>14.28</u>	36.91	52.07	93.33	125.64
E2F2C	59.67	57.48	56.2	51.3	48.12
eSBR	50.12	60.28	71.49	101.08	119.67
NJL	45.67	42.13	37.67	<u>35.29</u>	<u>31.26</u>

TABLE A.4: Delays in seconds to inform the last vehicle on the Valencia scenario for the considered car densities, highlighting the lowest delays for each density and weight factors combination (part 2 — weight factor combinations 6–10).

Car density	25	50	100	150	200
Weight factors combination 6					
HM	19.79	20.67	27.9	40.58	70.69
HMwF	18.9	24.26	31.48	46.06	78.14
EN2IwF	15.18	37.9	53.77	92.08	126.38
E2F2C	61.29	59.8	57.03	53.56	49.77
eSBR	48.97	57.65	69.53	97.08	116.46
NJL	44.38	41.05	36.02	34.79	30.6
Weight factors combination 7					
HM	18.47	19.64	25.8	36.47	66.9
HMwF	18.02	21.58	29.74	45.97	76.15
EN2IwF	16.08	39.66	54.17	93.8	127.9
E2F2C	63.2	58.7	56.46	53.11	48.79
eSBR	46.7	55.68	67.09	96.8	115.28
NJL	46.79	43.28	39.7	35.2	31.72
Weight factors combination 8					
HM	20.79	26.47	28.62	38.55	68.08
HMwF	19.63	23.47	31.28	47.55	78.9
EN2IwF	17.29	41.28	56.77	95.09	129.78
E2F2C	65.48	61.2	58.08	55.61	49.93
eSBR	43.28	52.79	65.07	95.11	110.74
NJL	48.79	46.05	42.17	37.98	33.65
Weight factors combination 9					
HM	22.78	29.47	32.6	40.79	70.21
HMwF	21.47	25.6	33.45	49.8	80.47
EN2IwF	19.48	42.04	58.1	96.9	127.2
E2F2C	67.48	63.9	60.2	57.4	52.18
eSBR	45.81	54.26	67.08	96.8	113.48
NJL	50.17	48.97	45.6	41.27	36.45
Weight factors combination 10					
HM	24.17	31.2	36.75	42.18	73.64
HMwF	23.65	28.95	35.48	51.02	78.4
EN2IwF	22.31	44.78	61.29	95.4	131.74
E2F2C	69.55	66.05	62.31	59.8	56.47
eSBR	47.12	56.8	69.08	98.11	115.47
NJL	52.47	49.8	46.75	43.29	37.84

TABLE A.5: Sum of the percentages of vehicles informed on the Valencia scenario across all densities, highlighting the highest sum for each weight factors combination (part 1 — weight factor combinations 1–5).

Car density	25	50	100	150	200	SUM
Weight factors combination 1						
HM	100	100	97.6	94.2	93.5	485.3
HMwF	100	98.95	94.6	92.14	89.4	475.09
EN2IwF	95.7	97.76	96.18	94.71	92.64	476.99
E2F2C	46.24	52.47	58.6	63.81	71.8	292.92
eSBR	84.95	86.2	87.4	88.1	90.5	437.15
NJL	82.8	83.7	85.6	87.4	89.2	428.7
Weight factors combination 2						
HM	100	100	98.2	96.2	94.18	488.58
HMwF	100	99.2	95.7	93.8	92.4	481.1
EN2IwF	96.77	94.82	92.14	90.8	87.24	461.77
E2F2C	37.63	41.6	47.4	52.18	56.9	235.71
eSBR	62.36	65.2	71.2	76.75	82.3	357.81
NJL	87.1	89.8	92.7	94.68	96.7	460.98
Weight factors combination 3						
HM	100	100	97.8	95.4	92.34	485.54
HMwF	100	98.65	95.13	92.78	90.4	476.96
EN2IwF	96.77	91.6	90.8	87.48	84.2	450.85
E2F2C	34.25	38.9	41.26	46.78	51.4	212.59
eSBR	66.4	69.27	72.8	78.9	84.97	372.34
NJL	89.6	92.6	94.78	96.23	98.84	472.05
Weight factors combination 4						
HM	100	99.4	95.68	93.27	90.48	478.83
HMwF	98.92	96.59	94.1	90.68	87.49	467.78
EN2IwF	95.18	93.67	91.8	89.25	86.4	456.3
E2F2C	31.18	34.79	38.65	42.38	47.96	194.96
eSBR	78.5	79.87	82.34	84.1	86.9	411.71
NJL	93.55	94.8	95.62	97.69	99.3	480.96
Weight factors combination 5						
HM	100	99.1	94.7	92.14	87.56	473.5
HMwF	98.2	95.48	91.05	89.7	84.4	458.83
EN2IwF	96.77	91.6	90.8	87.48	84.2	450.85
E2F2C	30.79	32.16	36.7	39.48	41.26	180.39
eSBR	79.5	81.82	83.69	85.7	88.2	418.91
NJL	94.89	96.2	96.9	98.48	99.5	485.97

TABLE A.6: Sum of the percentages of vehicles informed on the Valencia scenario across all densities, highlighting the highest sum for each weight factors combination (part 2 — weight factor combinations 6–10).

Car density	25	50	100	150	200	SUM
Weight factors combination 6						
HM	95.7	95.13	94.6	92.79	91.5	<u>469.72</u>
HMwF	95.7	94.78	92.18	90.6	87.42	460.68
EN2IwF	94.62	92.76	91.02	89.46	87.8	455.66
E2F2C	34.4	35.78	37.9	40.42	43.6	192.1
eSBR	88.5	84.76	81.8	77.49	74.6	407.15
NJL	80.65	78.7	76.28	71.9	67.1	374.63
Weight factor combination 7						
HM	98.6	96.7	95.6	94.32	92.08	<u>477.3</u>
HMwF	97.9	95.82	94.16	92.73	89.62	470.23
EN2IwF	95.47	94.6	92.84	90.69	88.5	462.1
E2F2C	33.74	34.69	36.2	38.79	41.2	184.62
eSBR	92.18	90.7	86.24	81.68	77.9	428.7
NJL	84.69	81.4	78.9	73.46	69.08	387.53
Weight factors combination 8						
HM	100	98.14	96.79	95.8	94.6	<u>485.33</u>
HMwF	98.92	97.14	96.9	94.76	91.2	478.92
EN2IwF	96.5	95.8	94.62	92.89	90.6	470.41
E2F2C	32.26	35.9	37.24	40.8	44.2	190.4
eSBR	96.7	94.81	88.9	84.76	79.29	444.46
NJL	87.1	83.69	80.5	76.47	71.2	398.96
Weight factors combination 9						
HM	100	98.9	97.48	96.9	95.78	<u>489.06</u>
HMwF	97.8	96.42	94.95	93.46	90.7	473.33
EN2IwF	96.77	95.4	94.12	92.26	89.74	468.29
E2F2C	30.97	36.7	38.24	42.6	45.3	193.81
eSBR	91.69	89.1	85.74	82.38	76.48	425.39
NJL	90.3	86.75	82.8	78.29	73.67	411.81
Weight factors combination 10						
HM	100	99.4	98.62	97.5	96.9	<u>492.42</u>
HMwF	96.9	95.28	93.01	91.9	88.76	465.85
EN2IwF	96.81	96	95.28	94.73	91.09	473.91
E2F2C	29.03	37.91	40.8	44.55	47.85	200.14
eSBR	82.8	81.06	78.9	76.47	74.18	393.41
NJL	93.55	90.86	86.9	81.37	77.49	430.17

TABLE A.7: Sum of the delays in seconds to inform the last vehicle on the Valencia scenario across all densities, highlighting the lowest sum for each weight factors combination (part 1 — weight factor combinations 1–5).

Car density	25	50	100	150	200	SUM
Weight factors combination 1						
HM	22.9	26.1	34.08	48.95	78.09	<u>210.12</u>
HMwF	26.2	31.34	37.9	66.48	86.4	248.32
EN2IwF	19.3	38.7	49.08	110.8	145.7	363.58
E2F2C	55.7	52.06	49.71	42.8	36.45	236.72
eSBR	59.4	68.38	78.49	111.55	136.92	454.74
NJL	68	63.26	61.79	50.6	36.4	280.05
Weight factors combination 2						
HM	23.4	24.8	32.9	46.78	76.05	<u>203.93</u>
HMwF	18.97	26.8	30.29	49.73	82.02	207.81
EN2IwF	11.2	32.69	46.23	89.65	130.46	310.23
E2F2C	56.9	53.14	50.84	44.16	38.9	243.94
eSBR	57.7	66.94	76.45	108.26	131.72	441.07
NJL	50.02	47.62	43.29	41.08	35.89	217.9
Weight factors combination 3						
HM	23.2	25.1	33.68	47.91	77.96	207.85
HMwF	16.74	24.92	27.69	46.8	79.05	<u>195.2</u>
EN2IwF	12.3	33.95	48.9	91.25	127.64	314.04
E2F2C	57.08	55.96	53.48	46.7	41.08	254.3
eSBR	54.28	63.8	75.96	106.74	126.4	427.18
NJL	49.1	46.07	41.8	40.2	35.02	212.19
Weight factors combination 4						
HM	22.6	24.1	31.79	45.6	75.4	199.49
HMwF	15.2	21.9	24.67	42.38	76.4	<u>180.55</u>
EN2IwF	13.6	35.78	50.28	92.3	128.5	320.46
E2F2C	58.12	56.47	54.59	48.2	46.7	264.08
eSBR	52.81	62.25	73.48	102.6	123.47	414.61
NJL	47.69	45.2	40.1	38.68	34.12	205.79
Weight factors combination 5						
HM	20.6	22.89	28.75	42.17	72.38	<u>186.79</u>
HMwF	16.47	23.68	26.98	44.05	77.48	188.66
EN2IwF	14.28	36.91	52.07	93.33	125.64	322.23
E2F2C	59.67	57.48	56.2	51.3	48.12	272.77
eSBR	50.12	60.28	71.49	101.08	119.67	402.64
NJL	45.67	42.13	37.67	35.29	31.26	192.02

TABLE A.8: Sum of the delays in seconds to inform the last vehicle on the Valencia scenario across all densities, highlighting the lowest sum for each weight factors combination (part 2 — weight factor combinations 6–10).

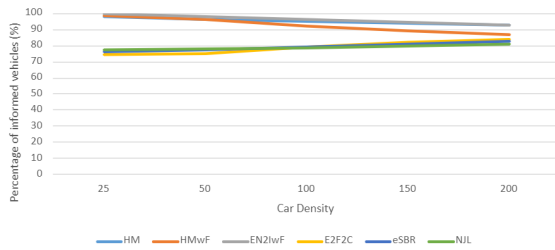
Car density	25	50	100	150	200	SUM
Weight factors combination 6						
HM	19.79	20.67	27.9	40.58	70.69	179.63
HMwF	18.9	24.26	31.48	46.06	78.14	198.84
EN2IwF	15.18	37.9	53.77	92.08	126.38	325.31
E2F2C	61.29	59.8	57.03	53.56	49.77	281.45
eSBR	48.97	57.65	69.53	97.08	116.46	389.69
NJL	44.38	41.05	36.02	34.79	30.6	186.84
Weight factors combination 7						
HM	18.47	19.64	25.8	36.47	66.9	167.28
HMwF	18.02	21.58	29.74	45.97	76.15	191.46
EN2IwF	16.08	39.66	54.17	93.8	127.9	331.61
E2F2C	63.2	58.7	56.46	53.11	48.79	280.26
eSBR	46.7	55.68	67.09	96.8	115.28	381.55
NJL	46.79	43.28	39.7	35.2	31.72	196.69
Weight factors combination 8						
HM	20.79	26.47	28.62	38.55	68.08	182.51
HMwF	19.63	23.47	31.28	47.55	78.9	200.83
EN2IwF	17.29	41.28	56.77	95.09	129.78	340.21
E2F2C	65.48	61.2	58.08	55.61	49.93	290.3
eSBR	43.28	52.79	65.07	95.11	110.74	366.99
NJL	48.79	46.05	42.17	37.98	33.65	208.64
Weight factors combination 9						
HM	22.78	29.47	32.6	40.79	70.21	195.85
HMwF	21.47	25.6	33.45	49.8	80.47	210.79
EN2IwF	19.48	42.04	58.1	96.9	127.2	343.72
E2F2C	67.48	63.9	60.2	57.4	52.18	301.16
eSBR	45.81	54.26	67.08	96.8	113.48	377.43
NJL	50.17	48.97	45.6	41.27	36.45	222.46
Weight factors combination 10						
HM	24.17	31.2	36.75	42.18	73.64	207.94
HMwF	23.65	28.95	35.48	51.02	78.4	217.5
EN2IwF	22.31	44.78	61.29	95.4	131.74	355.52
E2F2C	69.55	66.05	62.31	59.8	56.47	314.18
eSBR	47.12	56.8	69.08	98.11	115.47	386.58
NJL	52.47	49.8	46.75	43.29	37.84	230.15

A.2 DATA AND FIGURES OF THE SAN FRANCISCO SCENARIO

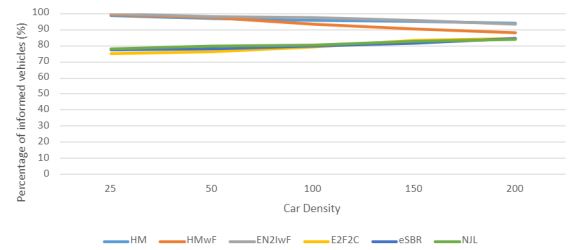
Along the same lines, charts and tables for the percentages of vehicles informed on the San Francisco map are presented on Figure A.5 (part 1 — weight factor combinations 1 through 5) and on Figure A.6 (part 2 — weight factor combinations 6 through 10) and Table A.9 (part 1) and Table A.10 (part 2). The values highlighted on both tables correspond to the ones in Table 6.4.

Similarly, charts and tables for the delays to inform the last vehicle on the San Francisco map are shown on Figure A.7 (part 1) and Figure A.8 (part 2) and Table A.11 (part 1) and Table A.12 (part 2). Highlighted values are the ones used in Table 6.6.

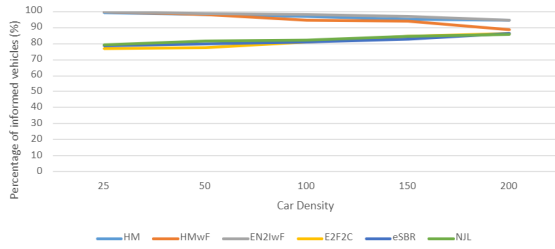
And finally, considering a single communication method along all densities, the percentages of informed vehicles are shown in Table A.13 (part 1) and Table A.14 (part 2) (values used in Table 6.8), and delays to inform the last vehicle in Table A.15 (part 1) and Table A.16 (part 2) (values used in Table 6.10).



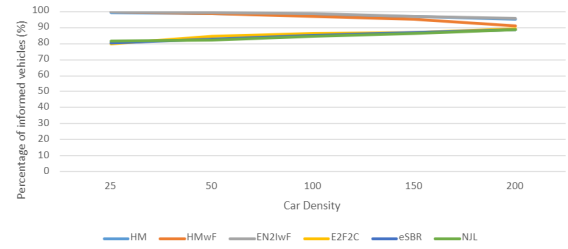
(A) Weight factors combination 1 — $wf1 = 1, wf2 = 0, wf3 = 0$



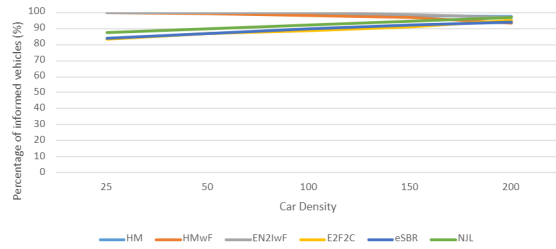
(B) Weight factors combination 2 — $wf1 = 2/3, wf2 = 1/3, wf3 = 0$



(C) Weight factors combination 3 — $wf1 = 2/3, wf2 = 0, wf3 = 1/3$

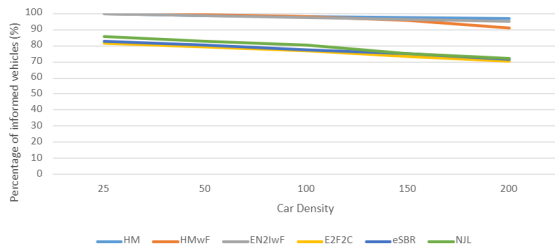


(D) Weight factors combination 4 — $wf1 = 1/3, wf2 = 2/3, wf3 = 0$

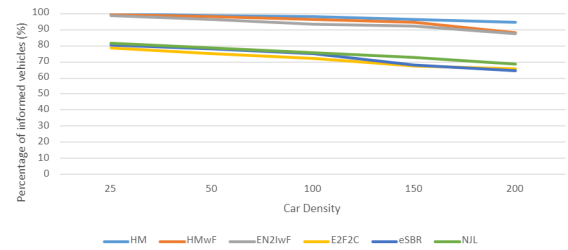


(E) Weight factors combination 5 — $wf1 = 1/3, wf2 = 1/3, wf3 = 1/3$

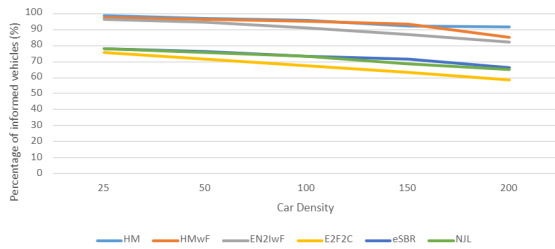
FIGURE A.5: Percentage of informed vehicles crossing car densities for the San Francisco scenario with different weight-factor combinations in the VANET for all proposed methods and benchmarks (part 1 — weight factor combinations 1–5).



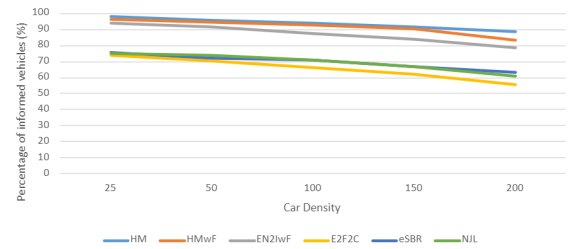
(A) Weight factors combination 6 — $wf1 = 1/3, wf2 = 0, wf3 = 2/3$



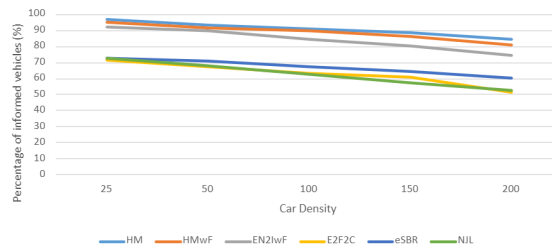
(B) Weight factors combination 7 — $wf1 = 0, wf2 = 1, wf3 = 0$



(C) Weight factors combination 8 — $wf1 = 0, wf2 = 2/3, wf3 = 1/3$



(D) Weight factors combination 9 — $wf1 = 0, wf2 = 1/3, wf3 = 2/3$



(E) Weight factors combination 10 — $wf1 = 0, wf2 = 0, wf3 = 1$

FIGURE A.6: Percentage of informed vehicles crossing car densities for the San Francisco scenario with different weight-factor combinations in the VANET for all proposed methods and benchmarks (part 2 — weight factor combinations 6–10).

TABLE A.9: Percentage of vehicles informed on the San Francisco scenario for the considered car densities, highlighting the highest percentage for each density and weight factors combination (part 1 — weight factor combinations 1–5).

Car density	25	50	100	150	200
Weight factors combination 1					
HM	98.1	96.04	95.21	93.87	92.6
HMwF	98.9	96.28	92.17	89.24	86.7
EN2IwF	<u>100</u>	<u>97.76</u>	<u>96.18</u>	<u>94.71</u>	<u>92.64</u>
E2F2C	74.72	75.14	78.9	82.4	83.6
eSBR	76.48	77.4	79.2	80.69	82.78
NJL	77.5	78.1	78.64	79.82	81.2
Weight factors combination 2					
HM	98.9	96.64	95.7	94.9	<u>93.79</u>
HMwF	99.3	97.4	93.2	90.13	87.9
EN2IwF	<u>100</u>	<u>98.1</u>	<u>97.3</u>	<u>95.68</u>	93.12
E2F2C	75.1	76.31	79.01	83.4	84.59
eSBR	77.18	78.2	79.67	81.29	84.72
NJL	78.2	79.49	80.14	82.47	83.68
Weight factors combination 3					
HM	99.34	97.89	96.78	95.18	<u>94.7</u>
HMwF	99.7	98.2	94.79	93.67	88.47
EN2IwF	<u>100</u>	<u>98.67</u>	<u>97.8</u>	<u>96.89</u>	94.26
E2F2C	76.87	77.58	80.67	84.7	86.2
eSBR	78.41	79.67	80.9	82.47	86.4
NJL	79.29	81.7	82.14	84.3	85.48
Weight factors combination 4					
HM	99.42	98.6	97.4	96.89	95.24
HMwF	99.8	98.4	96.7	95.13	91.2
EN2IwF	<u>100</u>	<u>99.2</u>	<u>98.35</u>	<u>97.14</u>	<u>95.64</u>
E2F2C	79.87	84.2	86.2	87.1	89.46
eSBR	80.26	82.47	84.9	86.7	88.6
NJL	81.6	82.2	84.75	86.3	88.4
Weight factors combination 5					
HM	<u>100</u>	99.6	98.6	98.2	<u>97.6</u>
HMwF	<u>100</u>	99.4	98.2	96.98	93.6
EN2IwF	<u>100</u>	<u>100</u>	<u>99.6</u>	<u>98.5</u>	97
E2F2C	83.48	86.9	88.4	91.2	95.12
eSBR	83.76	86.78	89.54	92.3	94.2
NJL	87.2	89.64	92.2	94.5	96.86

TABLE A.10: Percentage of vehicles informed on the San Francisco scenario for the considered car densities, highlighting the highest percentage for each density and weight factors combination (part 2 — weight factor combinations 6–10).

Car density	25	50	100	150	200
Weight factors combination 6					
HM	100	98.9	98.2	97.4	96.58
HMwF	99.8	99.1	97.9	95.4	91.2
EN2IwF	100	98.6	97.42	96.39	95.15
E2F2C	81.78	79.4	76.9	73	70.2
eSBR	82.8	80.6	77.4	75.2	71.58
NJL	85.4	82.7	80.1	74.8	72.1
Weight factors combination 7					
HM	99.8	98.6	98.2	96.4	94.78
HMwF	99.2	98.08	96.28	94.67	88.2
EN2IwF	98.6	96.48	93.48	91.97	87.2
E2F2C	78.4	74.79	72.21	67.26	65.8
eSBR	80.2	77.8	74.9	68.05	64.29
NJL	81.39	78.6	75.7	72.4	68.3
Weight factors combination 8					
HM	98.4	96.7	95.8	92.04	91.38
HMwF	97.68	96.18	94.8	93.2	85.2
EN2IwF	96.4	94.3	90.8	86.9	82.3
E2F2C	75.4	71.8	67.4	63.2	58.4
eSBR	78.2	76.4	73.29	71.48	66.28
NJL	78.2	75.9	73.2	68.5	64.8
Weight factors combination 9					
HM	97.8	95.6	93.7	91.4	88.48
HMwF	96.49	94.38	92.7	90.18	83.5
EN2IwF	94.2	91.6	87.4	83.9	78.4
E2F2C	73.6	70.2	66.2	61.9	55.62
eSBR	75.48	72.1	70.7	66.59	63.2
NJL	75.2	73.6	70.8	66.8	60.8
Weight factors combination 10					
HM	96.7	93.28	90.8	88.4	84.2
HMwF	95.1	91.7	89.6	86.2	80.8
EN2IwF	92.3	89.7	84.2	80.2	74.28
E2F2C	71.4	67.5	63.2	60.8	51.7
eSBR	72.5	70.8	67.4	64.24	60.28
NJL	72.5	68.2	62.48	57.2	52.8

TABLE A.11: Delays in seconds to inform the last vehicle on the San Francisco scenario for the considered car densities, highlighting the lowest delays for each density and weight factors combination (part 1 — weight factor combinations 1–5).

Car density	25	50	100	150	200
Weight factors combination 1					
HM	<u>26.8</u>	<u>32.4</u>	<u>38.78</u>	68.6	81.2
HMwF	30.2	36.7	41.25	70.2	90.8
EN2IwF	26.8	52.6	68.2	140.5	162.8
E2F2C	58.4	56.7	53.6	<u>46.8</u>	40.2
eSBR	73.5	76.9	82.5	120.9	140.9
NJL	138	120.6	112.08	92.6	<u>39.9</u>
Weight factors combination 2					
HM	24.4	<u>30.7</u>	<u>35.26</u>	60.9	76.4
HMwF	28.5	34.95	38.6	67.52	84.23
EN2IwF	<u>22.07</u>	46.3	65.9	126.4	145.7
E2F2C	51.7	46.8	41.3	<u>33.6</u>	<u>28.03</u>
eSBR	69.59	63.7	76.1	108.4	127.4
NJL	130.8	110.4	106.9	83.28	32.7
Weight factors combination 3					
HM	20.96	<u>26.7</u>	<u>31.6</u>	53.1	68.9
HMwF	24.8	31.09	33.4	60.9	78.2
EN2IwF	<u>17.6</u>	37.28	56.94	101.48	125.05
E2F2C	47.68	40.9	37.6	<u>26.4</u>	<u>20.75</u>
eSBR	54.89	55.2	63.8	86.5	113.26
NJL	118.9	103.26	94.7	76.8	32.7
Weight factors combination 4					
HM	18.1	<u>22.2</u>	<u>34.68</u>	59.6	76.4
HMwF	25.3	26.4	36.1	63.4	86.74
EN2IwF	<u>12.4</u>	38.2	51.03	132.6	150.7
E2F2C	47.8	45.3	42.78	<u>41.06</u>	39.87
eSBR	67.94	71.6	78.94	110.2	146.4
NJL	124	110.48	104.9	84.1	<u>23.7</u>
Weight factors combination 5					
HM	<u>12.7</u>	<u>20.9</u>	<u>26.3</u>	47.21	56.84
HMwF	22.76	28.69	30.5	49.7	62.8
EN2IwF	16.4	32.18	51.39	89.78	106.8
E2F2C	42.9	34.59	31.26	<u>20.4</u>	<u>16.5</u>
eSBR	47.6	51.74	59.6	73.48	116.2
NJL	107.01	96.28	88.97	71.49	30.5

TABLE A.12: Delays in seconds to inform the last vehicle on the San Francisco scenario for the considered car densities, highlighting the lowest delays for each density and weight factors combination (part 2 — weight factor combinations 6–10).

Car density	25	50	100	150	200
Weight factors combination 6					
HM	14.8	26.5	29.4	56.8	59.46
HMwF	25.9	33.6	36.78	57.49	67.8
EN2IwF	21.49	37.4	58.5	97.15	108.4
E2F2C	44.7	39.78	36.29	23.4	20.64
eSBR	51.28	58.47	67.45	78.29	121.05
NJL	117.5	99.68	93.58	79.62	40.6
Weight factors combination 7					
HM	17.8	30.2	36.5	61.7	67.89
HMwF	28.9	38.05	41.25	62.38	72.6
EN2IwF	26.94	41.89	66.8	106.84	118.54
E2F2C	57.68	48.6	39.4	28.7	22.6
eSBR	57.49	63.48	73.4	82.6	130.26
NJL	124.57	110.6	98.7	96.48	51.7
Weight factors combination 8					
HM	19.8	32.6	42.8	66.2	72.35
HMwF	34.8	43.64	47.94	66.8	78.4
EN2IwF	30.3	47.94	69.02	104.7	112.4
E2F2C	55.4	42.37	34.7	30.2	25.8
eSBR	64.79	68.74	76.4	84.5	124.14
NJL	117.2	106.5	99.8	94.2	59.4
Weight factors combination 9					
HM	23.5	37.48	49.67	69.18	79.2
HMwF	39.14	49.6	57.42	69.01	82.9
EN2IwF	36.89	49.75	75.9	112.9	121.7
E2F2C	59.8	51.7	38.4	33.46	30.7
eSBR	69.14	82.48	93.59	105.48	119.6
NJL	123.46	118.4	106.2	99.74	68.49
Weight factors combination 10					
HM	29.48	46.78	53.62	72.49	88.49
HMwF	47.65	55.8	63.45	72.3	87.48
EN2IwF	46.5	59.4	82.64	126.48	149.7
E2F2C	67.48	59.38	54.71	42.15	38.74
eSBR	78.45	91.6	98.48	121.4	142.5
NJL	135.8	124.6	113.25	100.6	86.57

TABLE A.13: Sum of the percentages of vehicles informed on the San Francisco scenario across all densities, highlighting the highest sum for each weight factors combination (part 1 — weight factor combinations 1–5).

Car density	25	50	100	150	200	SUM
Weight factors combination 1						
HM	98.1	96.04	95.21	93.87	92.6	475.82
HMwF	98.9	96.28	92.17	89.24	86.7	463.29
EN2IwF	100	97.76	96.18	94.71	92.64	481.29
E2F2C	74.72	75.14	78.9	82.4	83.6	394.76
eSBR	76.48	77.4	79.2	80.69	82.78	396.55
NJL	77.5	78.1	78.64	79.82	81.2	395.26
Weight factors combination 2						
HM	98.9	96.64	95.7	94.9	93.79	479.93
HMwF	99.3	97.4	93.2	90.13	87.9	467.93
EN2IwF	100	98.1	97.3	95.68	93.12	484.2
E2F2C	75.1	76.31	79.01	83.4	84.59	398.41
eSBR	77.18	78.2	79.67	81.29	84.72	401.06
NJL	78.2	79.49	80.14	82.47	83.68	403.98
Weight factors combination 3						
HM	99.34	97.89	96.78	95.18	94.7	483.89
HMwF	99.7	98.2	94.79	93.67	88.47	474.83
EN2IwF	100	98.67	97.8	96.89	94.26	487.62
E2F2C	76.87	77.58	80.67	84.7	86.2	406.02
eSBR	78.41	79.67	80.9	82.47	86.4	407.85
NJL	79.29	81.7	82.14	84.3	85.48	412.91
Weight factors combination 4						
HM	99.42	98.6	97.4	96.89	95.24	487.55
HMwF	99.8	98.4	96.7	95.13	91.2	481.23
EN2IwF	100	99.2	98.35	97.14	95.64	490.33
E2F2C	79.87	84.2	86.2	87.1	89.46	426.83
eSBR	80.26	82.47	84.9	86.7	88.6	422.93
NJL	81.6	82.2	84.75	86.3	88.4	423.25
Weight factors combination 5						
HM	100	99.6	98.6	98.2	97.6	494
HMwF	100	99.4	98.2	96.98	93.6	488.18
EN2IwF	100	100	99.6	98.5	97	495.1
E2F2C	83.48	86.9	88.4	91.2	95.12	445.1
eSBR	83.76	86.78	89.54	92.3	94.2	446.58
NJL	87.2	89.64	92.2	94.5	96.86	460.4

TABLE A.14: Sum of the percentages of vehicles informed on the San Francisco scenario across all densities, highlighting the highest sum for each weight factors combination (part 2 — weight factor combinations 6–10).

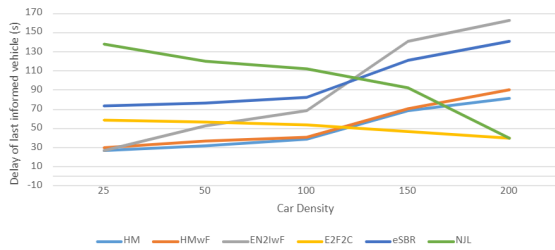
Car density	25	50	100	150	200	SUM
Weight factors combination 6						
HM	100	98.9	98.2	97.4	96.58	491.08
HMwF	99.8	99.1	97.9	95.4	91.2	483.4
EN2IwF	100	98.6	97.42	96.39	95.15	487.56
E2F2C	81.78	79.4	76.9	73	70.2	381.28
eSBR	82.8	80.6	77.4	75.2	71.58	387.58
NJL	85.4	82.7	80.1	74.8	72.1	395.1
Weight factors combination 7						
HM	99.8	98.6	98.2	96.4	94.78	487.78
HMwF	99.2	98.08	96.28	94.67	88.2	476.43
EN2IwF	98.6	96.48	93.48	91.97	87.2	467.73
E2F2C	78.4	74.79	72.21	67.26	65.8	358.46
eSBR	80.2	77.8	74.9	68.05	64.29	365.24
NJL	81.39	78.6	75.7	72.4	68.3	376.39
Weight factors combination 8						
HM	98.4	96.7	95.8	92.04	91.38	474.32
HMwF	97.68	96.18	94.8	93.2	85.2	467.06
EN2IwF	96.4	94.3	90.8	86.9	82.3	450.7
E2F2C	75.4	71.8	67.4	63.2	58.4	336.2
eSBR	78.2	76.4	73.29	71.48	66.28	365.65
NJL	78.2	75.9	73.2	68.5	64.8	360.6
Weight factors combination 9						
HM	97.8	95.6	93.7	91.4	88.48	466.98
HMwF	96.49	94.38	92.7	90.18	83.5	457.25
EN2IwF	94.2	91.6	87.4	83.9	78.4	435.5
E2F2C	73.6	70.2	66.2	61.9	55.62	327.52
eSBR	75.48	72.1	70.7	66.59	63.2	348.07
NJL	75.2	73.6	70.8	66.8	60.8	347.2
Weight factors combination 10						
HM	96.7	93.28	90.8	88.4	84.2	453.38
HMwF	95.1	91.7	89.6	86.2	80.8	443.4
EN2IwF	92.3	89.7	84.2	80.2	74.28	420.68
E2F2C	71.4	67.5	63.2	60.8	51.7	314.6
eSBR	72.5	70.8	67.4	64.24	60.28	335.22
NJL	72.5	68.2	62.48	57.2	52.8	313.18

TABLE A.15: Sum of the delays in seconds to inform the last vehicle on the San Francisco scenario across all densities, highlighting the lowest sum for each weight factors combination (part 1 — weight factor combinations 1–5).

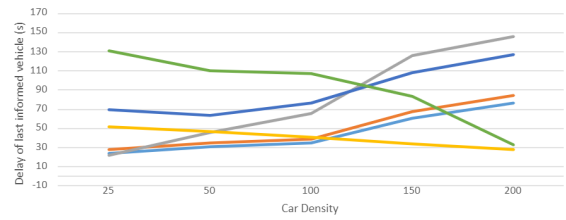
Car density	25	50	100	150	200	SUM
Weight factors combination 1						
HM	26.8	32.4	38.78	68.6	81.2	247.78
HMwF	30.2	36.7	41.25	70.2	90.8	269.15
EN2IwF	26.8	52.6	68.2	140.5	162.8	450.9
E2F2C	58.4	56.7	53.6	46.8	40.2	255.7
eSBR	73.5	76.9	82.5	120.9	140.9	494.7
NJL	138	120.6	112.08	92.6	39.9	503.18
Weight factors combination 2						
HM	24.4	30.7	35.26	60.9	76.4	227.66
HMwF	28.5	34.95	38.6	67.52	84.23	253.8
EN2IwF	22.07	46.3	65.9	126.4	145.7	406.37
E2F2C	51.7	46.8	41.3	33.6	28.03	201.43
eSBR	69.59	63.7	76.1	108.4	127.4	445.19
NJL	130.8	110.4	106.9	83.28	32.7	464.08
Weight factors combination 3						
HM	20.96	26.7	31.6	53.1	68.9	201.26
HMwF	24.8	31.09	33.4	60.9	78.2	228.39
EN2IwF	17.6	37.28	56.94	101.48	125.05	338.35
E2F2C	47.68	40.9	37.6	26.4	20.75	173.33
eSBR	54.89	55.2	63.8	86.5	113.26	373.65
NJL	118.9	103.26	94.7	76.8	32.7	426.36
Weight factors combination 4						
HM	18.1	22.2	34.68	59.6	76.4	210.98
HMwF	25.3	26.4	36.1	63.4	86.74	237.94
EN2IwF	12.4	38.2	51.03	132.6	150.7	384.93
E2F2C	47.8	45.3	42.78	41.06	39.87	216.81
eSBR	67.94	71.6	78.94	110.2	146.4	475.08
NJL	124	110.48	104.9	84.1	23.7	447.18
Weight factors combination 5						
HM	12.7	20.9	26.3	47.21	56.84	163.95
HMwF	22.76	28.69	30.5	49.7	62.8	194.45
EN2IwF	16.4	32.18	51.39	89.78	106.8	296.55
E2F2C	42.9	34.59	31.26	20.4	16.5	145.65
eSBR	47.6	51.74	59.6	73.48	116.2	348.62
NJL	107.01	96.28	88.97	71.49	30.5	394.25

TABLE A.16: Sum of the delays in seconds to inform the last vehicle on the San Francisco scenario across all densities, highlighting the lowest sum for each weight factors combination (part 2 — weight factor combinations 6–10).

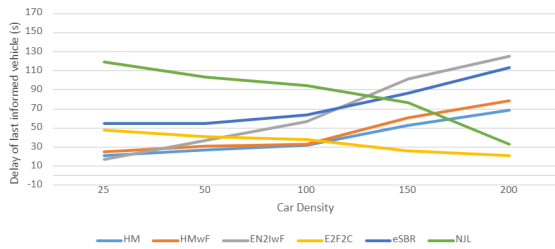
Car density	25	50	100	150	200	SUM
Weight factors combination 6						
HM	14.8	26.5	29.4	56.8	59.46	186.96
HMwF	25.9	33.6	36.78	57.49	67.8	221.57
EN2IwF	21.49	37.4	58.5	97.15	108.4	322.94
E2F2C	44.7	39.78	36.29	23.4	20.64	164.81
eSBR	51.28	58.47	67.45	78.29	121.05	376.54
NJL	117.5	99.68	93.58	79.62	40.6	430.98
Weight factors combination 7						
HM	17.8	30.2	36.5	61.7	67.89	214.09
HMwF	28.9	38.05	41.25	62.38	72.6	243.18
EN2IwF	26.94	41.89	66.8	106.84	118.54	361.01
E2F2C	57.68	48.6	39.4	28.7	22.6	196.98
eSBR	57.49	63.48	73.4	82.6	130.26	407.23
NJL	124.57	110.6	98.7	96.48	51.7	482.05
Weight factors combination 8						
HM	19.8	32.6	42.8	66.2	72.35	233.75
HMwF	34.8	43.64	47.94	66.8	78.4	271.58
EN2IwF	30.3	47.94	69.02	104.7	112.4	364.36
E2F2C	55.4	42.37	34.7	30.2	25.8	188.47
eSBR	64.79	68.74	76.4	84.5	124.14	418.57
NJL	117.2	106.5	99.8	94.2	59.4	477.1
Weight factors combination 9						
HM	23.5	37.48	49.67	69.18	79.2	259.03
HMwF	39.14	49.6	57.42	69.01	82.9	298.07
EN2IwF	36.89	49.75	75.9	112.9	121.7	397.14
E2F2C	59.8	51.7	38.4	33.46	30.7	214.06
eSBR	69.14	82.48	93.59	105.48	119.6	470.29
NJL	123.46	118.4	106.2	99.74	68.49	516.29
Weight factors combination 10						
HM	29.48	46.78	53.62	72.49	88.49	290.86
HMwF	47.65	55.8	63.45	72.3	87.48	326.68
EN2IwF	46.5	59.4	82.64	126.48	149.7	464.72
E2F2C	67.48	59.38	54.71	42.15	38.74	262.46
eSBR	78.45	91.6	98.48	121.4	142.5	532.43
NJL	135.8	124.6	113.25	100.6	86.57	560.82



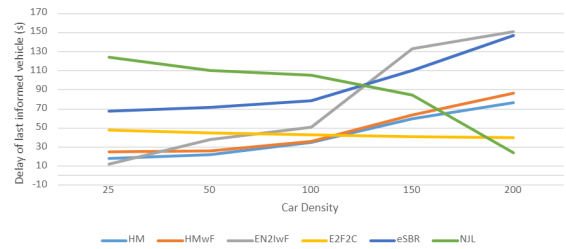
(A) Weight factors combination 1 — $wf1 = 1, wf2 = 0, wf3 = 0$



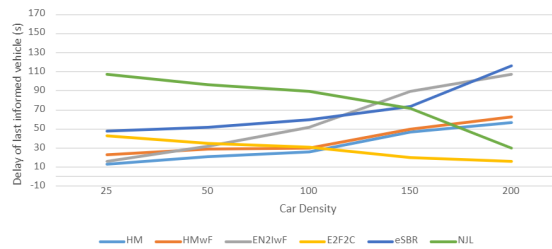
(B) Weight factors combination 2 — $wf1 = 2/3, wf2 = 1/3, wf3 = 0$



(C) Weight factors combination 3 — $wf1 = 2/3, wf2 = 0, wf3 = 1/3$

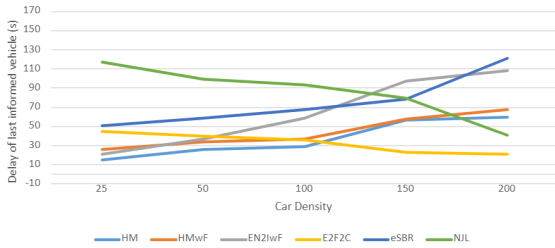


(D) Weight factors combination 4 — $wf1 = 1/3, wf2 = 2/3, wf3 = 0$

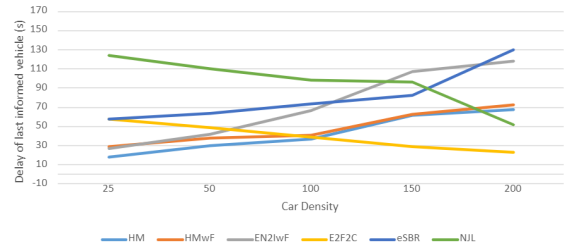


(E) Weight factors combination 5 — $wf1 = 1/3, wf2 = 1/3, wf3 = 1/3$

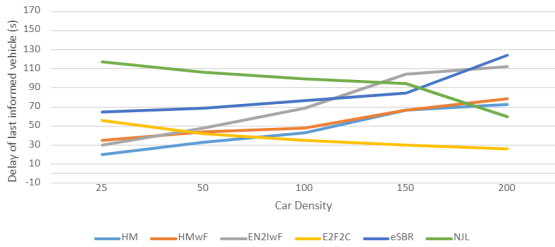
FIGURE A.7: Delays to inform the last vehicle crossing car densities for the San Francisco scenario with different weight-factor combinations in the VANET for all proposed methods and benchmarks (part 1 — weight factor combinations 1–5).



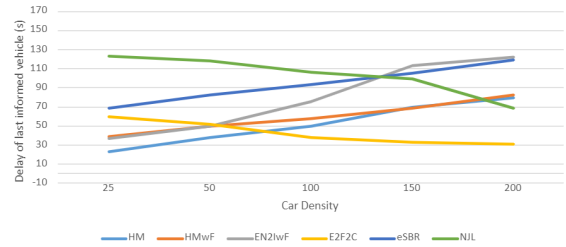
(A) Weight factors combination 6 — $wf1 = 1/3, wf2 = 0, wf3 = 2/3$



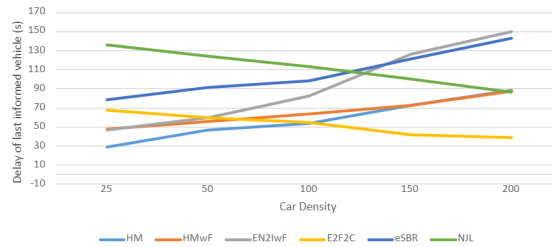
(B) Weight factors combination 7 — $wf1 = 0, wf2 = 1, wf3 = 0$



(C) Weight factors combination 8 — $wf1 = 0, wf2 = 2/3, wf3 = 1/3$



(D) Weight factors combination 9 — $wf1 = 0, wf2 = 1/3, wf3 = 2/3$



(E) Weight factors combination 10 — $wf1 = 0, wf2 = 0, wf3 = 1$

FIGURE A.8: Delays to inform the last vehicle crossing car densities for the San Francisco scenario with different weight-factor combinations in the VANET for all proposed methods and benchmarks (part 2 — weight factor combinations 6–10).

APPENDIX B

CLUSTER MERGING IMPLEMENTATION IN OMNET++

Since the cluster merging is the scheme used in all proposals shown in this thesis, we present the two versions of the code — 2-factor and 3-factor cluster merging —, which covers all the contribution chapters. First, the 2-factor cluster merging code is shown in Listing B.1.

```

1 void VeinsInetManager::startClusterMerging(int Clust0, int Clust1) {
2     EV_INFO << "Merging Clusters" << endl;
3     int wIndex = par("weightIndex");
4     float wf1 = 0.9;
5     float wf2 = 0.1;
6     float bestBeta = 0.0;
7     std::string bestVehicle;
8     int mergedCars = 0;
9     for (std::map<std::string, cModule*>::const_iterator i = hosts.begin
10         (); i != hosts.end(); ++i) {
11         float speedFactor = 0;
12         cModule *hostNode = i->second;
13
14         auto appModule = dynamic_cast<VeinsInetSampleApplication*>(
15             hostNode->getSubmodule("app", 0));
16         if (appModule->par("clusterNumber").intValue() == Clust0 ||
17             appModule->par("clusterNumber").intValue() == Clust1) {
18             appModule->par("clusterNumber").setIntValue(Clust0);
19             appModule->par("isClusterMaster").setBoolValue(false);
20             hostNode->setDisplayString("i=veins/node/car;is=vs");
21             auto mobilityModules = getSubmodulesOfType<VeinsInetMobility>(
22                 hostNode);
23             inet::Coord nSpeedV = mobilityModules[0]->getCurrentVelocity();
24             double nSpeed = nSpeedV.squareLength();
25             for (std::map<std::string, cModule*>::const_iterator iter =
26                 hosts.begin(); iter != hosts.end(); ++iter) {
27                 cModule *hostNeigh = iter->second;

```

```

23     auto appNeigh = dynamic_cast<VeinsInetSampleApplication*>(
hostNeigh->getSubmodule("app", 0));
24     if (appNeigh->par("clusterNumber").intValue() == Clust0 ||
appNeigh->par("clusterNumber").intValue() == Clust1) {
25         auto mobilityModulesN = getSubmodulesOfType<
VeinsInetMobility>(hostNeigh);
26         inet::Coord kSpeedV = mobilityModulesN[0]->
getCurrentVelocity();
27         double kSpeed = kSpeedV.squareLength();
28         speedFactor += abs(nSpeed - kSpeed);
29     }
30 }
31 speedFactor /= numberOfOneHopNeighbors[hostNode->getFullName()].
numberOfNeighbors;
32 float leadershipValue = 1/(1 + speedFactor);
33 EV_INFO << "Leadership value for vehicle " << hostNode->
getFullName() << ": " <<
34     leadershipValue << endl;
35     numberOfOneHopNeighbors[hostNode->getFullName()].beta = wf1 *
numberOfOneHopNeighbors[hostNode->getFullName()].numberOfNeighbors
+ wf2 * leadershipValue;
36     EV_INFO << "Beta for vehicle " <<
37     hostNode->getFullName() << ": " <<
38     numberOfOneHopNeighbors[(i->second)->getFullName()].beta <<
endl;
39     if (numberOfOneHopNeighbors[hostNode->getFullName()].beta >=
bestBeta) {
40         bestBeta = numberOfOneHopNeighbors[hostNode->getFullName()].
beta;
41         bestVehicle = hostNode->getFullName();
42     }
43 }
44 }
45
46 EV_INFO << "Best vehicle: " << bestVehicle << endl;
47
48 cModule *bestV = getModuleByPath(bestVehicle.c_str());

```

```

49 bestV->setDisplayString("i=veins/node/car,gold;is=vs");
50 auto appModule = dynamic_cast<VeinsInetSampleApplication*>(bestV->
    getSubmodule("app", 0));
51 appModule->par("isClusterMaster").setBoolValue(true);
52 }

```

LISTING B.1: 2-Factor Cluster Merging Implementation (C++ code)

The mentioned code is in the `VeinsInetManager` class, which is responsible for several functions regarding the network vehicles mobility and interactions with each other. The version of the code shown in B.1 was used to merge clusters on the contributions in Chapters 3 and 4. The differences on the contributions are the communication chains added in Chapter 4.

With every simulation step, the vehicles positions are updated and their one-hop neighbors are re-calculated. When a CM is detected as a one-hop neighbor of another CM, the method in Listing B.1 is called. More details on the code operation are shown after the modifications explained next.

However, for Chapters 5 and 6, the third weight factor was added and we decided to normalize the number of neighbors and the new estimated received power from the BS factors. The last version of the code is presented in Listing B.2.

```

1 void VeinsInetManager::startClusterMerging(int Clust0, int Clust1) {
2     EV_INFO << "Merging Clusters" << endl;
3     int wIndex = par("weightIndex");
4     float wf1 = we1[wIndex];
5     float wf2 = we2[wIndex];
6     float wf3 = we3[wIndex];
7     float bestBeta = 0.0;
8     std::string bestVehicle;
9     int mergedCars = 0;
10    for (std::map<std::string, cModule*>::const_iterator i = hosts.begin
        (); i != hosts.end(); ++i) {
11        float speedFactor = 0;
12        cModule *hostNode = i->second;
13
14        auto appModule = dynamic_cast<VeinsInetSampleApplication*>(
            hostNode->getSubmodule("app", 0));

```

```

15     if (appModule->par("clusterNumber").intValue() == Clust0 ||
16     appModule->par("clusterNumber").intValue() == Clust1) {
17         appModule->par("clusterNumber").setIntValue(Clust0);
18         appModule->par("isClusterMaster").setBoolValue(false);
19         hostNode->setDisplayString("i=veins/node/car;is=vs");
20         auto mobilityModules = getSubmodulesOfType<VeinsInetMobility>(
21     hostNode);
22         inet::Coord nSpeedV = mobilityModules[0]->getCurrentVelocity();
23         double nSpeed = nSpeedV.squareLength();
24         int Nmax = -1;
25         double maxRcvdPower = -1;
26         for (std::map<std::string, cModule*>::const_iterator iter =
27     hosts.begin(); iter != hosts.end(); ++iter) {
28             cModule *hostNeigh = iter->second;
29             auto appNeigh = dynamic_cast<VeinsInetSampleApplication*>(
30     hostNeigh->getSubmodule("app", 0));
31             if (appNeigh->par("clusterNumber").intValue() == Clust0 ||
32     appNeigh->par("clusterNumber").intValue() == Clust1) {
33                 auto mobilityModulesN = getSubmodulesOfType<
34     VeinsInetMobility>(hostNeigh);
35                 inet::Coord kSpeedV = mobilityModulesN[0]->
36     getCurrentVelocity();
37                 double kSpeed = kSpeedV.squareLength();
38                 speedFactor += abs(nSpeed - kSpeed);
39                 if (Nmax < 0 || Nmax < numberOfWorkOneHopNeighbors[hostNeigh->
40     getFullName()].numberOfNeighbors) {
41                     Nmax = numberOfWorkOneHopNeighbors[hostNeigh->getFullName()].
42     numberOfNeighbors;
43                 }
44                 if (maxRcvdPower < 0 || maxRcvdPower <
45     numberOfWorkOneHopNeighbors[hostNeigh->getFullName()].estRcvdPower) {
46                     maxRcvdPower = numberOfWorkOneHopNeighbors[hostNeigh->
47     getFullName()].estRcvdPower;
48                 }
49             }
50         }
51     }

```

```

40     speedFactor /= numberOfOneHopNeighbors[hostNode->getFullName()].
numberOfNeighbors;
41     float leadershipValue = 1/(1 + speedFactor);
42     EV_INFO << "Leadership value for vehicle " << hostNode->
getFullName() << ": " <<
43         leadershipValue << endl;
44     numberOfOneHopNeighbors[hostNode->getFullName()].beta = wf1 *
numberOfOneHopNeighbors[hostNode->getFullName()].numberOfNeighbors
/Nmax +
45     wf2 * leadershipValue + wf3 * numberOfOneHopNeighbors[
hostNode->getFullName()].estRcvdPower/maxRcvdPower;
46     EV_INFO << "Beta for vehicle " <<
47     hostNode->getFullName() << ": " <<
48     numberOfOneHopNeighbors[(i->second)->getFullName()].beta <<
endl;
49     if (numberOfOneHopNeighbors[hostNode->getFullName()].beta >=
bestBeta) {
50         bestBeta = numberOfOneHopNeighbors[hostNode->getFullName()].
beta;
51         bestVehicle = hostNode->getFullName();
52     }
53 }
54 }
55
56 EV_INFO << "Best vehicle: " << bestVehicle << endl;
57
58 cModule *bestV = getModuleByPath(bestVehicle.c_str());
59 bestV->setDisplayString("i=veins/node/car,gold;is=vs");
60 auto appModule = dynamic_cast<VeinsInetSampleApplication*>(bestV->
getSubmodule("app", 0));
61 appModule->par("isClusterMaster").setBoolValue(true);
62 }

```

LISTING B.2: 3-Factor Cluster Merging Implementation (C++ code)

In this case, the weight factors are no longer fixed at $wf1 = 0.9$ and $wf2 = 0.1$. The first step is to get the weight factor index defined in `VeinsInetManager.ned`, which is then used to get each of the weight factors defined in arrays in `VeinsInetManager.h`

with the exact same values shown in Table 6.1. For Chapter 5, though, only index 5 is used ($wf1 = wf2 = wf3 = 1/3$).

The best β found so far is initialized with 0 on line 7 of Listing B.2, which corresponds to line 13 of Algorithm 5.

Then, the *for* loop starting on line 10 of Listing B.2 sweeps all vehicles on the network looking for vehicles in the merging clusters — represented by `Clust0` and `Clust1` — and making all of them members of the first merging cluster. Both CMs lose their CM status (line 17), since a new one will be elected for the new cluster.

As mentioned before, the calculation of the number of one-hop neighbors, indicated on Algorithm 5 in line 7, is carried out prior to the beginning of a cluster merging procedure and is, therefore, already available.

After that, an inner *for* loop starting on line 24 sweeps all vehicles to enable the comparison — between the current vehicle for the outer loop and the one for the inner loop — of speeds, the search for the maximum number of one-hop neighbors, and the search for the maximum estimated received power from the BS. Also in the inner loop, the leadership values and, finally, the suitability value, β , is calculated for each vehicle. By the end of the loop, the best vehicle to become the CM is discovered. Ultimately, on line 61, the vehicle with the best β changes its status to CM.